โครงการการเรียนการสอนเพื่อเสริมประสบการณ์

การเกิดแร่ทองคำ-เงิน และการแปรเปลี่ยนชนิดอีพิเทอร์มอล
จังหวัด พิจิตร

โดย

นาย สิรวิชญ์ แก้วผลึก
เลขประจำตัวนิสิต 5732752623

โครงการนี้เป็นส่วนหนึ่งของการศึกษาระดับปริญญาตรี
ภาควิชาธรณีวิทยา คณะวิทยาศาสตร์ จุฬาลงกรณ์มหาวิทยาลัย
ปีการศึกษา 2560

EPITHERMAL GOLD-SILVER MINERALIZATION AND ALTERATION OF B-PROSPECT, PHICHIT PROVINCE

Mr. Sirawit Kaewpaluk

A Report submitted in Partial Fulfillment of the Requirements

For the Degree of Bachelor of Science

Department of Geology

Faculty of Science

Chulalongkorn University

Academic Year 2017

การเกิดแร่ทองคำ-เงิน และการแปรเปลี่ยนชนิดอีพิเทอร์มอล ของพื้นที่สำรวจบี จังหวัดพิจิตร

นาย สิรวิชญ์ แก้วผลึก

รายงานฉบับนี้เป็นส่วนหนึ่งของการศึกษาตามหลักสูตรปริญญาวิทยาศาสตร์บัณฑิต
ภาควิชาธรณีวิทยา คณะวิทยาศาสตร์ จุฬาลงกรณ์มหาวิทยาลัย
ปีการศึกษา 2560

Title	EPITHERMAL GOLD-SILVER MINERALIZATION AND ALTERATION OF B-PROSPECT, PHICHIT PROVINCE
Researcher	Sirawit Kaewpaluk
Department	Geology
Advisor	Dr. Abhisit Salam

Date of submission

_____/_____/_____

Date of approval

_____/_____/_____

Signature

_____

(Dr. Abhisit Salam)

EPITHERMAL GOLD-SILVER MINERALIZATION AND ALTERATION OF B-PROSPECT, PHICHIT PROVINCE

Researcher: Sirawit Kaewpaluk

Advisor: Dr.Abhisit Salam

Department of Geology, Faculty of Science, Chulalongkorn University

Abstract

The study area (B prospect) is located about 3 km south-east of Chatree deposit. The rocks in the prospect area can be grouped into 4 units namely, 1) Polymictic breccia unit (Unit 1), 2) Volcanogenic sedimentary unit (Unit 2), 3) Fiamme breccia unit (Unit 3) and 4) Andesitic polymictic breccia unit (Unit 4). The coherent rocks occur as dykes, it can be categorized into 3 types namely, 1) Hornblende-plagioclase phyric andesite, 2) Plagioclase phyric andesite and 3) Hornblende phyric andesite. Gold mineralization occurs as quartz ± carbonate – sulfides – electrum veins/veinlets and stock works hosted in volcanics and volcaniclastic rocks of Late Permian-Early Triassic. Mineralizations consist of 3 stages namely, 1) Quartz -pyrite veins, 2) Quartz ± carbonate – sulfides – electrum veins and 3) Quartz ± carbonate veins. The main gold stage (Stage 2) is characterized by typical textures of low sulfidation epithermal deposit which consists of mainly quartz and minor calcite gangue. Pyrite is a major sulfide with minor sphalerite. Gold identifies both as inclusion in sulfide particularly pyrite and free grain associates with quartz and calcite. EPMA analysis confirms that gold occurs as electrum with fineness ranging from 595 to 632. Petrographic and XRD study suggested that the hydrothermal alteration at B prospect can be divided into 3 types: 1) Quartz - adularia, 2) Adularia – sericite – illite – quartz ± calcite and 3) Sericite – illite ± chlorite ± calcite ± adularia ± quartz. The mineralization at B prospect can be distinguished from Chatree deposit by its simple mineral assemblages. And it can be classified as a low-sulfidation epithermal deposit.

Keywords: Low-sulfidation epithermal deposit, Mineralization stage, Electrum, Fineness

การเกิดแร่ทองคำ-เงิน และการแปรเปลี่ยนชนิดอีพิเทอร์มอลของพื้นที่สำรวจบี จังหวัดพิจิตร

ผู้วิจัย: สิรวิชญ์ แก้วผลึก

อาจารย์ที่ปรึกษางานวิจัย: อาจารย์ ดร.อภิสิทธิ์ ซาลำ

ภาควิชา ธรณีวิทยา คณะวิทยาศาสตร์ จุฬาลงกรณ์มหาวิทยาลัย

บทคัดย่อ

ทองคำ เงิน และ ทองแดง ในประเทศไทยนั้นพบอยู่มากในแนวชั้นหินคดโค้งเลย (Loei fold belt) เช่น แหล่งแร่อีพิเอทร์มอล (ชาตรี) และ แหล่งแร่สการ์น (ภูทับฟ้า และ เขาพนมพา) ทองคำในชาตรี เกิดในรูปแบบของแหล่งแร่อีพิเทอร์มอลอุณหภูมิต่ำ อยู่ในหินภูเขาไฟและหินตะกอนภูเขาไฟช่วงยุคเพอร์เมียนตอนปลาย ถึงยุคไทรแอสซิกตอนต้น (Late Permian-Early Triassic) พื้นที่ศึกษาในที่นี้คือพื้นที่สำรวจบี (B prospect) ซึ่งอยู่ทางตะวันออกเฉียงใต้ ประมาณ 3 กิโลเมตรจากแหล่งแร่ชาตรี โดยลักษณางด้านธรณีวิทยาของพื้นที่สำรวจบีสามารถแบ่งหน่วยหินได้ 4 หน่วยหินดังนี้ 1) หน่วยหินกรวดเหลี่ยมหลากชนิด (Polymictic breccia unit) 2) หน่วยหินตะกอนต้นกำเนิดจากภูเขาไฟ (Volcanogenic sedimentary unit) 3) หน่วยหินกรวดเหลี่ยมภูเขาไฟแสดงริ้ว (Fiamme breccia unit) และ 4) หน่วยหินกรวดเหลี่ยมแอนดีไซต์หลากชนิด (Andesitic polymictic breccia unit) นอกจากนั้นยังพบหินที่เย็นตัวโดยตรงจากแมกม่า (Coherent rocks) เกิดในรูปผนังหิน (Dykes) ได้แก่ 1) ฮอร์นเบลนด์-พลาจิโอเคลส แอนดิไซต์เนื้อละเอียด (Hornblende-plagioclase phyric andesite) 2) พลาจิโอเคลส แอนดิไซต์เนื้อละเอียด (Plagioclase phyric andesite) และ 3) ฮอร์นเบลนด์ แอนดิไซต์เนื้อละเอียด (Hornblende phyric andesite) ในพื้นที่สำรวจบีนั้น ทองคำเกิดในสายแร่ควอตซ์-คาร์บอนเนต (Quartz-carbonate veins) และ สายแร่ร่างแห (Stock works) ซึ่งประกอบด้วย 3 ระยะการเกิดแร่คือ 1) สายแร่ควอตซ์ – ไพไรต์ (Quartz-pyrite veins) 2) สายแร่ควอตซ์ ± คาร์บอเนต – แร่ซัลไฟด์ – อีเล็กตรัม (Quartz ± carbonate – sulfides – electrum veins) และ 3) สายแร่ควอตซ์ ± คาร์บอนเนต (Quartz ± carbonate veins) มีระยะหลักที่พบทองประกอบด้วยแร่ ควอตซ์ และ แคลไซต์ โดยที่แร่ซัลไฟด์นั้น มีไพไรต์เป็นแร่หลัก และพบสฟาเลอไรต์เป็นแร่รอง ทองคำมีสองลักษณะคือ เป็นมลทินในไพไรต์ และเป็นแร่อิสระ อยู่กับควอตซ์ และ แคลไซต์ ซึ่งเกิดในรูปแบบของอีเล็กตรัมจากการศึกษาด้วยเครื่อง EPMA ซึ่งมีค่าความบริสุทธิ์ของทอง (Fineness) อยู่ในช่วง 595 ถึง 632 และการศึกษาการแปรเปลี่ยน โดยศึกษาศิลาวรรณา และXRD พบว่าสามารถแบ่งการแปรเปลี่ยน (Alteration) ได้ทั้งหมด 3 ชนิดคือ 1. บริเวณควอตซ์-อะดูลาเรีย (Quartz-Adularia zone) 2. บริเวณอะดูลาเรีย-เซอรีไซต์-อีลไลต์-ควอตซ์±แคลไซต์ (Adularia-Sericite-Illite-Quartz±Calcite zone) 3.บริเวณเซอรีไซต์-อีลไลต์±คลอไลต์±แคลไซต์±อะดูลาเรีย±ควอตซ์ (Sericite-Illite±Chlorite±Calcite±Adularia±Quartz) โดยการเกิดแร่ของพื้นที่สำรวจบีนั้นเป็นชนิดแหล่งแร่อีพิเทอร์มอลอุณหภูมิต่ำแต่มีความแตกแตกจากชาตรีเนื่องจากมีแร่องค์ประกอบน้อยกว่า

คำสำคัญ: แหล่งแร่ชนิดอีพิเทอร์มอลอุณหภูมิต่ำ ระยะการเกิดแร่ อีเล็กตรัม ความบุริสุทธิของทอง

ACKNOWLEDGEMENTS

Department of Geology, Faculty of Science, Chulalongkorn University provided a partial funding for this study. I honestly thank my Advisor, Dr. Abhisit Salam of Chulalongkorn University for his supports, valuable ideas, encouragements, critically advises and reviews of this research. And I would also like to thank Ms. Sopit Pumpuang, Mr. Prachin Thongprachum and Mr. Suriya Chokmor for technical support.

Furthermore, I am appreciated to Akara Mining to provide me a necessary data and to study a drill cores and collecting samples.

I would also like to thank Mr. Tanad Soisa, Mr. Smith Leknettip and Mr. Sigawat Sriprapaporn for great teamwork and all supporting.

Finally, I thank my family and my classmate, Geo'58 for their support and encouragement throughout this time of hardship.

Contents

Contents

List of figures

List of tables

Chapter 1

Introduction

1.1 Background and rationale

Gold, silver, and copper are important for world economy. In Thailand, gold and silver deposits are mainly found in the Loei Fold Belt (Salam, et al., 2014) for instance Phu Thap Fah (Au skarn deposit) in Loei, Chatree (Au-Ag epithermal deposit) in Phichit-Phetchabun province. In addition, some small deposits include Khao Phanom Pha (Au skarn deposit) in Phichit and Khao Lek (Fe-Cu skarn) in Nakhon Sawan, central Thailand. Another small Au skarn deposit knows as French mine is located in Prachinburi eastern Thailand (Khin Zaw, 2007).

Chatree Au-Ag epithermal low sulfidation deposit locates at Phitchit-Phetchabun province, is considered as the biggest Au deposit in Thailand. It is about 3 km northwest of B-prospect. The Chatree deposit has been studied intensively by Salam (2013) on volcanic facies and architecture of the host volcanic sequence, petrochemistry of volcanic and its associated plutonic rocks, description of mineralization and mineralogy of mineralization and alteration, stable and radiogenic isotopes. Other aspects of study include fluid inclusions and trace element geochemistry in pyrite.

B-prospect which is considered as the one of the Chatree's settle-light deposits within the radius of 15 to 20 km (Salam, 2013) has not been any study in the past except unpublish Company reports. This prospect is located on the same structure (NNW-SSE trending fault) as Chatree deposit which has extensed at least about 15 kilometers (Salam, 2013). In this study, details geology, mineralization and alteration will be undertaken. Additional focus will also be given on study of minerals chemistry particularly gold fineness and sphalerite composition.

1.2 Objective

1) Geological characteristics of rock in the study area

2) Mineralization and alteration of the study area

1.3 Scope of this study

This study will be focused on stratigraphy of host volcanic rocks, mineralization and alteration of B-prospect. Due to limitation of diamond drill cores in this prospect and most of the cross section has limited diamond drill holes, section number 1800085N was selected for this study. This section consists 3 diamond drill holes namely, hole number 4562DD, 4564DD and 4576DD. Detailed drill core logging focusing on rock types, mineralization and alteration has been undertaken. All total 50 samples have been collected including rock type samples, vein sample and altered rock sample for further laboratory study (thin-sections, polish thin/mount and powdered sample).

1.4 Study area

The B-prospect is located in Thap Khlo district, Phichit Province about 3 kilometers southeast of Chatree deposit. In topographic map, scales 1:50000, the study area is located in between 1798500 to 1800000nN; 678000 to 679000nE.

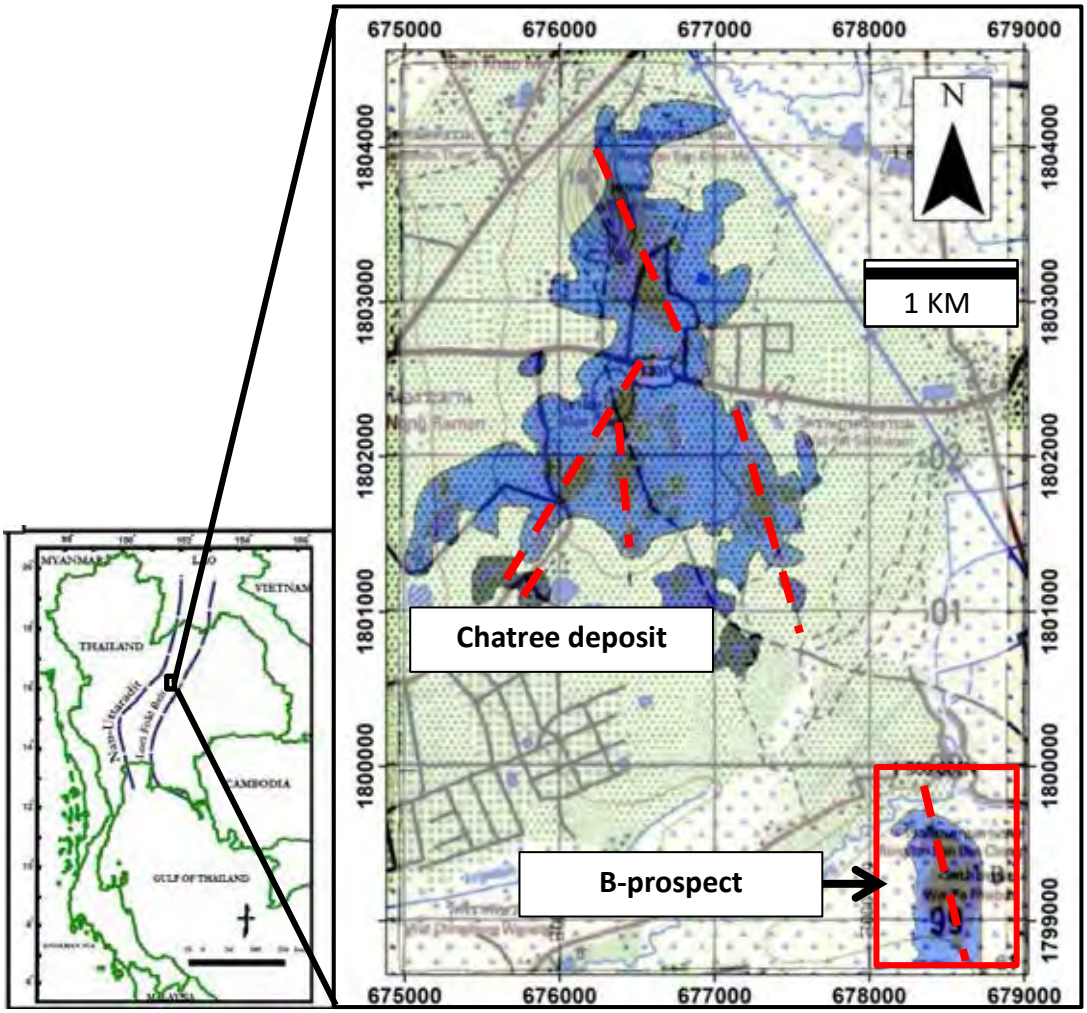

Fig. 1.1 Topographic map showing B-prospect locates southeast of Chatree deposit about 3 kilometers and the mineralization is confined to the same structure (fault) as the Chatree deposit (NNW-SSE) (Kromkhun, 2005)

Fig. 1.2 Google earth's map showing location of drill holes drill hole (number 4562DD, 4564DD and 4576DD) in section 1800085N (Google earth).

1.5 Outcome of study

1) Characteristics of rock units of B prospect

2) Characteristics of mineralization and alteration of B prospect

1.6 Theory and previous work

Geology and volcanic stratigraphy

Salam (2013) studied stratigraphy and volcanics facies of the Chatree deposit which is located in the Loei Fold Belt (LFB) extending from Lao DPR through Loei to Phichit-Phetchabun in central Thailand to Cambodia. The host volcanic rock of Chatree deposit has composition ranging from basaltic andesite to rhyolite represented by volcaniclastic and volcanogenic-sediment rocks of Late Permo-Early Triassic age (Salam et al., 2014). The stratigraphy of Chatree deposit can be divided into 4 units which include Fiamme breccia unit (Unit 1), Volcanogenic sedimentary unit (Unit 2), Polymictic mafic-intermediate breccia unit (Unit 3) and Porphyritic andesite unit (Unit 4).

Salam et al. (2014) studied petrochemistry and geochronology of host volcanics of the Chatree deposit. The result shows age of volcanic sequence (Host rock) is Late Permian-Early Triassic (258-240 Ma) and the Chatree volcanics was erupted in continental arc setting.

Mineralization

Salam et al. (2008) studied paragenesis sequence of Chatree deposit and divided into 7 stages. In several stages, pyrite is the most abundant sulfide minerals. Minor sulfide minerals are sphalerite, galena and chalcopyrite. Gold has been identified in Stage 4, usually forms as electrum and commonly associated with sulfide minerals specially pyrite. Summary of paragenesis stages are given below:

Pre Au-Ag mineralization stage

- Stage 1: microcrystalline quartz + pyrite
- Stage 2: Quartz-chlorite-sericite-pyrite
    - Stage 2A: Quartz-chlorite-sericite-pyrite

- Stage 2B: Quartz-sericite-+-chlorite-chalcopyrite-pyrite-sphalerite +-galena

- Stage 3: Quartz-carbonate-(K-feldspar) +-carbonate+-sulfide

Main Au-Ag stage

- Stage 4: Quartz + carbonate + chlorite + adularia + sulfide + electrum
  - Stage 4A: Quartz + carbonate + chlorite + adularia + sulfide-electrum
  - Stage 4B: Quartz +- carbonate –adularia-sulfide-electrum
  - Stage 4C: Carbonate+-quartz-adularia-sulfide-electrum-argentite-tetrahedrite

Post mineralization

- Stage 5: Quartz +- carbonate veins
- Stage 6: Quartz +- carbonate veins/veinlets
- Stage 7: Quartz-zeolite-carbonate

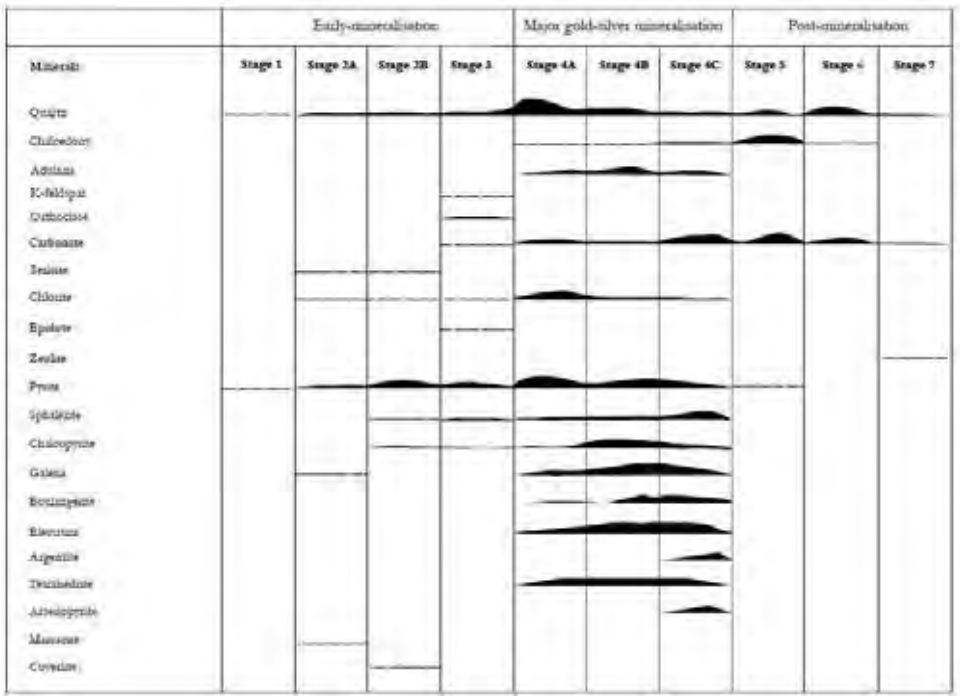

Fig. 1.3 Paragenesis sequence of Chatree deposit after Salam (2013)

Tangwattananukul et al. (2014) studied paragenesis sequence of Q-prospect and divided it into 5 stages in which electrum occurs in stage 1 and 4.

- Stage 1: Dark-grey quartz veins and veinlets consisting dominantly of microcrystalline quartz with small amounts of illite, calcite, adularia, pyrite, electrum, chalcopyrite and sphalerite.
- Stage 2: Quartz veins and veinlets consist chiefly of quartz with small amounts of calcite, illite, adularia, pyrite and chalcopyrite.
- Stage 3: Quartz veins and veinlets associated with trace amounts of calcite, adularia, illite, chlorite, pyrite and electrum.
- Stage 4: Quartz-calcite veins and stockworks consist mainly of quartz and calcite with a small amount of illite and lesser amounts of chlorite, adularia and laumontite in this stage. Large amounts (compared with those in the other stages) of ore minerals such as pyrite, sphalerite, chalcopyrite and electrum were precipitated in this stage.
- Stage 5: Greenish fine-grained quartz consists of a large amounts of quartz and small amounts of adularia, calcite and pyrite.

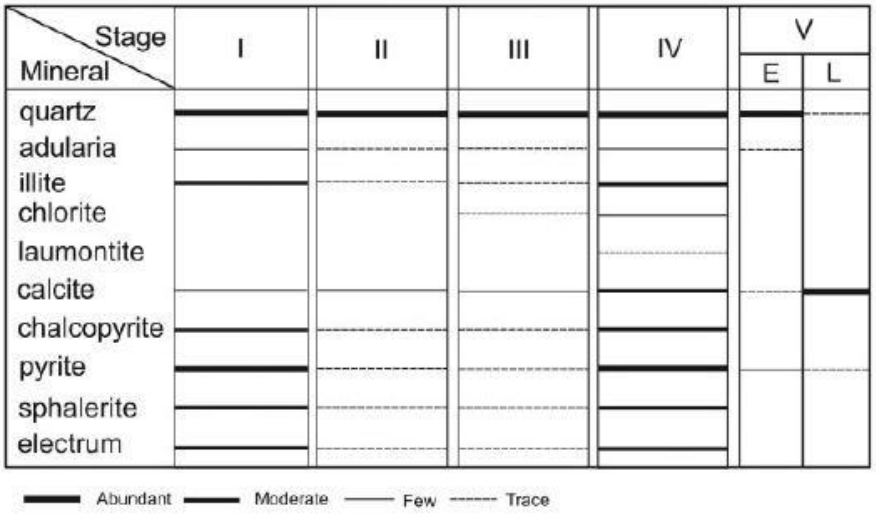

Fig. 1.4 Paragenesis sequence of Q prospect

Alteration

Salam et al. (2008) studied hydrothermal alteration by petrography and short wavelength infrared (SWIR) spectral analysis methods with extensive staining for adularia on drill cores. The alteration can be divided into 4 types.

- Silicic alteration is confined to the ore zones. K-feldspar staining of volcanic breccia, epiclastic sedimentary rocks show abundant adularia associated with quartz, illite and pyrite in this alteration zone.
- Argillic alteration is not common but highly focused, particularly in the fiamme breccia unit at the hanging wall to the H orebody.
- Phyllic alteration is widespread at the Chatree deposit and occurs in a large halo enveloping the silicic alteration zones. The mineralogy of this alteration style is characterized by illite, adularia, quartz, chlorite and pyrite.
- Propylitic alteration is distal to the ore zones and almost no adularia is present. The alteration assemblage comprises chlorite (Fe-chlorite and Mg-chlorite), calcite, epidote and pyrite.

Sangsiri (2008) studied the alteration of A prospect. The results show the alteration zone of host rock that proximal to ore zones are dominated by silicification, quartz-adularia alteration, followed by carbonates and finally Fe-sulfide-Fe-Ti-oxide-sphene/leucoxene assemblages. The alteration zone of host rock that distal from ore zones are dominated by propylitic alteration assemblage e.g. chlorite/serpentine and/or Fe-Ti oxides.

Isotope

Salam et al. (2008) studied oxygen isotope of Chatree deposit that mainly focuses on quartz vein that is Au-Ag bearing mineralization (Stage 2) and some quartz +- calcite veins of late stage 4. The oxygen isotope result of Au-Ag bearing quartz (stage 2) is 8.1 to 12.3 ‰ that is lowest values of general deeper occurrence level (140 m below the surface). In the other hand, the oxygen isotope results of stage 4 tend to higher values that are 11.9 to 12.0 ‰. The results of calculated oxygen isotope composition of the Chatree ore fluid have ranging between -1 to 6 ‰ that overlaps with the both meteoric and magmatic compositions. This shift in the result may relate to process such as water rock-interaction and/or mixing of meteoric and magmatic fluids. Mixing of magmatic fluids with lower temperature meteoric water is the cause of the lower oxygen isotope in the center of the main mineralization zone and higher in the rim of this zone.

Tangwattananukul et al. (2014) studied oxygen isotope of Q prospect by F_2-technique. The studying focuses on each stage of quartz veins and is determined by a mass spectrometer. The result of oxygen isotope shows the oxygen isotope value of quartz in stage 1 to 4 range from +10.4 to +11.6 ‰, except the values of stage 4 (+15.0‰). The increasing of oxygen isotope values of quartz in stage 4 can explain veins are precipitated by boiling. The boiling is processes to precipitate of veins. The temperature during quartz forming is approximately 200°C based on the mineral assemblage. The temperature of the hydrothermal solution prior to boiling is thought to be higher than 200°C. Thus, oxygen isotope of stage 4 is increase.

Texture of quartz

Tangwattananukul et al. (2014) studied texture of quartz each mineralized stage of Q prospect. The textures in each stage are different that shows the different composition of vein.

- Stage 1: Banded and brecciated structures are dominated. Microcrystalline quartz is intimately associated with a large amount of pyrite and with small amounts of chalcopyrite, sphalerite and electrum.
- Stage 2: Quartz in this stage is characterized by a banded structure and comb texture is dominated.
- Stage 3: Banded structure is common. The texture of quartz is characterized by chalcedonic and mosaic textures. Small amounts of pyrite and electrum were precipitated on the mosaic texture in this stage.
- Stage 4: Brecciated structure is common. The quartz is characterized by flamboyant and comb textures. Flamboyant and comb textures were formed in the early and late parts of this stage, respectively.
- Stage 5: Banded structure is composed of fine-grained quartz showing a mosaic texture.

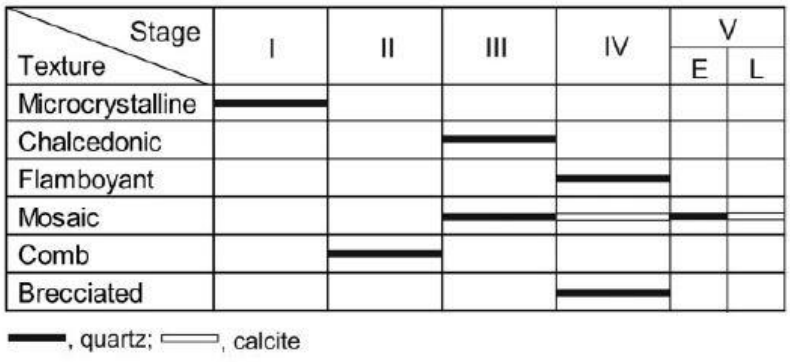

Fig. 1.5 Quartz textures and calcite texture in each stage.

Other deposit in Loei Fold Belt

Paipana (2014) studied Bo Thong deposit in eastern Thailand which is located on the northwestern edge of Chantaburi Terrane. This deposit is identified as antimony-fluorite-gold mineralization which occurs as veins/veinlets and minor breccia. The host rock is volcaniclastics and volcanogenic-sedimentary rocks. The volcaniclastic rocks are intermediate to felsic compositions which is intruded by a syenite intrusion. The host rocks and intrusive body are cut by basalt porphyry dykes. At Bo Thong, the mineralization is characterized by fracture filling hydrothermal veins and associated with breccia. The veins can be divided into 5 stages in which Stages 2, 3 and 4 are major mineralization stages. Based on mineral assemblages, alteration, fluid inclusion and sulphur isotope data the study suggested that the deposit has achateristics of an epithermal deposit.

de Little (2005) studied Wang Yai prospect locates in Wang Pong district, central Thailand. The prospect has been investigated in term of vein textures, mineralogy, fluid inclusions and stable isotopes. The vein systems can be divided into 2 types; mineralized veins and poorly mineralized veins. The mineralized veins are characterized by quartz-chalcedony-calcite ± adularia and poorly mineralized vein are characterized by chalcedony and opaline quartz. The host rocks are volcanic and volcanogenic-sedimentary units intruded by andesite and diorite. The age of host rock is Late-Permian to Early Triassic. Based on vein textures, mineralogy and alteration assemblages the mineralization at Wang Pong is comparable with the nearby Chatree low-sulfidation epithermal deposit. The Wang Yai prospects is likely to be the top of the broader epithermal system and therefore potential for high grade mineralization at depth exists.

Chapter 2

Geological tectonic setting

2.1 Tectonic setting

Thailand is composed of two major terranes in which Indochina terranes is on the east and Shan-Thai on the west. The two terranes are separated by Sukhothai Arc or Sukhothai Fold Belt (SFB) on the western side and Loei Fold Belt (LFB) on the eastern side (Bunopas, 1981; Fig. 2.1). The subduction of Shan-Thai under Indochina give rise to the emplacement of Late Permian-Early Triassic magmatism in both Sukhothai Arc and LFB and the collision of Shan-Thai with Indochina during middle Triassic maked by the closer of Paleotethys that lied between two terranes. As the result of the subduction, magmatism that emplaced along the Loie Fold Belt were responsible for major Au, Ag, Cu and Fe mineralization particularly in the LFB extending from Lao DPR to Loei (northeastern Thaialnd) through to Phichit-Phetchabun in central Thailand and Prachinburi in Eastern Thailand. This belt composes of tholeiite and calc-alkaline volcanics, volcaniclastic rocks and volanogenic-sedimentary rocks and minor intrusive rocks. Volcanic rock of the belt is felsic to mafic rocks of Late Permian-Triassic and subsequently followed by middle Triassic mostly occur as dykes. (Fig. 2.1)

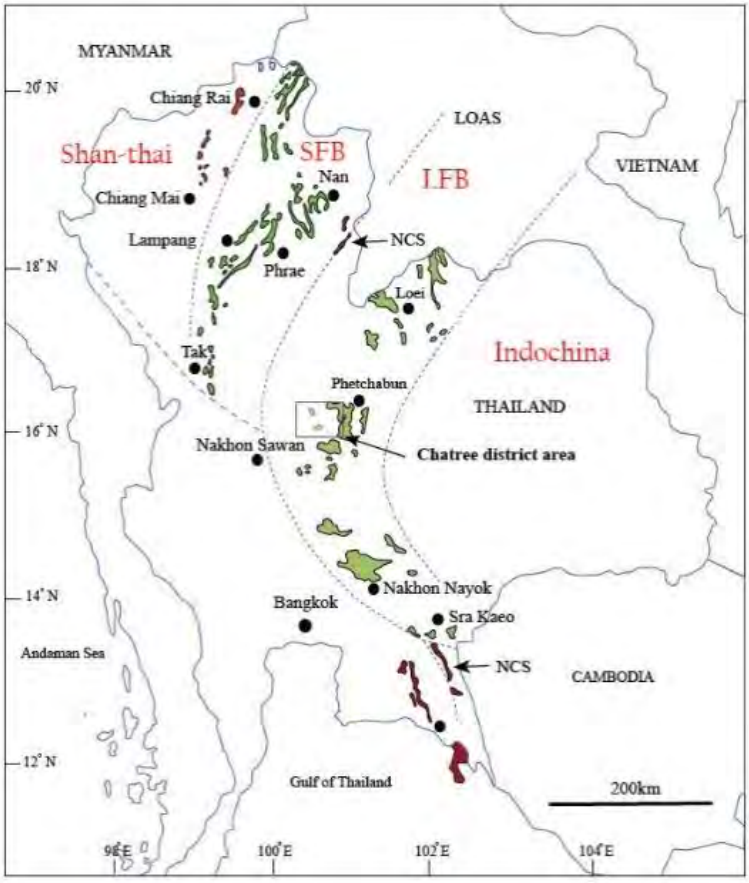

Fig. 2.1 Map of Thailand showing tectonic Shan-Thai terrane, Sukhothai Fold Belt, Loei Fold Belt and Indochina terrane from east to west respectively. (after Panjasawatwong et al., 1997, 2008).

2.2 Regional geology

The Chatree deposit covers areas of Thap Klo, Wang Sai Phun (Phichit Province), Chon Deang and Wang Pong (Phetchabun Province) and a part of Noen Maprang district (Phitsanulok Province). This section is focused on the main rock units in the area with emphasis on volcanic and plutonic units. (Fig. 2.2).

2.2.1 Carboniferous rocks.

The Carboniferous rock comprise of volcanogenic rhyolitic siltstone, sandstone, chert and minor limestone. The Carboniferous unit in this area was classified into dominant unit of Wang Sapung Formation. The limestone crops out at Dong Khui sub-district, whereas the volcanic and sedimentary rocks are widespread throughout the area (Fig. 2.2). The Carboniferous rocks are dominated by volcanogenic sedimentary rocks and limestone in the Chatree District. The sedimentary rocks mainly are laminated siltstone, sandstone, minor conglomerate and limestone. The rocks are widely distributed in the eastern part of the area from east of Dong Khui to Wang Pong, and have a strike of northwest-southeast. The volcanogenic siltstone and sandstone crop out locally at a cut-back near the town of Wang Pong and along Chon Daen-Wang Pong road. The sequences are composed of alternate siltstone (clay-rich) and siliceous beds.

2.2.2 Middle Permian limestone (Ratchaburi Group)

Middle Permian limestone overlies Carboniferous sedimentary rocks marked by basaltic conglomerate, and sandstone at the south-east of Wang Pong Township. The unit is known as Noen Maprang limestone of Saraburi Group (DMR, 1974). It is named after the place called “Noen Maprang District” north of the Wang Pong District. This unit consists of massive to thick-bedded, fossiliferous limestone (Crossing, 2004) interbedded with thin shale, siltstone and chert.

2.2.3 Late Permian volcanic rocks

The Late Permian volcanic rocks in the Chatree District have been described as Permo-Triassic volcanic/volcaniclastic rocks with a composition ranging from andesitic to rhyolitic, and characterized by andesite flows, breccia and rhyolite lava and breccia. In general, Late Permian volcanic rocks are characterized by basalt to andesite in the lower parts and by felsic compositions at the upper parts. Basaltic to andesitic rocks are commonly observed in the southern part of Chatree area but Rhyolitic rocks are abundant in the northern part of the area especially at Khao Keaw and east of Khao Sai which are stratigraphically equivalent to the upper part of the Late Permian. Most of middle Triassic rocks occur as dyke and sill (Salam 2013). Based on petrography, geochronology and geochemistry several distinct suites of dyke and sill have been recognized (e.g., Khin Zaw et al., 2007; Salam et al., 2014).

Andesite dyke

Dykes and sills are common in the Chatree deposit. They are andesite to basaltic andesite in composition and dark green in color. Most dykes cross-cut gold-silver bearing quartz-carbonate veins. At D lens, basaltic dyke contains diorite xenoliths which was dated using LA-ICPMS zircon U-Pb method and yields 238 ± 6 Ma (Khin Zaw et al., 2007). An andesitic dyke collected from east of Chatree also was dated in this study at 247.1 ± 5.1 Ma using the LA-ICPMS zircon U-Pb age method (Salam, 2013).

2.2.4 Plutonic rock

Plutonic rocks are poorly exposed in the Chatree district. However, small isolated outcrops of plutonic rocks can be observed east of Wong Pong District which may be called Wang Pong granite (Salam et al., 2014).). Other areas that identified the plutonic rocks are Dong Khui (Chon Daeng district), Khao Rub Chang (near Phichit township), Khao Chet Lok (10 km west of Chatree mine), N-prospect (1 km south of Chatree mine) and Singto (south of Wang Pong township).

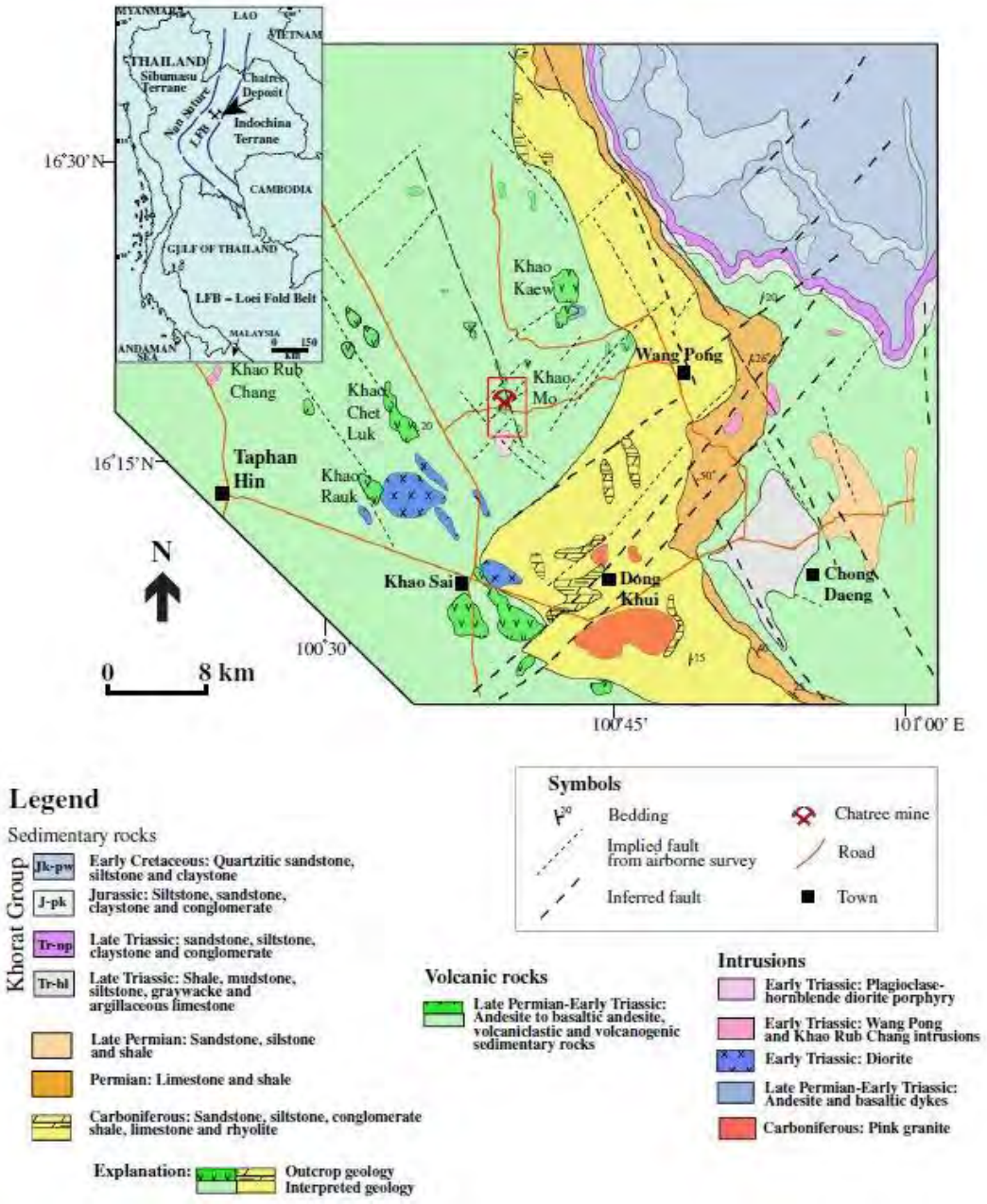

Fig. 2.2 Geological map of the Chatree District compiled by Salam (2013) based on map scale 1: 250000 of DMR (1976), subsurface RAB information from (Akara Mining Ltd). and new information of Salam (2013)

2.3 Rock units in Chatree deposit

Chatree deposit is located in Loei Fold Belt (LFB) which is associated with Late Permian-Early Triassic volcaniclastics and volcanogenic-sedimentary rocks. The Chatree deposit is dominated by two major faults namely, NNW-SSE and NE-SW faults. Mineralizations are confined to these two major faults which are represented by several ore lenses (Fig. 2.3).

Salam (2013) identified stratigraphy units of Chatree deposit into 4 units namely, Fiamme breccia unit (Unit 1), Volcanogenic sedimentary unit (Unit 2), Mafic-intermediate polymictic breccia unit (Unit 3) and Porphyritic andesite unit (Unit 4). (Fig. 2.4)

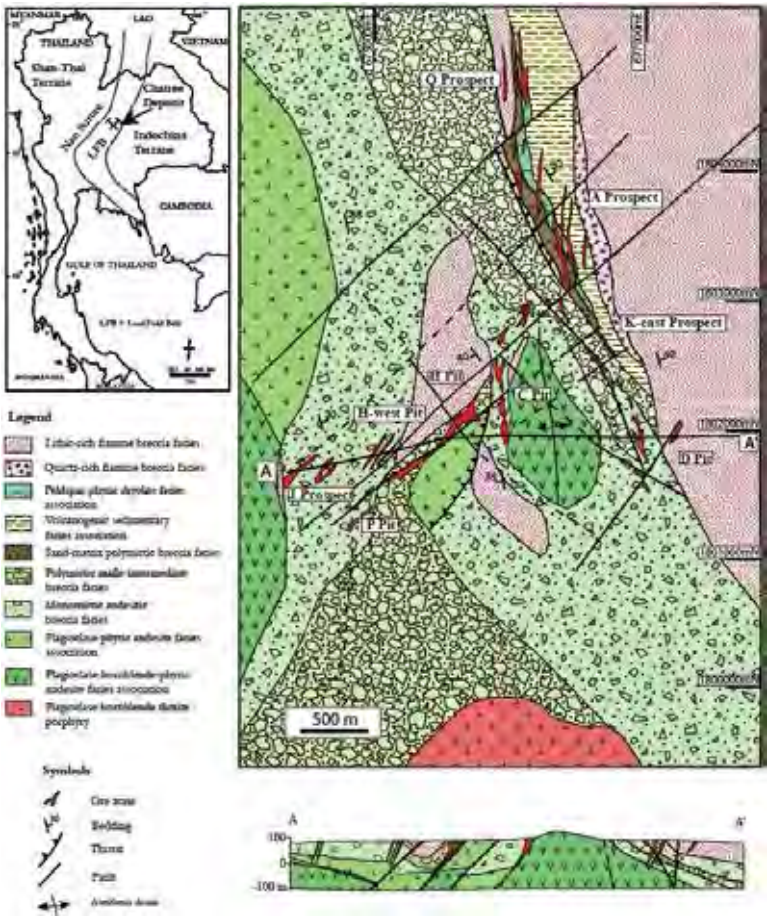

Fig. 2.3 Geological map of the Chatree deposit showing the relations among volcanic facies associations and ore lens

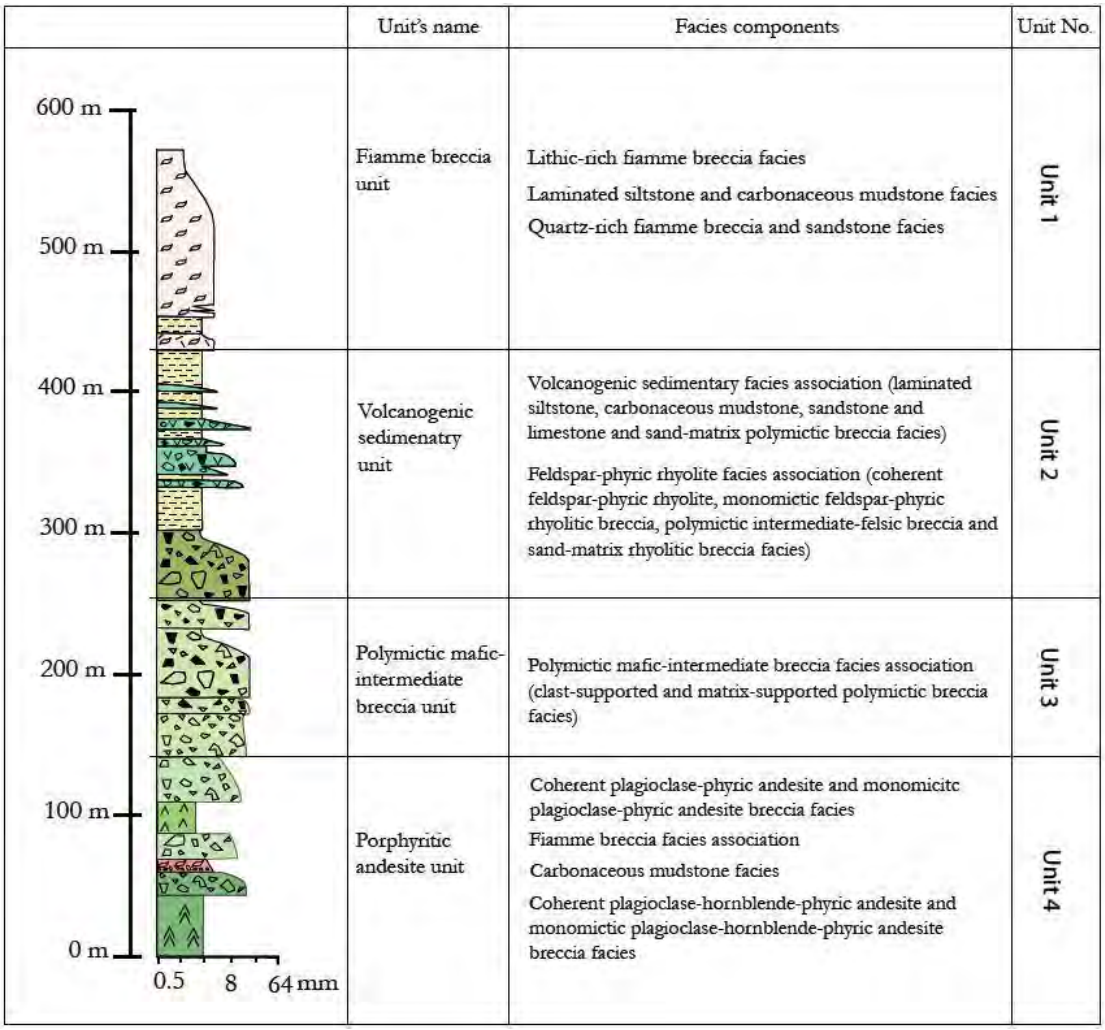

Fig. 2.4 Stratigraphy of Chatree deposit after Salam (2013).

Unit 1 Fiamme breccia unit

This unit includes lithic-rich fiamme breccia, laminated siltstone, carbonaceous mudstone, quartz-rich fiamme breccia and sandstone

Unit 2 Volcanogenic sedimentary unit

Unit 2 mainly consists of volcanogenic-sedimentary rocks that includes laminated siltstone, carbonaceous mudstone, sandstone and limestone and sand-matrix polymictic breccia

In addition, the unit includes feldspar-phyric rhyolite (coherent feldspar-phyric rhyolite, meromictic feldspar-phyric rhyolitic breccia, polymictic intermediate-felsic breccia and sand-matrix rhyolitic breccia)

Unit 3 Polymictic mafic-intermediate breccia unit

The unit consists of polymictic mafic-intermediate breccia that includes clast-supported and metrix-supported polymictic breccia

Unit 4 Porphyritic andesite

The unit consists of coherent plagioclase-phyric andesite and monomictic plagioclase-phyric andesite breccia, fiamme breccia, carbonaceous mudstone, coherent plagioclase-hornblende-phyric andesite and meromictic plagioclase-hornblende-phyric andesite breccia.

Chapter 3

Methodology

3.1 Studying general data and literature reviews

3.1.1 General geology of study area

3.1.2 Literature review and related work

3.1.3 Laboratory process

3.2 Field work

3.2.1 Diamond drill core logging

Logging the drill holes number 4562DD, 4564DD and 4576DD and create cross-section by logs correlation

3.2.2 Samples collecting

Representing to rock unit, mineralization and alteration

3.3 Laboratory work

3.3.1 Rock units

This process uses the polarized light microscope to study mineral assemblages and textures of host rock from thin section

3.3.2 Mineralization

Establishing paragenesis sequence of the deposit using cross-cutting relationship, mineral assemblages and textures. Reflected light microscope was used to study opaque minerals such as pyrite, chalcopyrite and electrum using polished mount and polished thin section. Electron Probe Micro Analysis (EPMA) is used to conform unidentified sulfide minerals and composition of some minerals such as electrum and sphalerite.

3.3.3 Hydrothermal alteration of host rocks

This part studies assemblages of altered mineral and textures of the wallrocks at proximal to distal from the veins or ore zones. This study was based on petrographic invistigation and X-Ray Diffractometion (XRD).

3.4 Data analysis

3.4.1 Rock units

3.4.2 Mineralization

3.4.3 Alteration

3.5 Discussion and conclusion

3.6 Presentation and book preparation

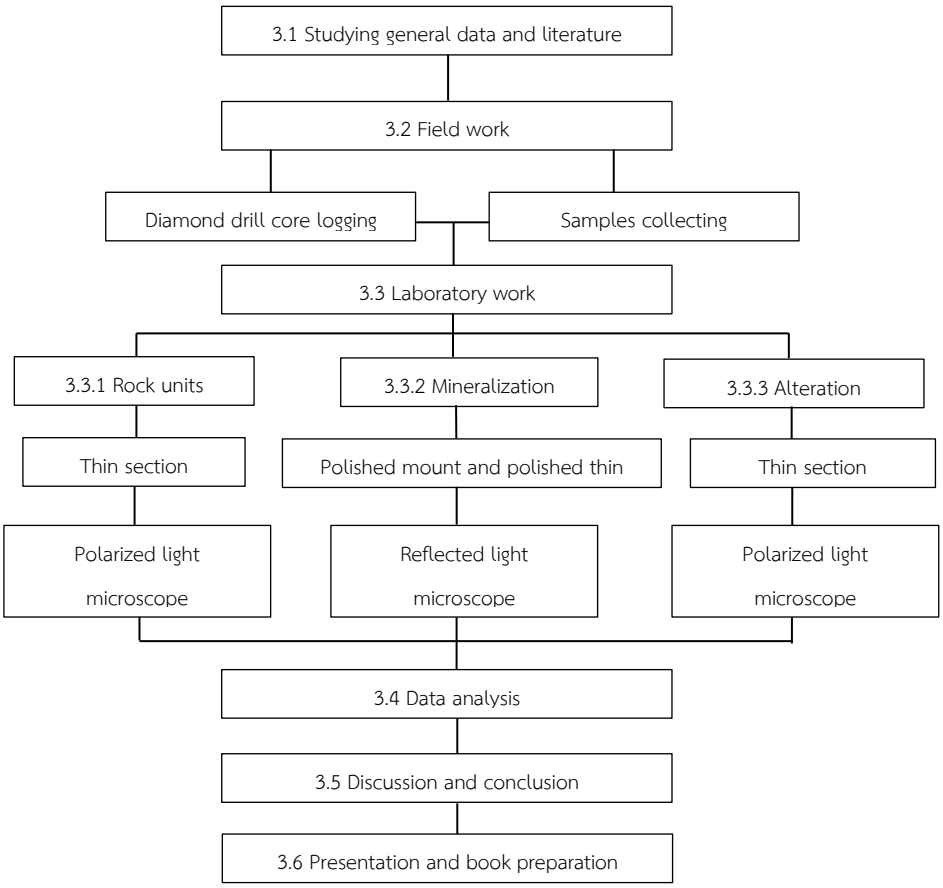

Fig. 3.1 flow chart of methodology showing field work and laboratory work

3.2 Field work

3.2.1 Diamond drill core logging

Study is focused on section 1800085N that has enough and located along the center of the ore zone. This EW section has 3 diamond drill holes namely, hole no. 4562DD, 4564DD and 4576DD (Fig. 3.2).

Fig. 3.2 Location of section 1800085N including drill hole number 4562DD, 4564DD and 4576DD

Stratigraphic logging that emphasize on 3 objectives; lithology, mineralization and alteration. After that, correlate 3 drill core logs to make the cross-sections of section 1800085N of B-prospect. The cross-sections are 3 types that are rock unit, mineralization zone and alteration zone.

3.2.2 Samples collecting

The samples are collected in 3 mainly objectives. First is collecting for study mineral assemblages under polarized light microscope to classify rock types and characterize rock units. Second step is veins collecting to study mineralization and paragenesis sequence. Third is samples collecting of alteration zone which focus on strong silicified rock, moderated silicified rock and weak silicified rock.

Table 3.1 Samples for laboratory preparing

Drill hole number	Sample number	Objectives		
		Rock units	Mineralization	Alteration
4562DD	4562-12.5	✓		
	4562-49.9	✓		
	4562-62.3	✓		
	4562-79.6		✓	
	4562-79.9	✓		✓
	4562-90.0	✓		
	4562-104.4	✓		
	4562-114.0	✓		✓
	4562-115.0	✓		
	4562-119.0	✓		✓
	4562-122.3	✓		✓
	4562-138.2	✓		
	4562-200.65	✓		
	4562-224.3	✓		
	4562-238.9	✓		✓
	4562-255.5	✓		
	4562-270.5	✓		

4564DD	4564-12.2	✓		
	4564-21.5		✓	
	4564-50.0		✓	
	4562-128.6		✓	
	4564-193.5	✓		✓
4576DD	4576-21.2	✓		✓
	4576-44.1	✓		✓
	4576-62.4	✓		
	4576-97.8	✓		✓
	4576-129.3	✓		✓
	4576-141.0	✓		

3.3 Laboratory work

3.3.1 Rock units

Thin sections of representative rock samples are prepared for petrographic study (e.g., mineral assemblage, and textures). These selected samples are also represented rock types identified in B-prospect. Total 24 samples have been prepared for thin sections to study petrography under polarized light microscope and X-Ray Diffractometer (XRD) respectively.

Thin sections preparation

Step one is cutting a slab. A suitable size slab for mounting on a slide is cut from a piece of rock or drill core with a diamond saw. After takes photos, cut into glass slide size. Next is added glass slide. After drying on a hot plate, a glass slide is glued to the lapped face of the slab with balsam. Then polish the slap to close the glass. Using a thin section polish, the slab is cut-off close to the slide. The thickness is further reduced on a thin section grinder. Finally, A finished thickness of 30 microns is achieved by lapping the section by hand on a glass plate with 600 grit and a fine grinding with 1000 grit.

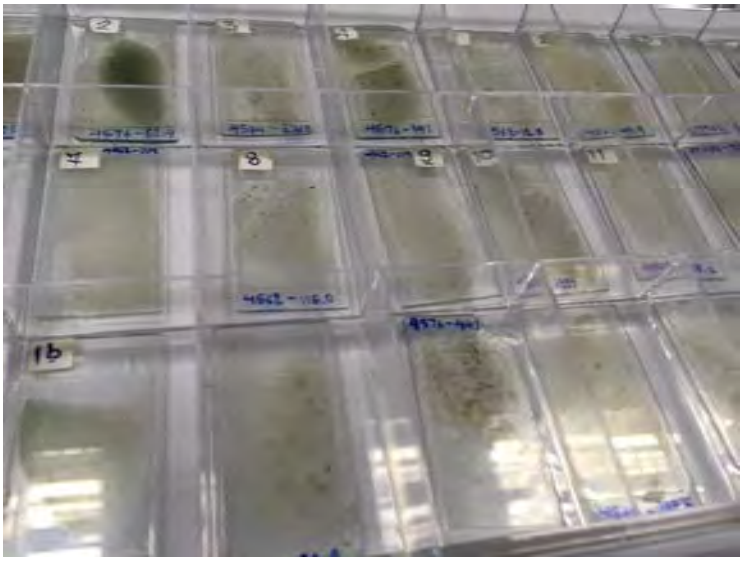

Fig. 3.3 thin sections

Studying of rock units

Thin section samples are studied minerals assemblage and textures by polarized light microscope.

3.3.2 Mineralization

Mineralization study, veins samples were selected for polished mounts and polished thin sections prepaaration. Both type of prepared samples (polished mount and polished thin sections) then use for petrographic study of opaque mineral under reflected light microscope. Moreover, polished thin sections are also used to study the relationship between opaque minerals (sulfide minerals). All together 6 samples have been prepared for polished mounts and polished thin sections.

Polished mount preparing

First, bring veins samples that expect to have sulfide minerals to cut and put in mounts. After that, pour the epoxy (Resin) into the mount and use desiccator to make vacuum condition. Gas will leave out from the sample. When all gas in the samples is gone, leave the sample in the room temperature and wait about 8 hours, epoxy will be setting. Then, bring sample out from the mounts. Next, polish the sample by polishing powder size 600 and 1000 girt respectively until the samples are flat. Finally, polish the sample with Grinding-polishing (Fig. 3.4) at 6,3 and 1 micron respectively until the samples are flat and lustrous. (Fig. 3.5)

Fig. 3.4 Grinding polishing machine of 6 μ

Fig. 3.5 Polished mounts

Polished thin section preparing

First, select sulfide lens in quartz vein. Then, prepare same as the thin section and polish the sample with Grinding-polishing at 6,3 and 1 micron respectively until the samples are flat and lustrous.

Studying of mineralization

Polished mounts are studied opaque minerals and ore minerals by reflected light microscope and use Electron Prove Micro Analysis (EPMA) to confirm the mineral type by chemical composition and examine ratio of gold and silver in electrum. For polished thin section is not only studied like the polished mounts but is also studied in relationship between quartz and opaque minerals.

3.3.3 Alteration

For alteration samples use the host rocks that are altered. Observation of color and hardness of rock can guide the alteration zone. Moreover, the intensity of alteration is depended on distance between mineralization zone and this sample. The representing samples are collected in much alteration intensity that can study mineral assemblages and texture to make the alteration zone of cross-section.

This section has 10 samples for thin sections that use to study petrography under polarized light microscope and X-Rays Diffraction (XRD) respectively.

Samples preparing of X-Rays Diffraction (XRD)

First, bring the excess sample from thin section preparing to crush into fine size as powder. Second, compress the sample powder into XRD mount. Then, use XRD to analyze and show the results in graph between 2θ and intensity value. Finally, select mineral that 2θ peak same as the graph and calculate the content of minerals in percent of whole rock

Chapter 4

Results

4.1 Introduction

This chapter describes results of this study which include geology setting (stratigraphy of the host volcanic rocks), mineralization (paragenesis and mineralogy of veins) and hydrothermal alteration and minerals chemistry (sphalerite composition and fineness.

4.2 Geology

This study is based on the observation of drill core logging and petrographic investigation to establish volcanic stratigraphy and represented cross section of the area. The study is based on drill core section number 1800085N consisting three diamond drill cores (e.g., number 4562DD, 4564DD and 4576DD).

4.2.1 Stratigraphy

Terms and classification in this study is based on McPhie et al. (2005) and follows details study of Chatree volcanics by Salam (2013). The identification and interpretation of the rock types are based on detailed logging and thin section examinatoin. The stratigraphy is established on the basis of the geological data collected during this study. Two stratigraphic units (polymictic breccia unit 1 and andesitic breccia unit 4) consist of a single rock type (Figs. 4.1-4.4). The other two units consist of combinations of two or more rock types (volcanogenic-sedimentary unit 2 and fiamme breccia unit 3; Figs. 4.1-4.4). Figure 4.5 shows E-W cross section of B-prospect. Mafic to intermediate units are present at the base and intermediate to felsic units occur at the top of the sequence (Fig. 4.1). The andesitic polymictic breccia unit (bottom unit) has thickness of 50 meters. It is overlain by fiamme breccia unit (Unit 3) with gradational contact. The fiamme breccia unit (Unit 3) consists predominantly of fiamme breccia breccia and polymictic breccia. The contact between these two rock types is gradational contact. The fiamme brecia unit overlain

by volcanogenic-sedimentary unit. This unit is predominantly constituted of carbonaceous siltstone, carbonaceous mudstone and sandy-matrix polymicitc breccis. The relationship between carbonaceous siltstone and mudstone with sand-matrix polymicitc breccia is mostly shape contact but occasionaly gradual contact.

The fiamme breccia unit (Unit 3) consists of fiamme breccia with polymictic breccia. In which polymictic breccia tends to occur at the lower part of the unit. Whereas, fiamme breccia tends to occur in the upper part of the unit. At the middle part of the unit, especially drill hole number 4562DD and 4576DD fiamme breccia is interbedded with polymictic breccia. In addition, thin beds carbonaceous mudstone can be found in drill core number 4564DD. The thickness of unit is estimated about 100 meters. Fiamme breccia at the top of unit have more clasts of mudstone, and siltstone showing a gradational contact with upper volcanogenic sedimentary unit (Unit 2).

The volcanogenic sedimentary unit (Unit 2) consists of siltstone, sandstone, carbonaceous mudstone, and sandy matrix polymictic breccia. The major rock types in this unit are siltstone and carbonaceous mudstone. However, the thickness and composition of this unit are variable for instance sandy- matrix polymictic breccia has been intersected in drill hole number 4562DD but absent in drill hole number 4564DD and 4576DD in the same unit.

Polymictic breccia unit (Unit 1) overlain on volcanogenic-sedimentary unit and has been identified in drill hole number 4562DD and 4564DD but is absent in drill hole number 4576DD. The contact between polymictic breccia unit and underlaying volcanogenic-sedimentary unit is gradational contact. This polymictic breccia unit consists of polymictic breccia which has predominant clasts of plagioclase phyric andesite and minor mudstone clasts.

The volcanics succession at the study area (Fig. 4.5) indicates that the rock units is dipping slightly to the east which is consistence with the regional dipping of

the Chatree volcanics (Salam, 2013). The coherent rock which occurs as dykes have intruded the host volcanic with steep dipping.

These several types of coherent rocks (dykes) have intersected all of drill holes (e.g., 4562DD, 4564DD and 4576DD) and all of them cross cut gold-silver bearing quartz-carbonate veins/veinlets or post dated Au-Ag mineralization (Salam, 2013). The coherent rocks can be divided into 3 rock types: Hornblende-plagioclase phyric andesite that found in top of 4562DD, plagioclase phyric andesite that found in bottom of 4564DD and hornblende phyric andesite (found at the bottom of 4564DD and top of 4576DD). Hornblende phyric andesite in 4564DD and 4576DD can be considered as a dyke.

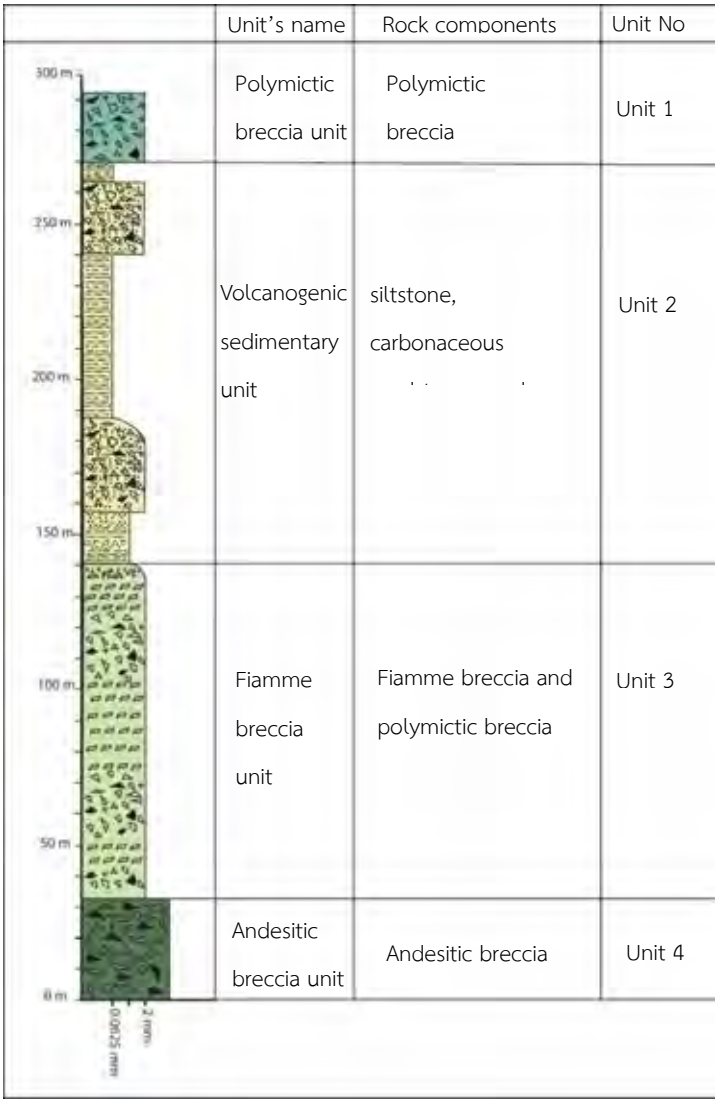

Fig. 4.1 Stratigraphy of the B-prospect, Phichit province.

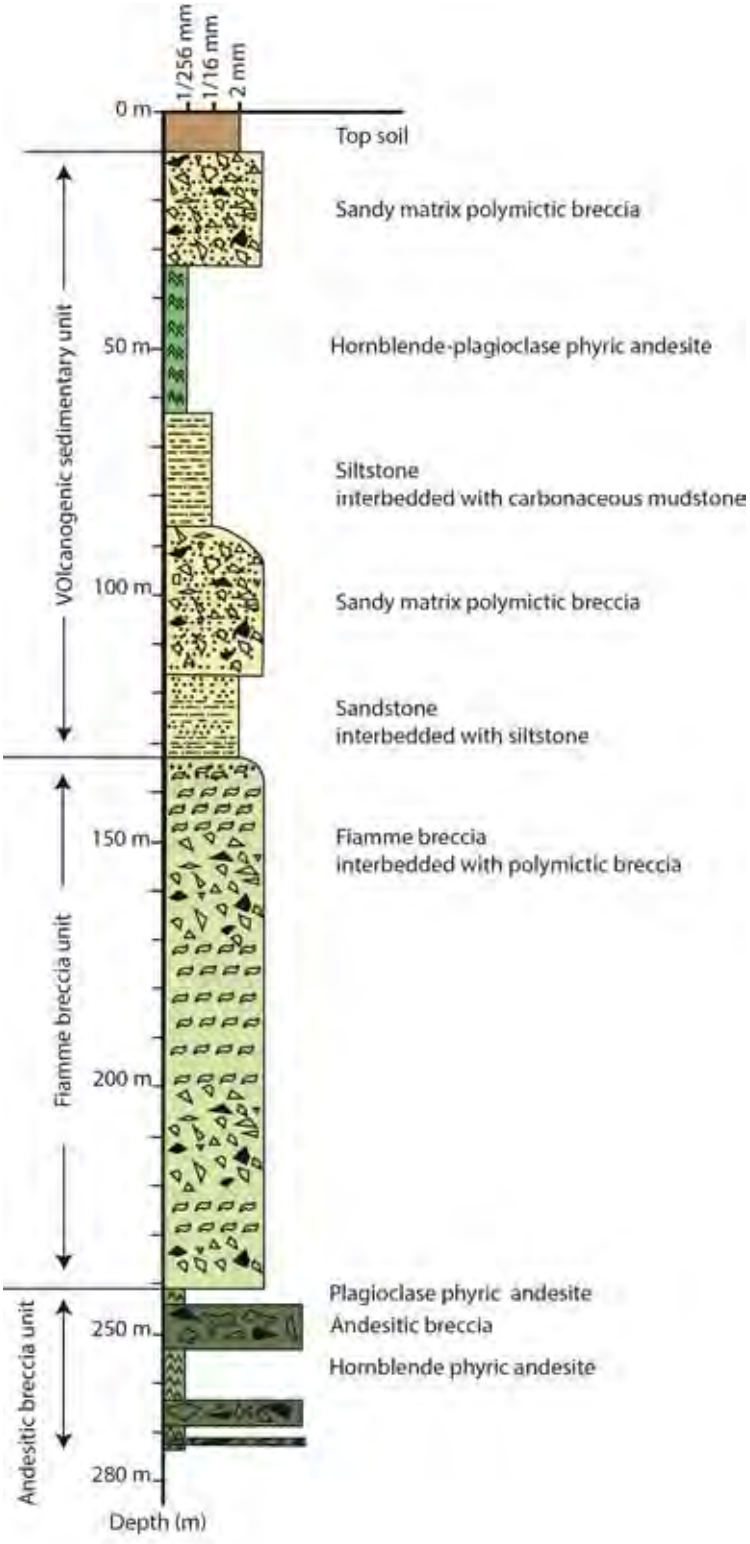

Fig. 4.2 Volcanic stratigraphy of drill hole number 4562DD

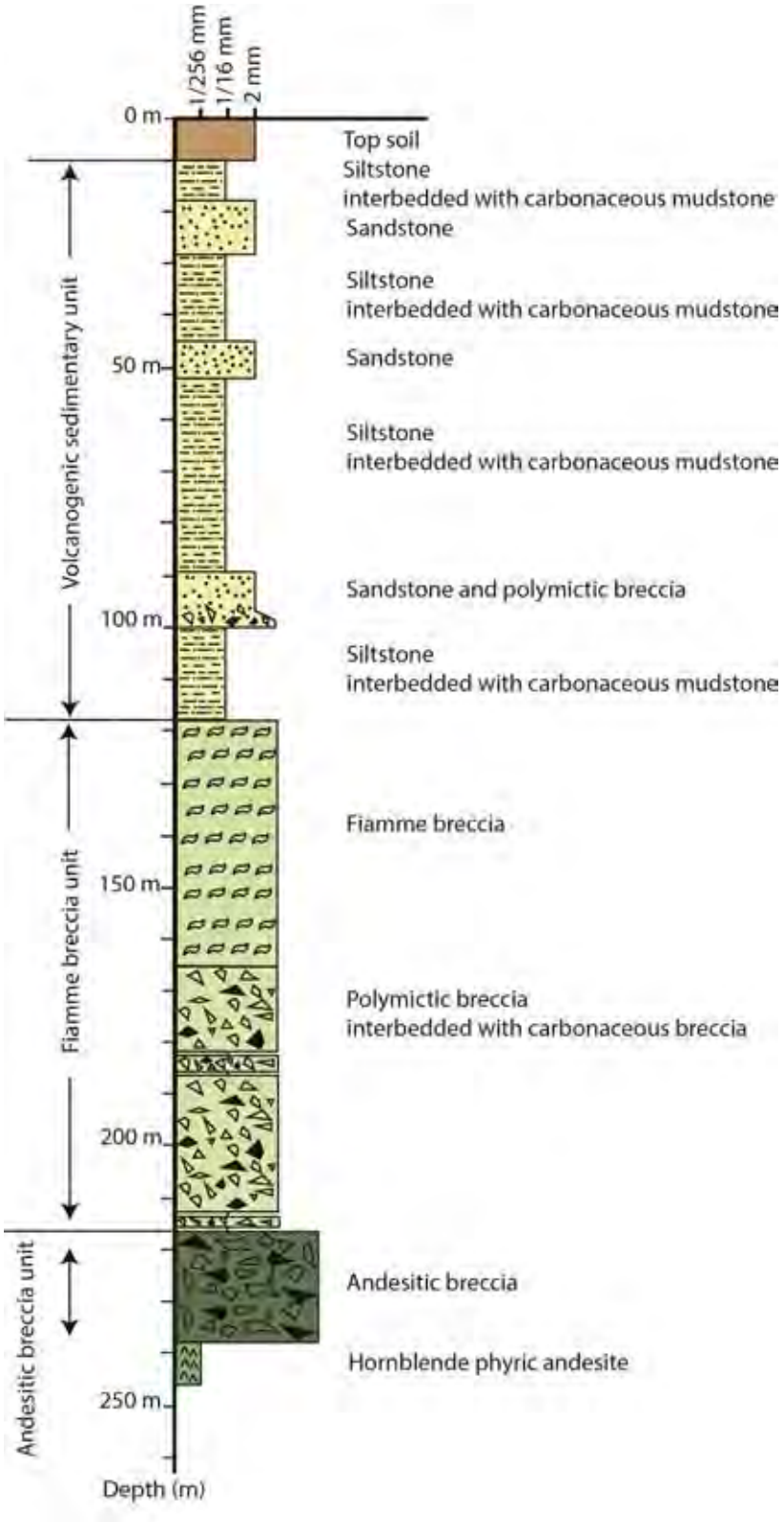

Fig. 4.3 Volcanic stratigraphy of drill hole number 4564DD

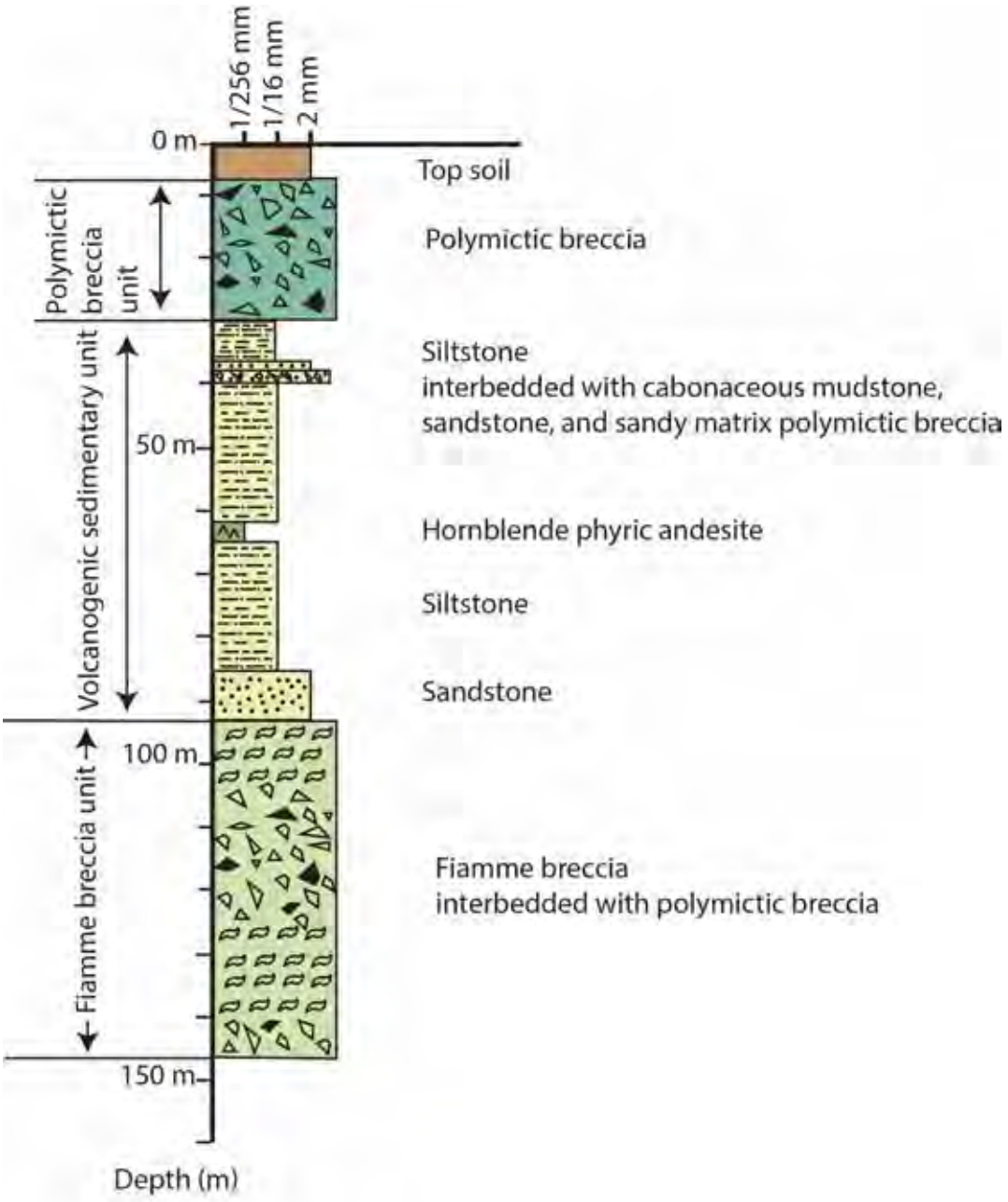

Fig. 4.4 Volcanic stratigraphy of drill hole number 4576DD.

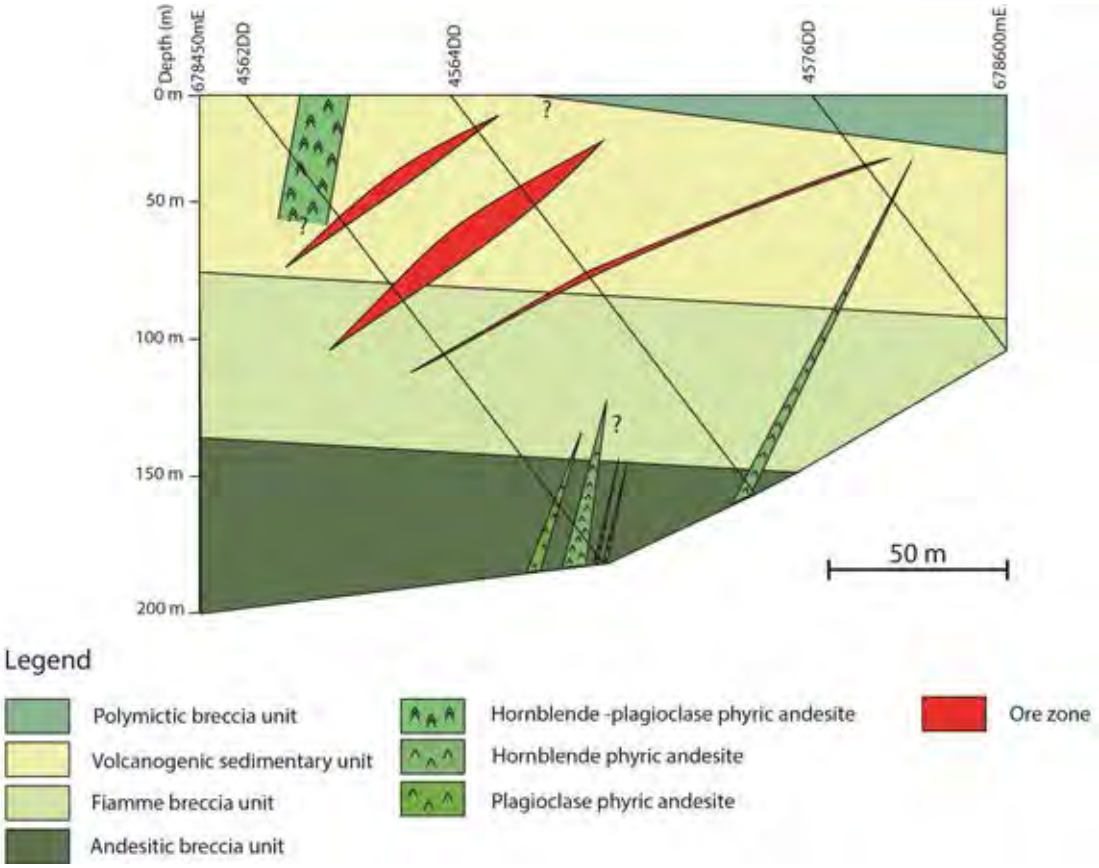

Fig. 4.5 Cross section of section 1800085N showing rock units dipping to east

In this study, six rock types are identified on the basis of their primary texture, mineralogy and composition: These rock types at B-prospect will be described and discussed in the following sections.

Andesitic polymictic breccia

Andesitic polymictic breccia identified in Unit 4 (andesitic polymictic breccia unit. The rock composes multiple clast types including plagioclase-phyric andesite, hornblende-plagioclase-phyric andesite and mudstone clasts in matrix that have similar composition to the clasts. The andesitic breccia has been identified mainly in andesitic polymictic breccia unit, elsewhere in the sequence is less predominant (Fig. 4.6). The rock makes up of multiple clast types mainly include plagioclase-phyric andesite clast, mudstone clast, siltstone clast. Crystal components consist of quartz and feldspar. The plagioclase-phyric andesite clasts of this rock are ranging in size from 2 to 5 mm. However, it is occasionally can be range from 5 to 10 cm in diameter in drill hole number 4564 DD at 236.5 meter of depth. Clast of mudstone and siltstone ranging from 1 to 5 mm. In general. All clasts have low sphericity with angular to sub-angular shape and they are very poor sorted. Matrix of this rock is same as the clasts.

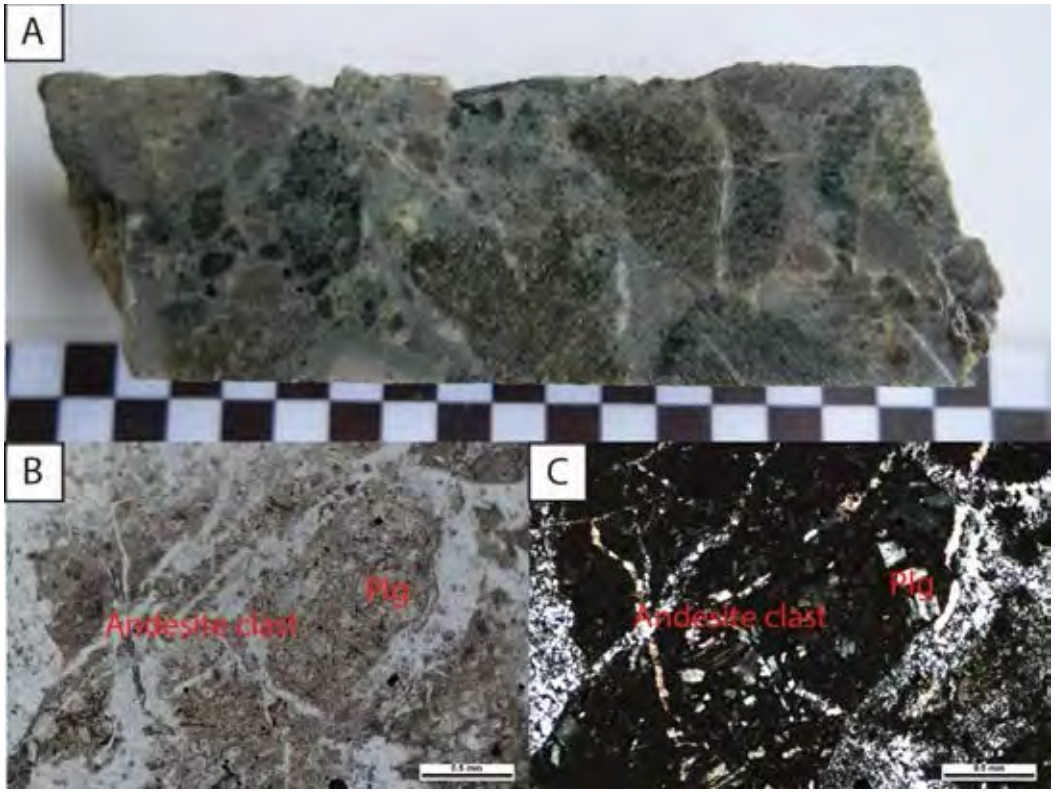

Fig. 4.6 Characteristics of andesitic breccia, sample no. 4564-236.5 (A) Photograph of diamond drill core showing andesitic breccia with large andesite clasts, partly silicified particularly in matrix and cross cut by quartz veinlets (B) Photomicrograph showing andesite clast with plagioclase phenocryst in PPL (C) Same as Fig. B highlight strong silicified matrix in XPL. Abbreviation: Plg = Plagioclase.

Fiamme breccia

The fiamme breccia mainly identified in unit fiamme breccia unit (Unit 3; Fig. 4.7). Based on drill core logging, fiamme breccia is interbedded with polymictic breccia (Fig. 4.1, 4.2 and 4.3) and at some parts are also interbedded with carbonaceous mudstone particularly in hole 4564DD. (Fig. 4.2) The fiamme breccia is here defined as polymictic breccia with clasts mainly compose of pumice with lens-like texture call “fiamme” (McPhie et al., 2005). This due to pumice clasts have been deformed due load compression during deposition. Lithic clasts increase toward the contact with polymictic breccia. Crystal-rich fiamme breccia may also present but less predominant compares to lithic-rich fiamme breccia. Fiamme breccia at B-prospect is commonly contained some percent of pumice clasts. The other clasts are mudstone clast and andesite clast. In general, all types of clasts are ranging in size from 0.2 mm to 3 mm (Fig. 4.7). They are characterized by low sphericity, poor sorting and sub-angular shape. Andesite clasts consist of plagioclase-phyric andesite and hornblende-plagioclase-phyric andesite. For hornblende-plagioclase-phyric andesite is typically shown phenocryst of feldspar. The matrix of fiamme breccia is characterized by very fine particle of a similar composition that is difficult to observe.

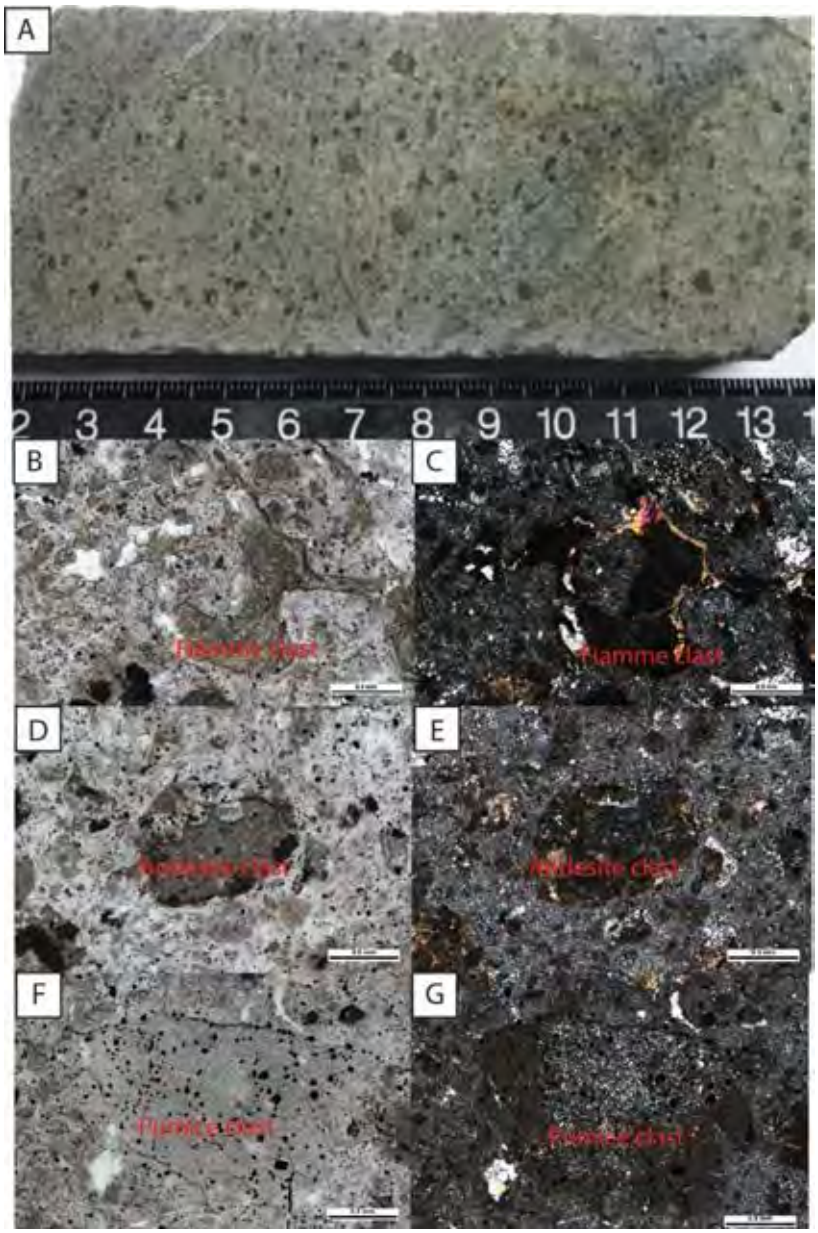

Fig. 4.7 Characteristics of fiamme breccia, (A) Photograph of diamond drill core showing fiamme breccia and some pumice clasts (dark) in matrix of moderately silicified. (Sample no. 4562-38.9) (B) Photomicrograph showing fiamme clast (glassy texture) with elongated shape in PPL, (C) Same as Fig. B in XPL (D) Photomicrograph showing andesite clast with plagioclase phenocryst in PPL (E) Same as Fig. D in XPL (F) Photomicrograph showing angular shape pumice clast (devitrified) in PPL (G) Same as Fig. F in PPL.

Siltstone, mudstone, sandstone and sandy-matrix polymictic breccia

Siltstone, mudstone, sandy-matrix polymictic breccia and sandstone mainly occur in volcanogenic-sedimentary rocks. Siltstone is most abundance rock type among volcanogenic-sedimentary rocks and usually interbedded with mudstone and is locally shown lamination (Fig. 4.8A and Fig. 4.8C). The color of siltstone is grey to light grey. The light grey color is partly due silicification. Siltstone are mainly composed of quartz and minor feldspar and mica with swell sorted (Fig. 4.8C). Quartz veinlets are commonly found cross cut siltstone (Fig. 4.8)

The mudstone can be divided into 2 types. First is deformed mudstone which is yellow color. Second is mudstone which is black color. The rock composes of sericite and some feldspar and quartz. Small quartz veins/veinlets common cross cut mudstone.

Another rock is sandy-matrix polymictic breccia (Fig. 4.9). This rock is polymictic breccia in which matrix is characterized by predominantly sand component. It constitutes multiple clast types such as plagioclase-phyric andesite sandstone, mudstone clasts. Majorities of clasts have low sphericity and high angularity. Sorting of this rock is poor sorting. The average size of mudstone, siltstone and plagioclase-phyric andesite is 2, 3, 1 and 0.5 mm respectively. However, some siltstone and mudstone clasts size can be up to 5cm or even up to 10 cm.

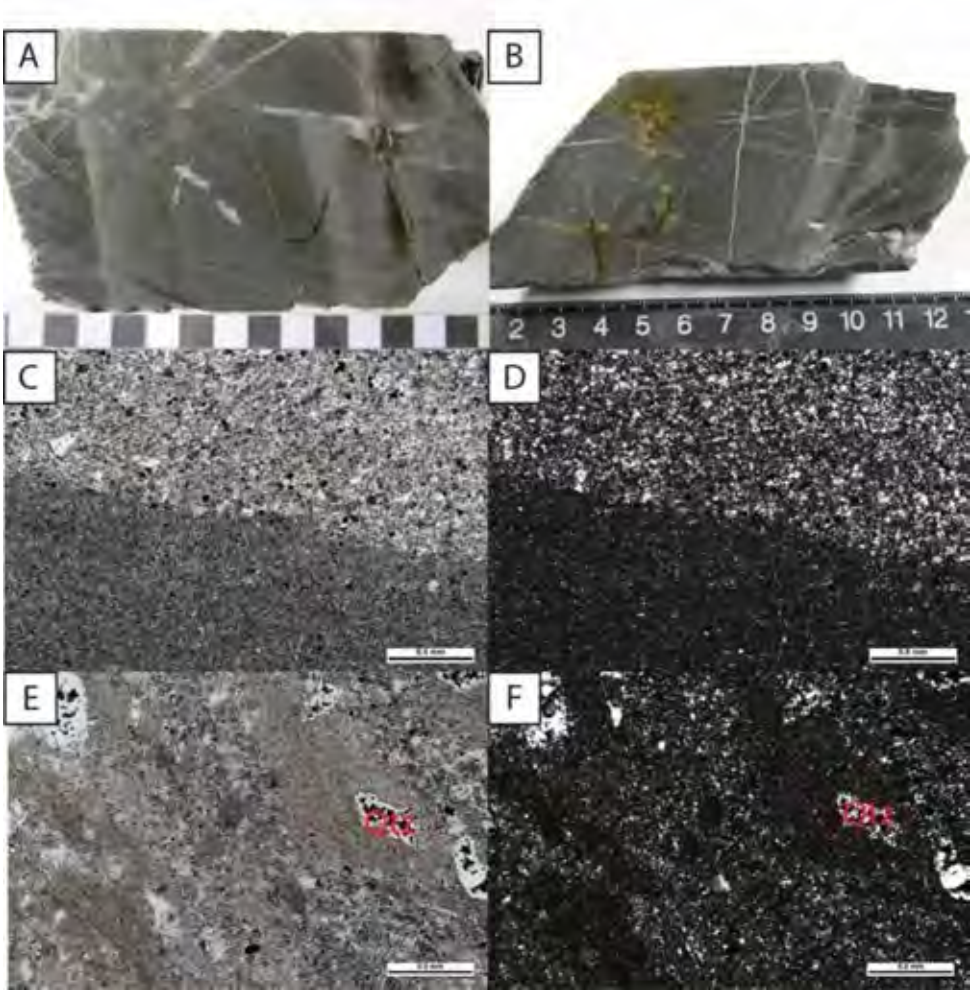

Fig. 4.8 Characteristic features of laminated siltstone, (**A**) Photograph of diamond drill core showing laminated siltstone (sample no. 4564-12.20), (**B**) Photograph of diamond drill core of carbonaceous mudstone showing some lamination (sample no. 4562-79.9), (**C**) Photomicrograph showing siltstone layer and mudstone layer, in PPL (**D**) Same as Fig. C in XPL (**E**) Photomicrograph showing mud size particles with microcrystalline quartz in vugs in PPL (**F**) Same as Fig. E in XPL Abbreviation: Qtz = quartz

\

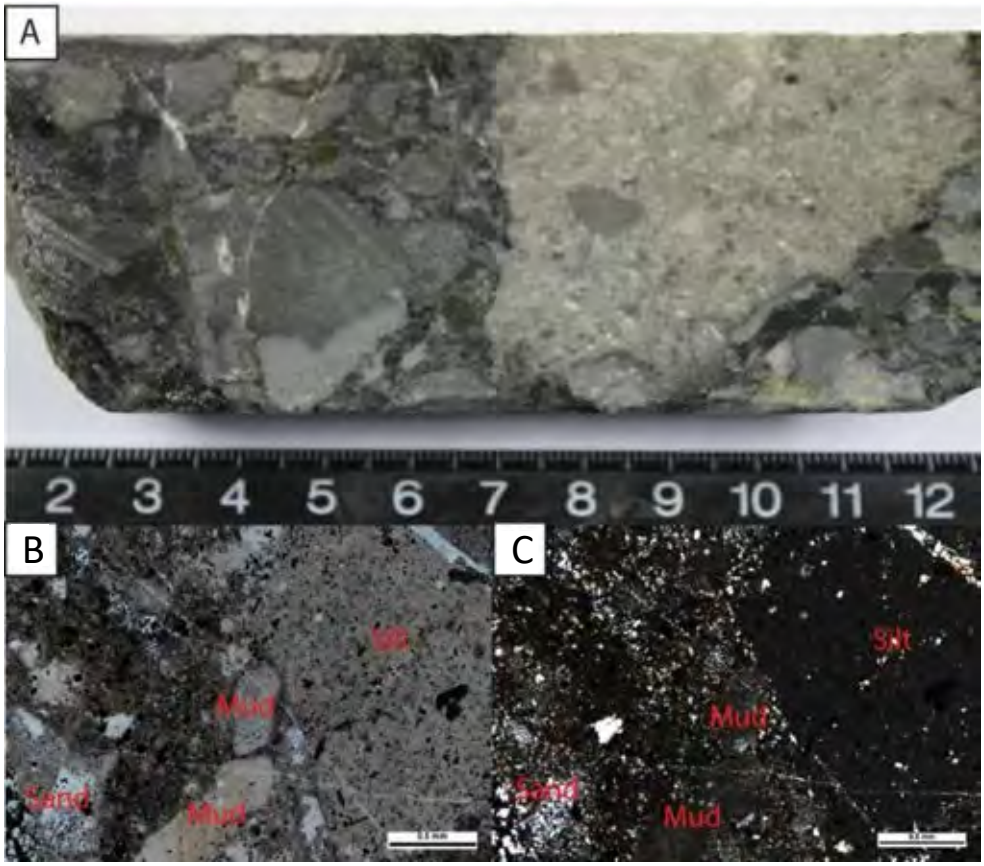

Fig. 4.9 Characteristics of sandy-matrix polymictic breccia (Sample no. 4562-90.0) (**A**) Photograph of diamond drill core showing sandy-matrix polymictic breccia with various clast types. (**B**) Photomicrograph showing siltstone, sandstone and mudstone clasts with sandy-matrix in PPL (C) Same as Fig. B in XPL. Abbreviation: Silt = siltstone clast, Mud = mudstone clast, Sand = sandstone clast

Polymictic breccia

The polymictic breccia identified mainly in unit polymictic breccia unit (Unit 1) in the top of the stratigraphic sequence (Fig. 4.10). This rock is characterized by grey to greyish brown color on fresh surface. The rock comprises multiple clasts types mainly include plagioclase-phyric andesite clast, plagioclase-hornblende-phyric andesite clasts, mudstone clast and sandstone clast (Fig. 4.10B) ranging in size from 0.5 mm. to 3 cm. In addition, at some depth in drill holes this rock may contain high proportion of crystals (quartz and plagioclase) (Fig. 4.10C). The plagioclase-phyric andesite clasts in polymictic breccia mainly contain plagioclase phenocryst size of 1 mm. (Fig. 4.10E) and most of clasts are roundness to sub-angular. The other clasts are ranging 0.5 to 5 mm and poorly sorting.

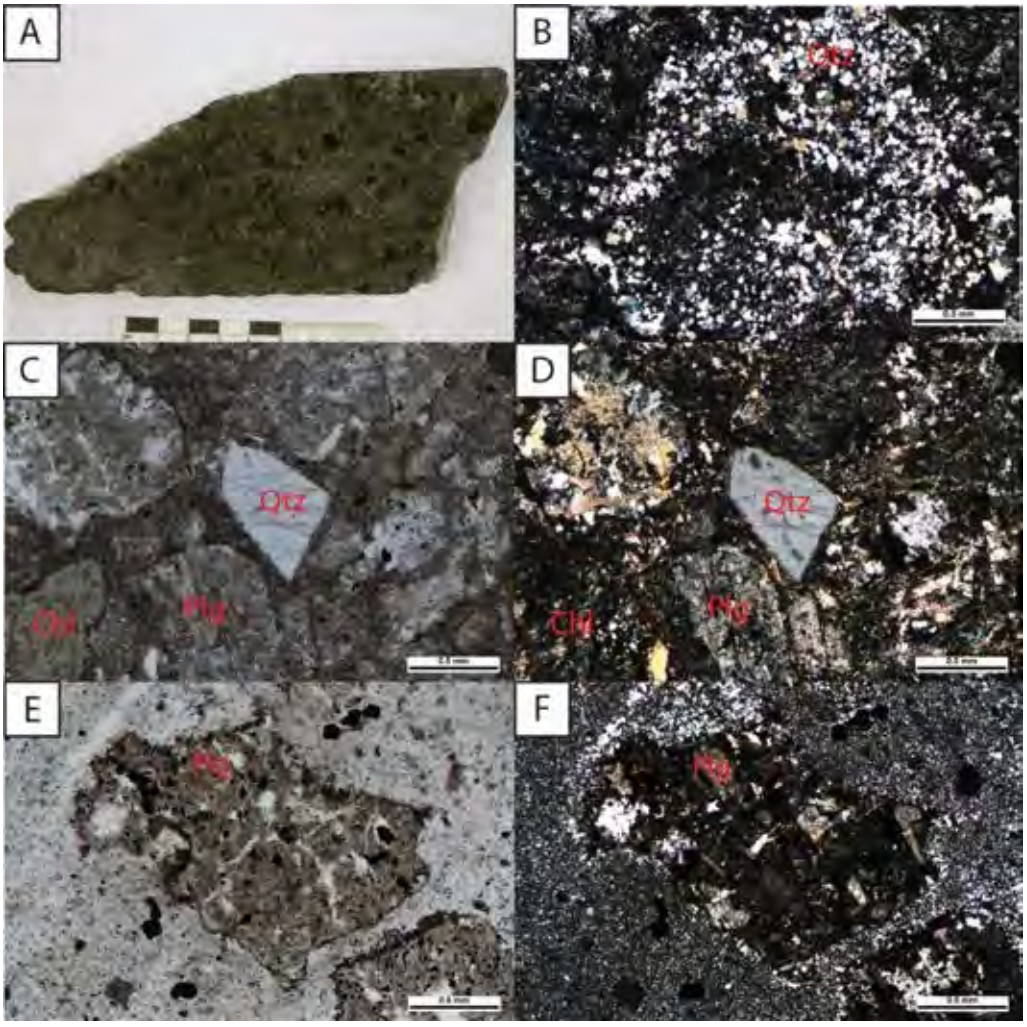

Fig. 4.10 Characteristics of polymictic breccia, (**A**) Photograph of diamond drill core showing various types of clast (**B**) Photomicrograph showing strongly altered sandstone clast, XPL (sample no. 4576-21.2) (**C**) Photomicrograph showing quartz and plagioclase crystals in PPL (sample no. 4576-21.2) (**D**) Same Fig. as Fig. C in XPL, (E) Photomicrograph of plagioclase-phyric andesite clast showing phenocryst of altered plagioclase in matrix of strongly silicified in PPl (sample no. 4576-21.2) (F) Same as Fig. E in XPL. Abbreviation: Qtz=quartz, Chl=chlorite, Plg = plagioclase

Coherent rocks (dyke)

Coherent rock here is defined as those rocks that form from crystallization of magma or lava (McPhie et al. 2005). At B-prospect, the coherent volcanic rock form as dyke or sill intruded the host volcanic sequence. Salam (2013) studied dykes in Chatree deposit and reported that most dykes cross cut gold bearing quartz veins or post-dated gold mineralization. The coherent volcanic rocks at B-prospect can be divided into 3 types; Hornblende-plagioclase phyric andesite, Plagioclase-phyric andesite and Hornblende phyric andesite.

Hornblende-plagioclase phyric andesite

Hornblende-plagioclase phyric andesite (Fig. 4.11A and Fig. 4.11B) is orange and green. Based on diamond drill core logging, it is intersected in several drill holes (Fig. 4.5). The hornblende-plagioclase phyric andesite can be implied to dyke. The minerals assemblage of the rock are mainly plagioclase feldspar, hornblende and potassium feldspar. It has porphyritic texture in which plagioclase feldspar and hornblende become its phenocrysts (Figs. 4.10C and Fig. 4.10D) Phenocrysts of plagioclase feldspar ranges from 2 mm to 1 cm in diameter. The groundmass is mainly composed of plagioclase feldspar, K-feldspar and minor hornblende. However, some grains of hornblende and feldspar are partly altered to chlorite and sericite respectively.

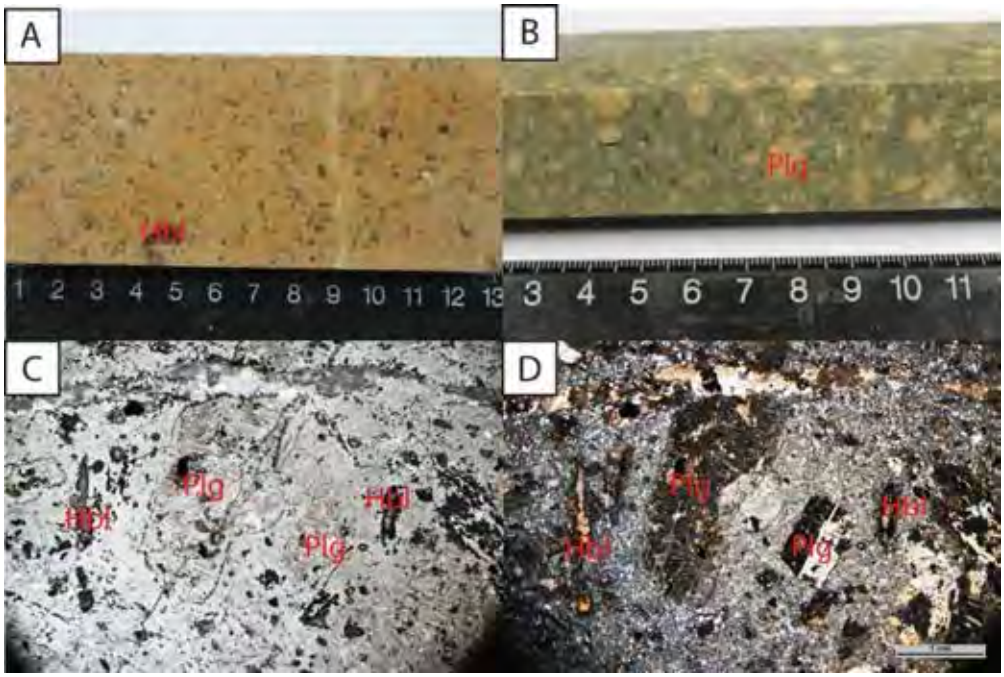

Fig. 4.11 Characteristics of hornblende-plagioclase phyric andesite, (**A**) Photography of diamond drill core showing hornblende-plagioclase phyric andesite (Orange) which has hornblende grain and plagioclase grain as porphyritic texture (B) Photograph of diamond drill core showing similar features to Fig. A but has green color and clearly shown hornblende and plagioclase phenocrysts (C) Photomicrograph showing plagioclase and hornblende as porphyritic texture in PPL (D) Same as Fig. C in XPL. Abbreviation: Plg = plagioclase, Hb = hornblende

Plagioclase phyric andesite

Plagioclase phyric andesite occurs as dyke (Fig. 4.5). It occurs as very fine-grained and equigranular texture (Fig. 4.12A). This rock consists mainly of plagioclase feldspar and K-feldspar with minor hornblende (mafic mineral; Fig. 4.12B and Fig. 4.12C). Size of plagioclase feldspars range 0.5 to 1 mm in larger grain and smaller grains range 0.1 to 0.2 mm. Moreover, pyrite, chlorite also found as alteration minerals.

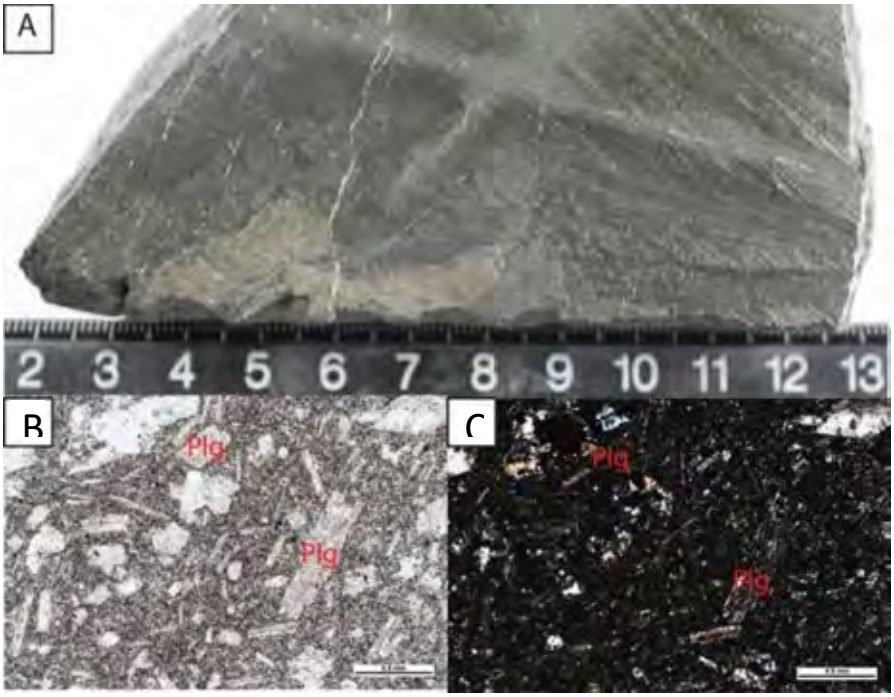

Fig. 4.12 Characteristics of plagioclase phyric andesite, (A) Photograph of diamond drill core showing plagioclase phyric andesite (B) Photomicrograph showing plagioclase as phenocryst in PPL (C) Same as Fig. B in XPL. Abbreviation: Plg = Plagioclase

Hornblende phyric andesite

Hornblende phyric andesite also occurs as dyke and typically characterized by slightly porphyritic texture (Fig. 4.13A). The rock consists of mainly plagioclase feldspar and minor K-feldspar. Hornblende is most abundance mafic mineral in this rock and its size ranging from 0.2 to 1 mm. (Fig. 4.13B and Fig. 4.13C). Feldspar both plagioclase and K-feldspar are partly altered to sericite, calcite. Hornblende is also partly altered to chlorite and carbonate minerals.

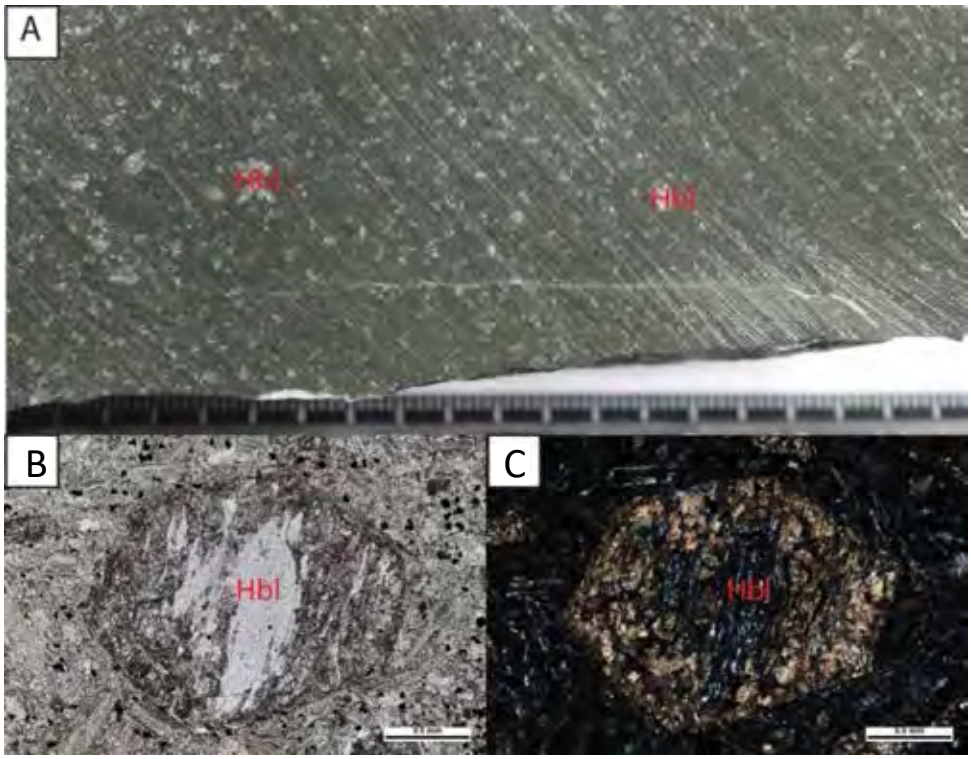

Fig. 4.13 Characteristics of hornblende phyric andesite, (A) Photograph of diamond drill core showing hornblende phyric andesite which has hornblende (B) Photomicrograph showing hornblende that altered to calcite and chlorite. Abbreviation: Hb = hornblende

4.3 Mineralization

This section describes mineralization at B-prospect based on drill core logging, examination of this sections, polished thin sections and mounts. This also includes establishing paragenesis sequence and characteristics of each mineralization stage (veins). The paragenesis sequence is the order of mineral occurrence and in this study, special focus is given to the gold mineralization stage. Regarding to mineralogy, characteristics of sulfide minerals and gold have also been focused using reflected light microscope.

4.3.1 Paragenesis sequence

The paragenesis sequence (Fig. 4.14) in this study is based on cross cutting relashipships, mineral assemblages and textures. Paragenesis sequence can be divided into 3 stages; pre Au-Ag mineralization stage (Stage 1), main Au-Ag mineralization stage (Stage 2) and post Au-Ag mineralization stage (Stage 3).

	Pre Au-Ag mineralization stage	Main Au-Ag mineralization stage	Post Au-Ag mineralization stage
Quartz			
Calcite			
Pyrite			
Sphalerite			
Electrum			

Fig. 4.14 Paragenesis sequence showing 3 stages of vein occurrences, gold as electrum can be found in stage 2.

Pre Au-Ag mineralization stage (Stage 1)

This stage is characterized by grey quartz veins with pyrite (Fig. 4.15A) and in some samples pyrite may occur as massive pyrite veins. The thickness of veins range from 1 to 3 cm . Texturally, veins of this stage are characterized by crustiform, colloform banding and comb texture. This stage found larger pyrite grains in the quartz veins and smaller pyrite grains along contact of vein and wall rock. Pyrites in quartz veins are mainly euhedral with cubic shape. (Fig. 4.15B) However, pyrites in massive pyrite veins are mainly subhedral to anhedral shape. (Fig. 4.15D).

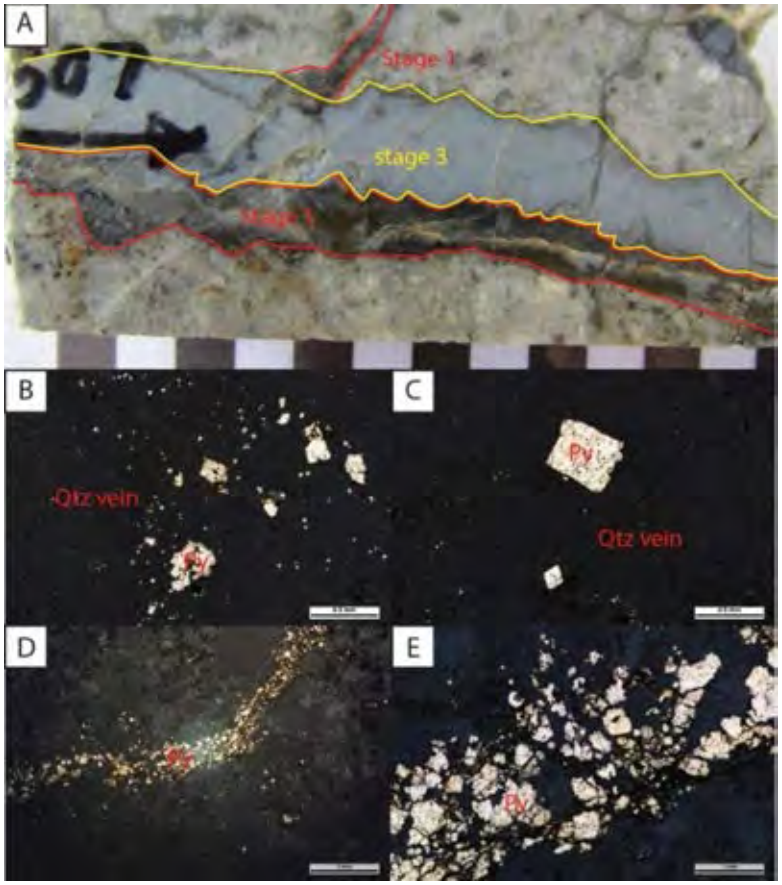

Fig. 4.15 Characteristics of vein in stage 1, (A) Photograph of diamond drill core showing quartz-pyrite vein in stage 1 (B) Photomicrograph showing pyrites occur with quartz vein (C) Photomicrograph showing pyrites have euhedral shape (D) Photomicrograph showing massive pyrite vein (E) Photomicrograph showing pyrites in massive pyrite vein which have anhedral shape. Abbreviation: Py = pyrite, Qtz = quartz veins

Main Au-Ag mineralization stage (Stage 2)

This stage is characterized by colorless quartz accompanied by gold (Fig. 4.16A). The thickness of Stage 2 veins can be ranging from 5 to 10 cm. Sulfide minerals often form as layer or band in Stage 2 quartz vein. Major sulfide minerals are pyrite and minor sphalerite. Gold is commonly associated with gold (Fig. 4.16B and Fig. 4.16C). Under microscope, quartz is clearly revealed crustiform and colloform textures. The colloform texture is indicated of hydrothermal vein that represents multiple time of vein precipitation. In addition, some parts of vein can be found quartz associated with carbonate minerals. Pyrites in this stage are relatively larger than those of Stage 1 and forms as anhedral. Pyrite is closely associated with sphalerite and electrum.

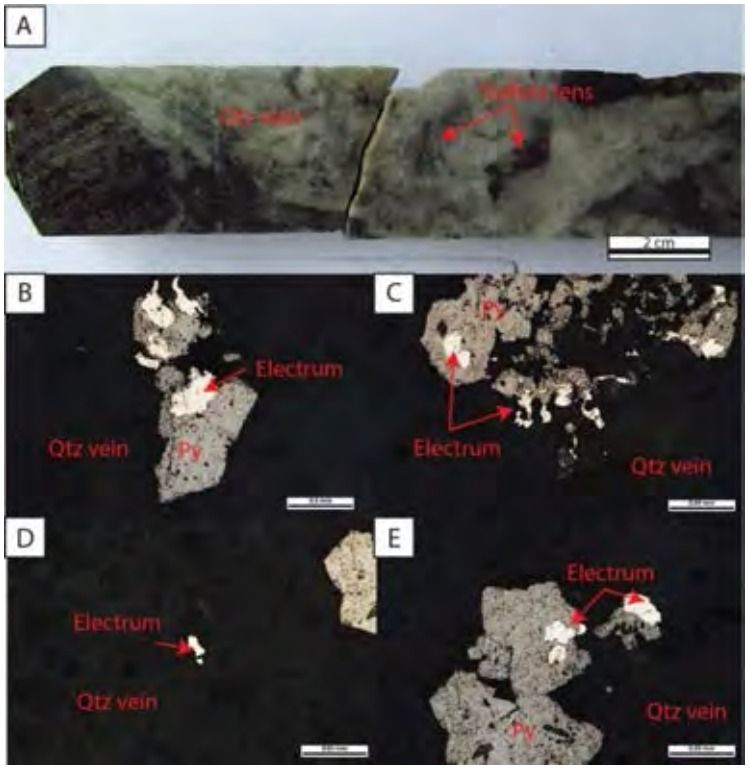

Fig. 4.16 Characteristics of stage 2 veins, (A) Photograph of diamond drill core showing quartz veins in stage 2 and sulfide lens that include sphalerite, pyrite and electrum. (B) Photomicrograph showing electrums are distributed all of sulfide lens (C) Photomicrograph showing electrum occur as irregular shape (D) Photomicrograph showing free grain electrum (E) Photomicrograph showing inclusion grain electrum. Abbreviation: Qtz vein = Quartz vein, Py = Pyrite

Electrum

Electrum (Fig. 4.16) occurs as irregular shape and has light golden color which brighter than pyrite. The light golden color electrum tends to have low fineness (Salam, 2013). The microscopic observation of polished mount and polished thin section samples show that gold occur as electrum into 2 characters: 1) free grain electrum (Occurs in silicate minerals such as quartz and calcite) and 2) Inclusion grain electrum (Occurs as inclusion with sulfide minerals such as pyrite and sphalerite). Pyrite is the most common sulfide containing electrum inclusion.

Sphalerite

Sphalerite (Fig. 4.17) is one of sulfide mineral which minor mineral in stage 2. Composition of sphalerite is ZnS. Sphalerites are grey to dark grey color and associate with pyrite. Sphalerite can be found with small pyrite range 0.02 to 0.05 mm. In microscopic observation, sphalerite is small grain as pyrite with subhedral to anhedral shape.

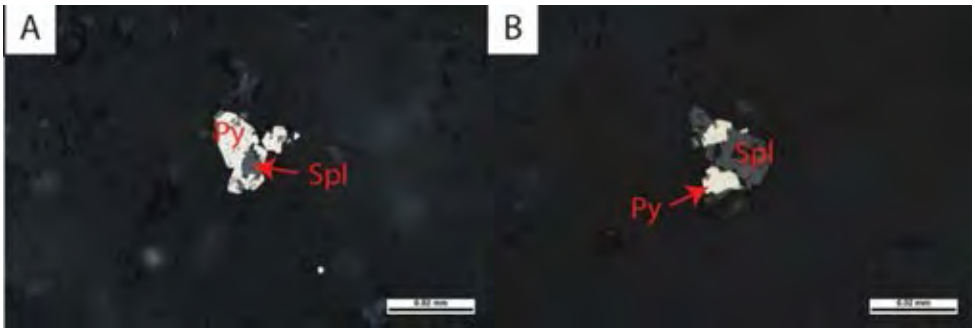

Fig. 4.17 Characteristics of stage 2 veins (A) Photomicrograph showing sphalerite that can be found with pyrite in the sulfide lens of quartz veins in stage 2 (B) Photomicrograph showing sphalerite occurs as inclusion in pyrite (C) Photomicrograph showing sphalerite occurs associated with pyrite

Post Au-Ag mineralization stage (Stage 3)

This stage found quartz veins without pyrite association and carbonate veins. (Fig. 4.18) The veins and veinlets size range 1 to 3 cm. Quartz veins show crustiform texture and grey color. Some pyrite can be found in the rim wall rock as the black bands that can be implied to be diagenetic pyrite in sedimentary rock and alteration pyrite in volcanic rock. Thus, pyrite in this stage isn't occurs with quartz veins in stage 3. Calcite veins in this stage occur cut the quartz veins.

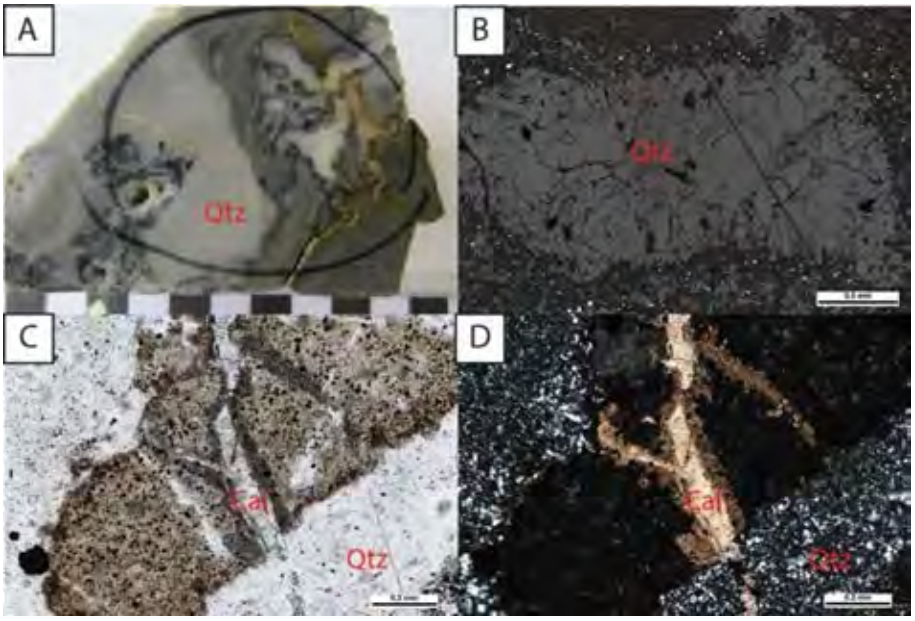

Fig. 4.18 Characteristics of vein in stage 3, (A) Photograph of diamond drill core showing quartz vein in stage 3 (B) Photomicrograph showing quartz veins occur without pyrite (C) Photomicrograph showing calcite vein in PPL (D) Photomicrograph showing calcite vein in XPL Abbreviation: Qtz = quartz, Cal = calcite.

4.3.2 Minerals Chemistry

The study of minerals chemistry is mainly focused on the Au-Ag mineralization stage (Stage 2) in which gold and sphalerite are present. This study uses Electron Probe Micro Analyzer (EPMA) to measure the mineral composition in term of elements. The results of EPMA analyzes can be confirmed the microscopic

observation. In addition, purity of gold is also aimed in this study in term of gold fineness. The results of EPMA analyzes are shown in Table 4.1.

The EPMA mapping of gold bearing veins (Stage 2) showed in Figure 4.19. EPMA image shows high iron (Fe) and sulfur (S) indicating pyrite and high zinc (Zn) and sulfur indicating sphalerite. Gold associated pyrite indicating by elevated in Ag and Au with low concentration of Cu. This result confirms that gold occurs as eletrum.

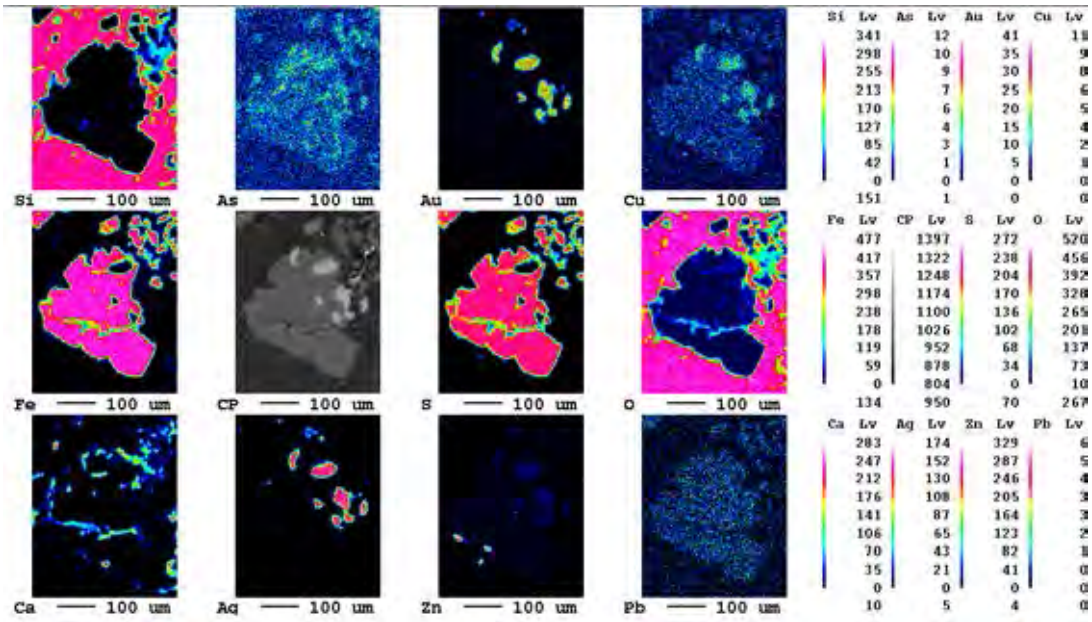

Fig. 4.19 EPMA Mapping of gold bearing quartz vein showing pyrite and electrum and sphalerite assembalge.

Fineness (purity of gold)

The purity of gold is measured in the term of fineness. The fineness is a ratio of Au per Au and Ag in each grain. The content of Au and Ag can be quantified by EPMA. This value can identify types of gold grains: electrum, and free gold (Shikazono and Shimzu, 1987). If the fineness value is more than 800, it can be identified as free grain gold. On the other hand, it can be identified as electrum when the value less than 800. The fineness can be calculated by this formula:

$$Fineness = \frac{(\mathrm{wt\%\ Au}) \times 1000}{(\mathrm{wt\%\ Au + wt\%\ Ag})}$$

In this study, 37 grains from the samples were detected for the content of Au and Ag to calculate the fineness. The average fineness is 619.64 which can be identified to be electrum. Moreover, this study also measured sizes of electrum grains and plotted the relation between fineness and sizes of electrum grains. The data can be divided into two types of grains; inclusion grain and free grain. The result of gold inclusion grain (Fig. 4.20) shows gradational increasing of fineness when grain size is increased. However, the result of the free grain remains constant.

Table 4.1 EPMA's result of sample number 4562-79.6-2 showing mineral compositions of sphalerite and electrum.

No.	S	As	Au	Ag	Fe	Pb	Cu	Zn	Total	Comment	Mineral
1	24.138	0	24.939	22.171	20.715	0	0.027	0	91.99	B1-G-1	Pyrite?
2	0.152	0	52.312	43.135	1.516	0.005	0.023	0	97.143	B1-G-2	Electrum
3	48.485	0.109	0.113	0.025	40.907	0	0.043	0.002	89.684	B1-G-3	Pyrite
4	30.164	0.12	0	0.217	23.633	0	0.263	19.107	73.504	B1-S-1	Sphalerite?
5	28.951	0.018	0	0	9.247	0	0.327	44.127	82.67	B1-S-2	Sphalerite?
6	25.343	0	0.426	0.013	2.177	0	0.527	54.463	82.949	B1-S-3	Sphalerite
7	25.994	0	0.752	0	2.943	0	0.527	54.347	84.563	B1-S2-1	Sphalerite?
8	46.234	0.046	0.188	1.008	37.636	0	0.156	3.505	88.773	B1-S2-2	Pyrite
9	45.373	0.029	0.525	4.413	37.924	0	0.482	0.134	88.88	B1-S2-3	Pyrite
10	26.601	0.029	0.275	0	1.002	0	0.003	55.573	83.483	B1-S3-1	Sphalerite
11	26.315	0.01	0.113	0	1.273	0	0.044	57.148	84.903	B1-S3-2	Sphalerite
12	25.777	0	0	0	1.133	0	0.133	54.854	81.897	B1-S3-3	Sphalerite

Table 4.2 Composition of gold grains analyzed by EPMA and calculated gold fineness.

Sample No.	Au_avg	Ag_avg	sum	Wt%Au	Wt%Ag	fineness	Size (mm)
1	58.487	36.83633	95.32333	61.35644	38.64356	613.5644	0.05
2	49.289	32.486	81.775	60.27392	39.72608	602.7392	0.06
3	58.3835	36.5615	94.945	61.49192	38.50808	614.9192	0.1
4	51.562	30.83067	82.39267	62.58081	37.41919	625.8081	0.01
5	56.259	34.346	90.605	62.0926	37.9074	620.926	0.01
6	61.10567	37.023	98.12867	62.27096	37.72904	622.7096	0.1
7	46.53867	29.471	76.00967	61.2273	38.7727	612.273	0.07
8	62.09733	36.81667	98.914	62.77911	37.22089	627.7911	0.03
9	59.118	36.7995	95.9175	61.63422	38.36578	616.3422	0.01
10	61.536	36.99867	98.53467	62.45112	37.54888	624.5112	0.03

11	59.0685	36.054	95.1225	62.0973	37.9027	620.973	0.01
12	61.68	36.75	98.43	62.66382	37.33618	626.6382	0.025
13	57.226	36.665	93.891	60.9494	39.0506	609.494	0.01
14	62.31033	36.792	99.10233	62.87474	37.12526	628.7474	0.025
15	60.37	36.787	97.157	62.13654	37.86346	621.3654	0.015
16	58.766	35.77467	94.54067	62.15949	37.84051	621.5949	0.05
17	62.15067	36.23633	98.387	63.16959	36.83041	631.6959	0.1
18	61.211	37.194	98.405	62.20314	37.79686	622.0314	0.02
19	62.08967	37.144	99.23367	62.56915	37.43085	625.6915	0.05
20	61.997	37.48133	99.47833	62.32211	37.67789	623.2211	0.04
21	56.54467	35.02933	91.574	61.74751	38.25249	617.4751	0.02
22	55.486	34.34433	89.83033	61.76755	38.23245	617.6755	0.025
23	37.84667	24.01967	61.86633	61.1749	38.8251	611.749	0.01
24	60.7375	37.222	97.9595	62.00266	37.99734	620.0266	0.025
25	51.60767	31.984	83.59167	61.73781	38.26219	617.3781	0.03
26	61.648	36.89767	98.54567	62.5578	37.4422	625.578	0.05
27	60.56433	38.38767	98.952	61.20577	38.79423	612.0577	0.05
28	61.025	36.956	97.981	62.28248	37.71752	622.8248	0.05
29	60.59067	36.86633	97.457	62.17169	37.82831	621.7169	0.04
30	61.67233	37.28333	98.95567	62.3232	37.6768	623.232	0.03
31	61.34133	36.85	98.19133	62.47123	37.52877	624.7123	0.04
32	60.589	37.30133	97.89033	61.89477	38.10523	618.9477	0.02
33	57.226	38.82267	96.04867	59.58021	40.41979	595.8021	0.025
34	59.95833	37.54033	97.49867	61.49657	38.50343	614.9657	0.02
35	61.32433	37.029	98.35333	62.35105	37.64895	623.5105	0.06
36	62.513	37.30633	99.81933	62.62614	37.37386	626.2614	0.1
AVG	58.38667	35.80244	94.18911	61.96375	38.03625	619.6375	0.039

.

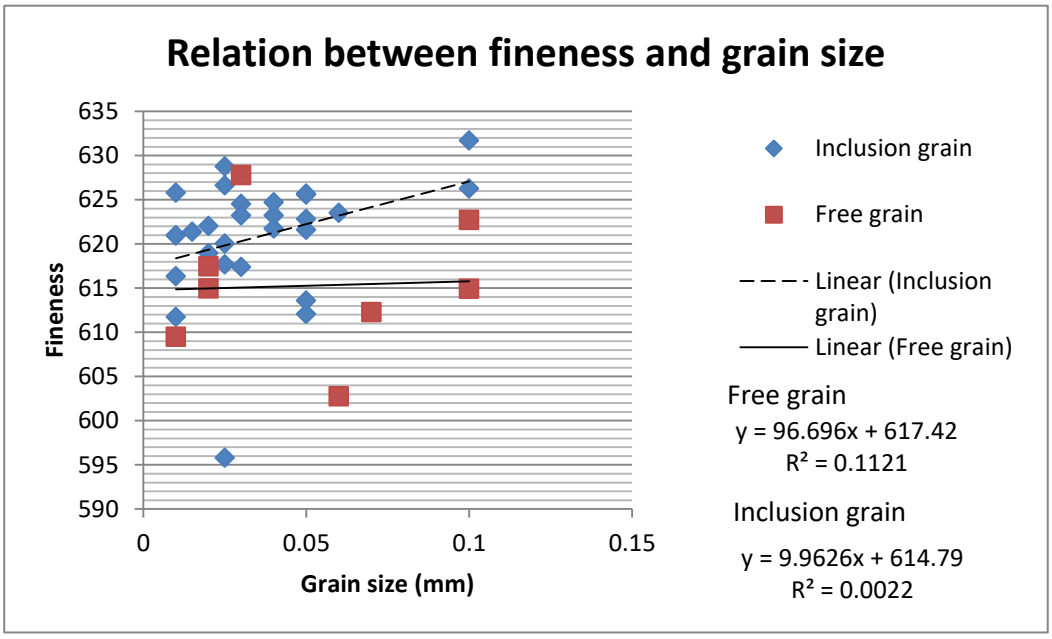

Fig. 4.20 Graph showing relation between gold fineness and grain size

4.4 Alteration

This section describes the hydrothermal alteration mineralogy and alteration zonation of B-prospect. The alteration mineral assemblages are varied from proximal to distal from ore zones. In this study, the alteration can be divided into 3 zones bases on dominated alteration minerals. Those 3 zones are 1) Quartz-Adularia (Silicic alteration), 2) Adularia-Sericite-Illite-Quartz-Calcite (Phyric alteration) and 3) Sericite-Illite-Chlorite-Calcite-Adularia-Quartz (Phyllic alteration; Fig. 4.24).

Quartz-Adularia zone (Silicic alteration)

This zone is dominated by silicic alteration which nearly ore zone. The zone ranges 1 to 2 m from the ore zone. In field observation, the altered rock of this zone is very hard implied to strong alteration. Color of altered rock of this zone is light brown to white. In microscopic investigation, major alteration mineral is quartz which is microcrystalline quartz (Fig. 4.21) in vug or open space. The minor alteration mineral is adularia which can found in rim of zone. The zone is represented to silicic alteration which high content of quartz, quartz replacement in vugs. In part of mineralogy study, microcrystalline quartz can be defined by texture and size. The texture of microcrystalline quartz is anhedral with small size.

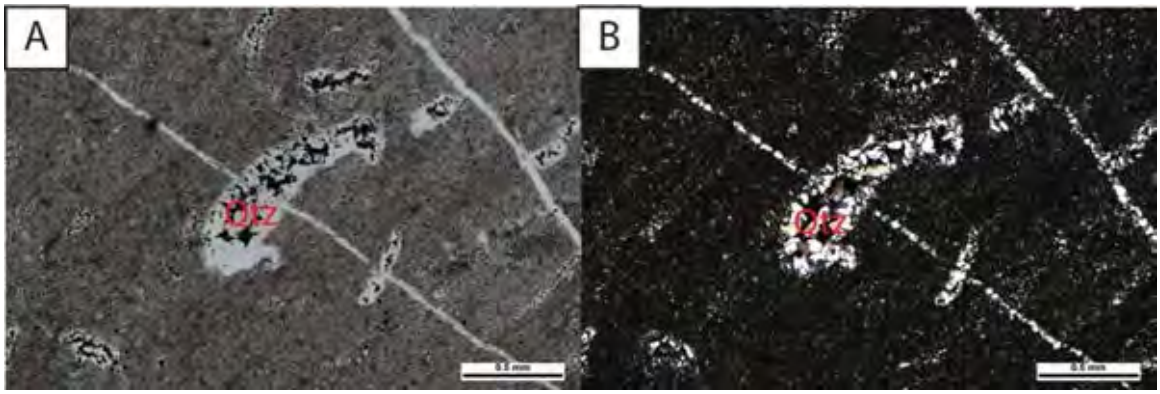

Fig. 4.21 Characteristics of Quartz-adularia zone, (A) Photomicrograph showing microcrystalline quartz in PPL (B) Same as Fig. B in XPL

Adularia-Sericite-Illite-Quartz-Calcite zone (Phyllic alteration)

This zone is next from the quartz-adularia zone and widely spread. In part of field observation, altered rock can be selected next from the strong alteration. The color of altered rocks is rather dark than silicic zone which moderated alteration. Major alteration minerals are adularia (Fig. 4.22A and Fig. 4.22B), sericite and illite, quartz and minor alteration mineral is calcite. In part of mineralogy study, adularia found in rhombohedral shape and occurs with quartz. Adularia can be identified by high relief and altered than quartz. Adularia also is indicator of hydrothermal low sulfidation system. All of mineral assemblages can be indicated to phyric alteration.

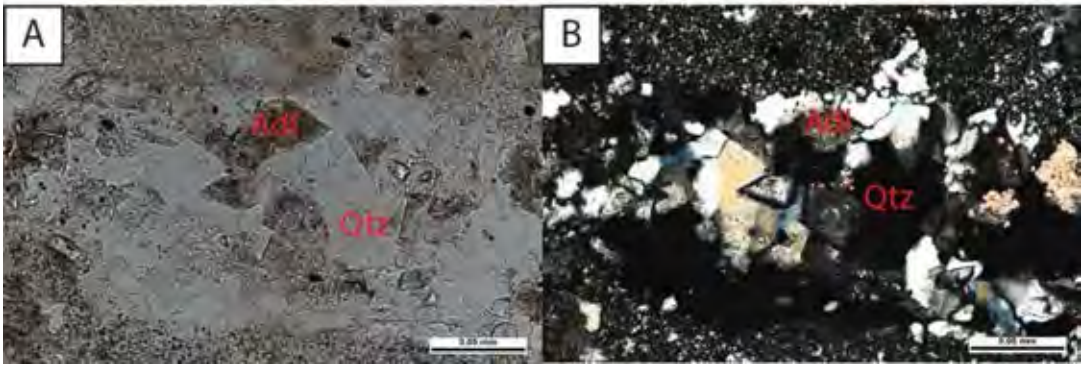

Fig. 4.22 Characteristics of Adularia-sericite-illite-quartz-calcite zone, (A) Photomicrograph showing adularia in microcrystalline quartz in PPL (B) Same as Fig. A in XPL

Sericite-Illite-Chlorite-Calcite-Adularia-Quartz zone (Phyllic alteration)

This zone occurs distal the veins. In field observation, the represented rocks are selected by altered rock which weak alteration. The weak alteration can be identified by color and distal distance from the ore zone. In microscopic observation, the representing minerals are sericite and illite (Fig. 4.23A and Fig. 4.23B). Minor minerals are chlorite, calcite (Fig. 4.23C and Fig. 4.23D), adularia and quartz. In mineralogy study, sericite and illite can't be separate under microscopic observation but XRD results can identify and separate them. Sericite and illite are altered from the feldspar, both plagioclase feldspar and alkaline feldspar, and show fine grain with high birefringence. In addition, chlorite can be found in green color in PPL and bow tie texture which altered from the hornblende. Some parts of this zone found calcite replacement.

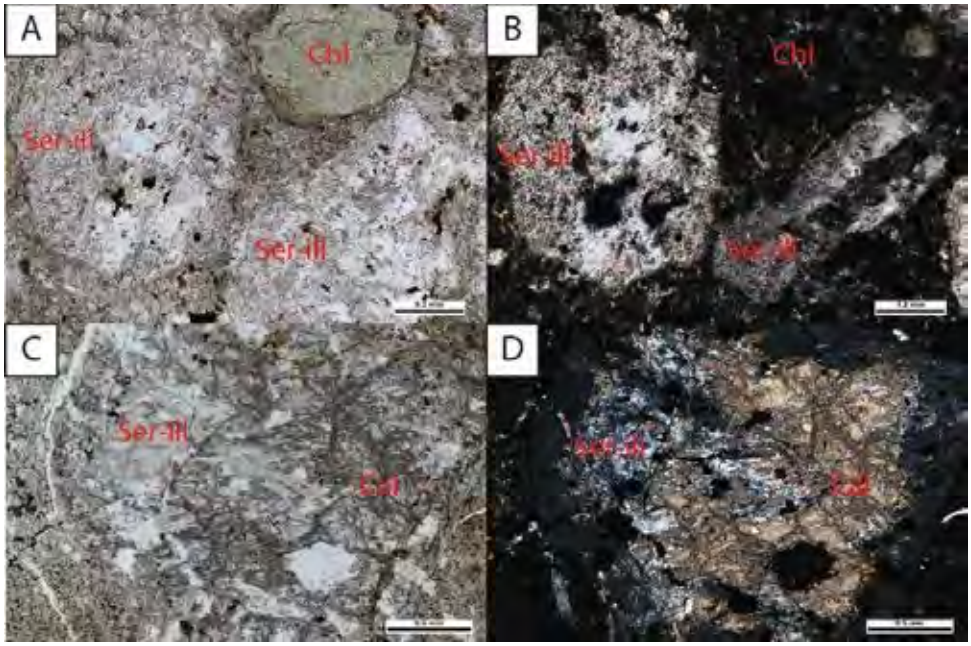

Fig. 4.23 Characteristics of sericite-illite-chlorite-adularia-quartz (A) Photomicrograph showing sericite-illite and chlorite in PPL (B) Same as Fig. A in XPL (C) Photomicrograph showing sericite-illite and calcite in PPL (D) Same as Fig. C in XPL Abbreviation: Ser = sericite, Ill = illite, Chl = chlorite, Cal = calcite

XRD results

XRD results (Table 4.3) are used to confirm the microscopic examination. Some of mineral are low content to observe in microscope. Sericite and illite can't be separate by microscope observation, XRD results can be used to separate them. However, XRD can't separate quartz between primary quartz and secondary quartz (Microcrystalline quartz or alteration quartz)

Table 4.3 XRD results of altered wall rocks

Sample	Quartz	Chlorite	Adularia	Sericite	Illite	Pyrite	Albite
4562-114.2	99.85	-	0.15	-	-	0.01	-
4562-238.9	90.88	0.05	0.26	0.09	0.13	0.21	8.36
4564-193.5	87.45	0.03	7.48	0.15	0.19	4.70	-
4576-21.2	73.05	7.83	0.12	0.15	0.06	0.05	18.74
4576-44.1	98.60	-	0.32	0.04	0.02	1.02	-
4576-97.8	99.79	-	0.14	-	-	0.08	-
4576-129.3	98.88	-	0.21	-	-	0.90	-

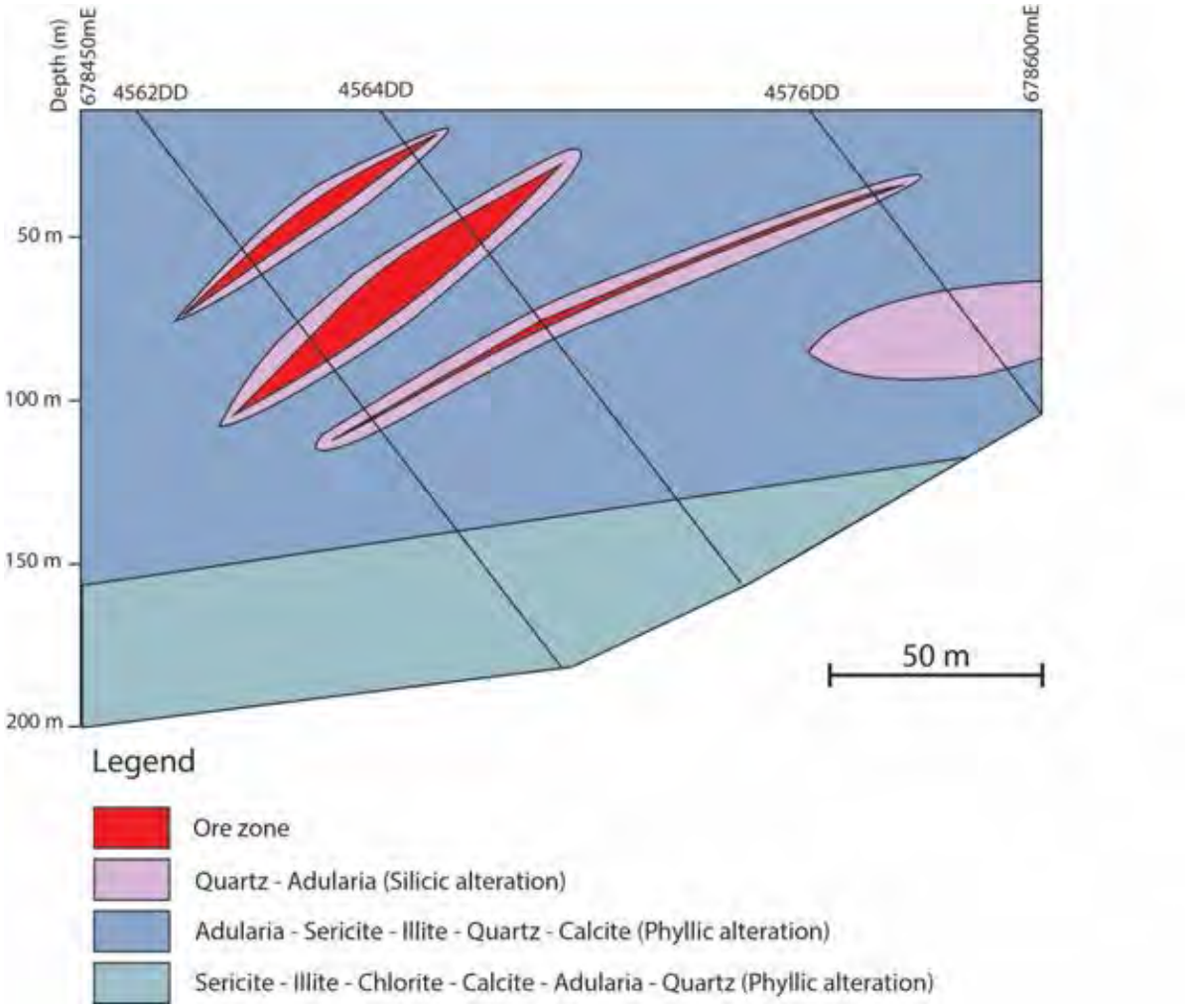

Fig. 4.24 E-W cross section (section no 1800085N) showing alteration zone representing by quartz-adularia zone (close to ore zone). However, some part quartz-adularia zone doesn't have ore zone closely. Adularia-sericite-illite-quartz-calcite zone and sericite-illite-chlorite-adularia-quartz are next from quartz-adularia zone, respectively

Chapter 5

Discussion and conclusion

5.2 Discussion

This chapter interprets and discusses all results from previous chapter in three aspects namely; geology, mineralization and hydrothermal alteration.

5.2.1 Geology

The whole volcanics sequence (Unit 1, 2, and 4) of the B-prospect can be compared to the volcanogenic sedimentary unit (Unit 2), polymivtic mafic-intermediate breccia unit (Unit 3), and upper porphyritic andesite unit (Unit 4) of the Chatree volcanics of Salam (2013; Fig. 5.1). The unit 1 and 2 of this study are equivalent to the volcanogenic sedimentary unit (Unit 2) of Chatree deposit. This study suggested to subdivide volcanogenic sedimentary unit of Salam (2013) into polymictic breccia (Unit 1) and volcanogenic sedimentary breccia (Unit 2). Because polymictic breccia in unit 1 shows the presence of plagioclase phyric andesite clast but sandy matrix polymictic breccia in unit 2 cannot be found. The fiamme breccia unit (Unit 3) can be equivalent to polymictic mafic-intermediate breccia (Unit 3) of Salam (2013) because fiamme breccia in this study can be found as two rock types; fiamme breccia, and polymictic breccia in this unit which have characteristics as polymictic mafic-intermediate breccia (Unit 3) of Salam (2013). It can be implied to variety of environmental deposit. In part of andesitic breccia unit (Unit 4) can be equivalent to the top of porphyritic andesitic unit (Unit 4) because the characteristics of andesitic breccia unit in this study is similar to plagioclase phyric andesite breccia facies.

In the part of stratigraphy, B-prospect cannot be found in the unit 1 and lower of the unit 4 (Salam, 2013) that can be interpreted as the erosion of fiamme breccia unit (Unit 1). The unit 4 is not found because the depth of drill core is not

enough. The setting of B-prospect can be compared to volcanic setting of Chatree deposit (Salam, 2013) based on rock types (Fig. 5.1) which rock unit is similar to A pit. (Fig. 5.2). B-prospect can be equivalent to A pit setting (Fig. 5.3).

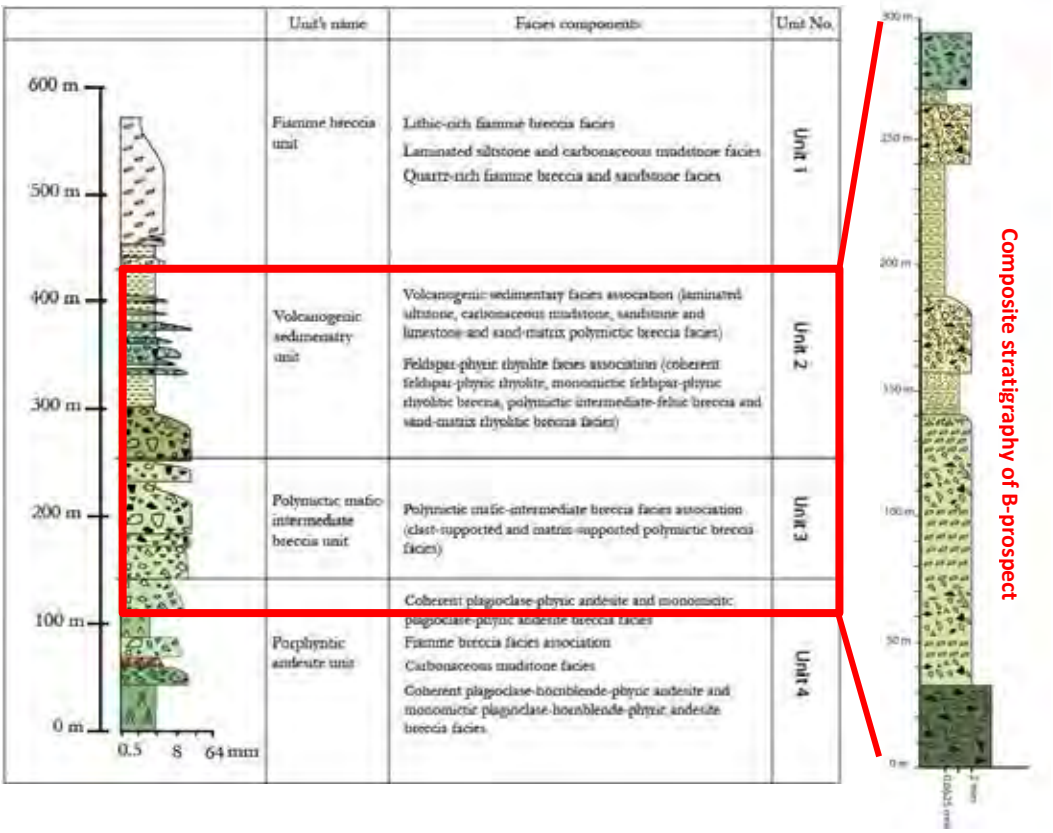

Fig. 5.1 Stratigraphy of Chatree deposit includes stratigraphy of B-prospect can be consider to unit 2, unit 3 and top of unit 4. (Salam, 2013)

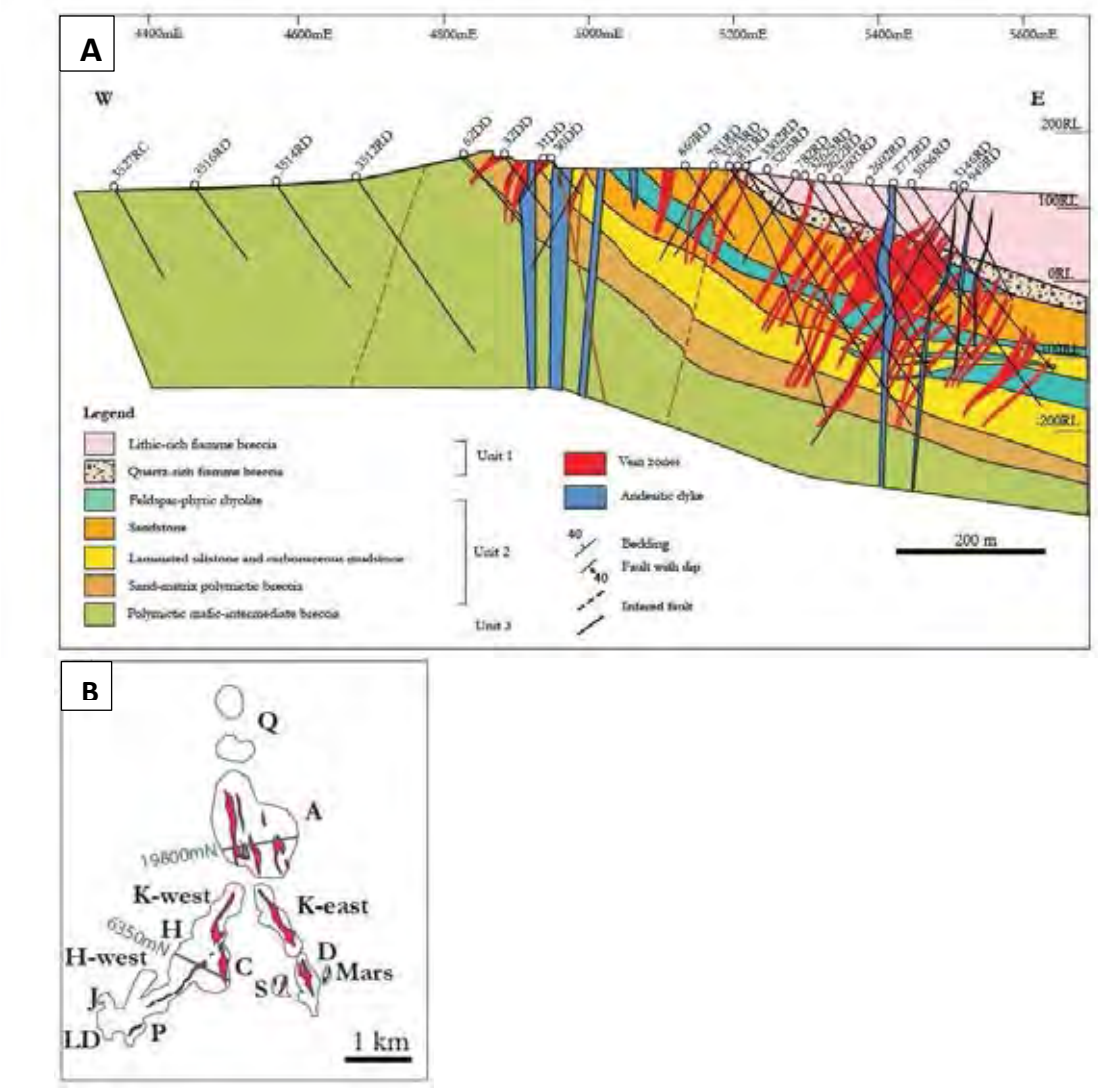

Fig. 5.2 (A) Cross section of A pit showing geology and ore body that same as the B prospect. (B) The location of cross section of A pit. (Salam, 2013)

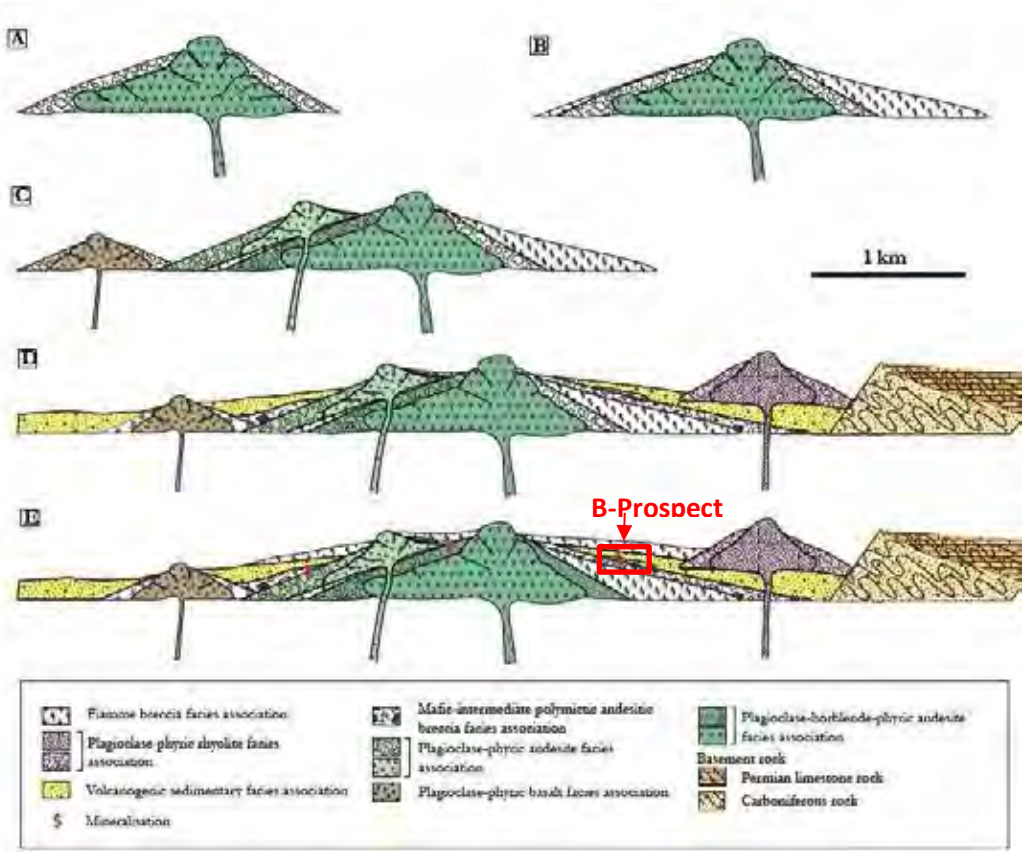

Fig. 5.3 Schematic volcanic setting and architecture of Chatree deposit. **A**. Emplacement of andesitic dome in the early stage of arc formation in graben structure consisting of coherent andesite and its associated monomictic andesitic breccia. **B**. Deposition of fiamme breccia facies association on the slope of early formed andesite dome from distal sources containing carbonaceous mudstone facies at the base of the unit. **C**. Formation of plagioclase-phyric andesite dome which has intruded the early andesite and fiamme breccia facies association on the western side comprising coherent and monomictic andesitic breccia. This facies association is widely distributed in the western part of Chatree south (C to J lenses). Basalt dome was also emplaced accompanied by monomictic basaltic breccia at Khao Ruak. **D**. Deposition of volcanogenic sedimentary facies association occurred in a calm environment mainly in the northern of Chatree and southwest of Khao Chet Lok district area. Plagioclase-phyric rhyolite facies association was emplaced in the northeast towards the end of sedimentation. **E**. Emplacement of fiamme breccia facies as a result of explosive eruption marked by the end of the main volcanism in the Chatree area. Note that mineralisation mainly occurred in the volcanic breccia (monomictic andesite breccia facies and mafic-intermediate polymictic breccia facies) and volcanogenic sedimentary facies association. (Salam, 2013)

5.2.2 Mineralization

Paragenesis sequence of B-prospect can be divided the mineralization stage into three stages (Fig. 4.14). The mineralization stage of Chatree deposit can be divided into seven stages (Salam, 2013) (Fig. 5.4) and the mineralization stage of Q prospect can be divided into five stages (Tangwathananukul, 2014) (Fig. 5.5). Because this study does not have enough samples to subdivide the mineralization stages. The criteria for dividing mineralization stages are cross-cutting relationship, mineral assemblages of veins and textures. However, this study focuses on section 1800085N so the samples in this study are not enough to subdivide mineralization stages. This study can only divide into pre-, main- and post- Au-Ag mineralization stage. In the comparison between this study and Salam, 2013, Pre Au-Ag mineralization stage of this study can be equivalent to stage 1, 2 and 3 of Chatree deposit and stage 2 and 3 of Q prospect. Main Au-Ag mineralization stage of this study can be equivalent to stage 4 of Chatree deposit and stage 4 of Q prospect. Post Au-Ag mineralization stage of this study can be equivalent to stage 5, 6 and 7 of Chatree deposit and stage 5 of Q prospect. The purity of gold (fineness) can be calculated by ratio of Au/Au+Ag. The fineness of B-prospect is 619.64 that can be identified to be electrum same as Chatree deposit.

In part of mineral types, B prospect and Q prospect are less than Chatree deposit in Salam, 2013. The locations of both prospects are southern and northern of Chatree deposit. (Fig. 5.6) There can be implied to the relation between location and mineral types. Chatree deposit may be center of epithermal low sulfidation system but B prospect and Q prospect are peripheral of the system.

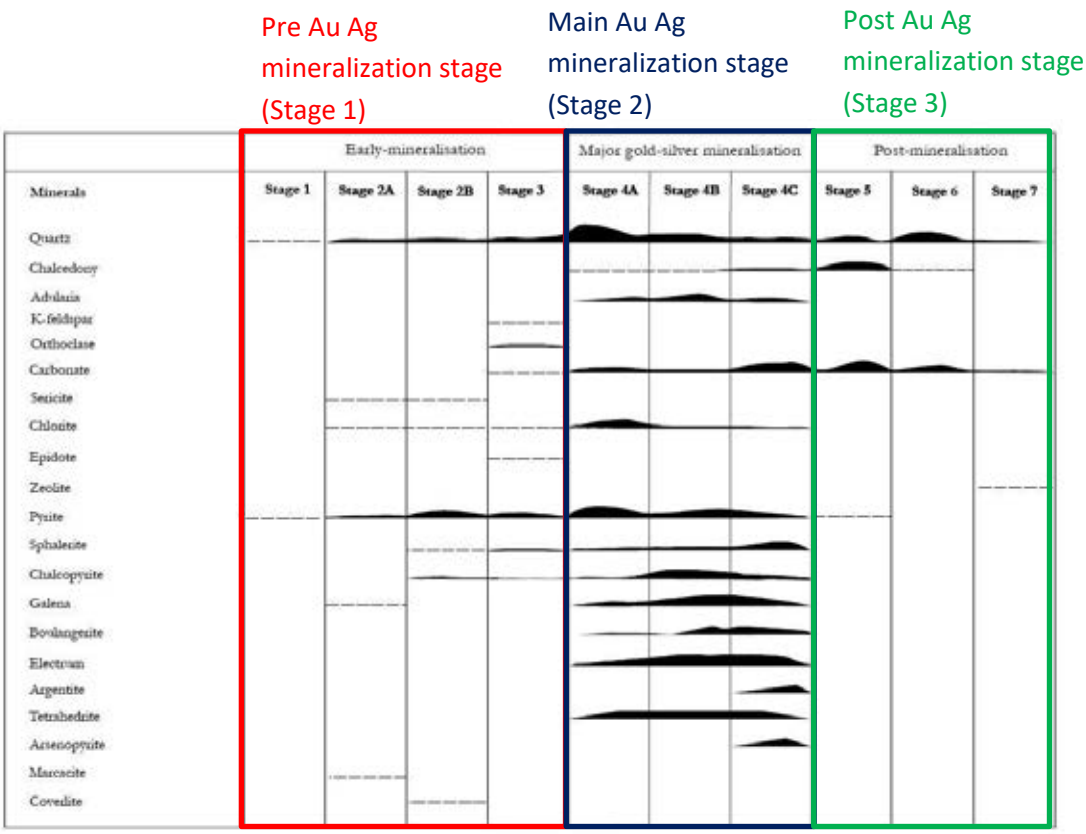

Fig. 5.4 Paragenesis diagram showing the occurrence and relative abundance of ore and gunge minerals of infill stage at the Chatree deposit compare to B prospect (Salam, 2013)

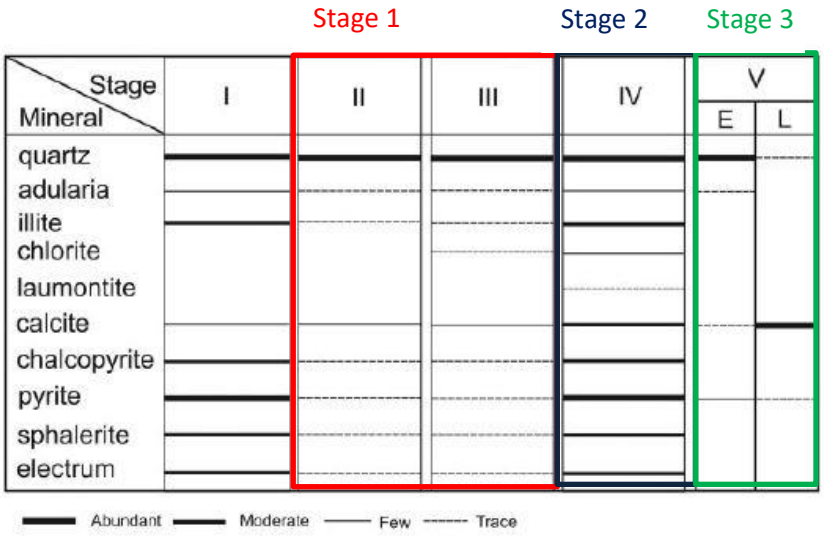

Fig. 5.5 Paragenesis sequence of gold mineralization at the Q prospect in the Chatree deposit compare to B prospect (Tangwattananukul, 2014)

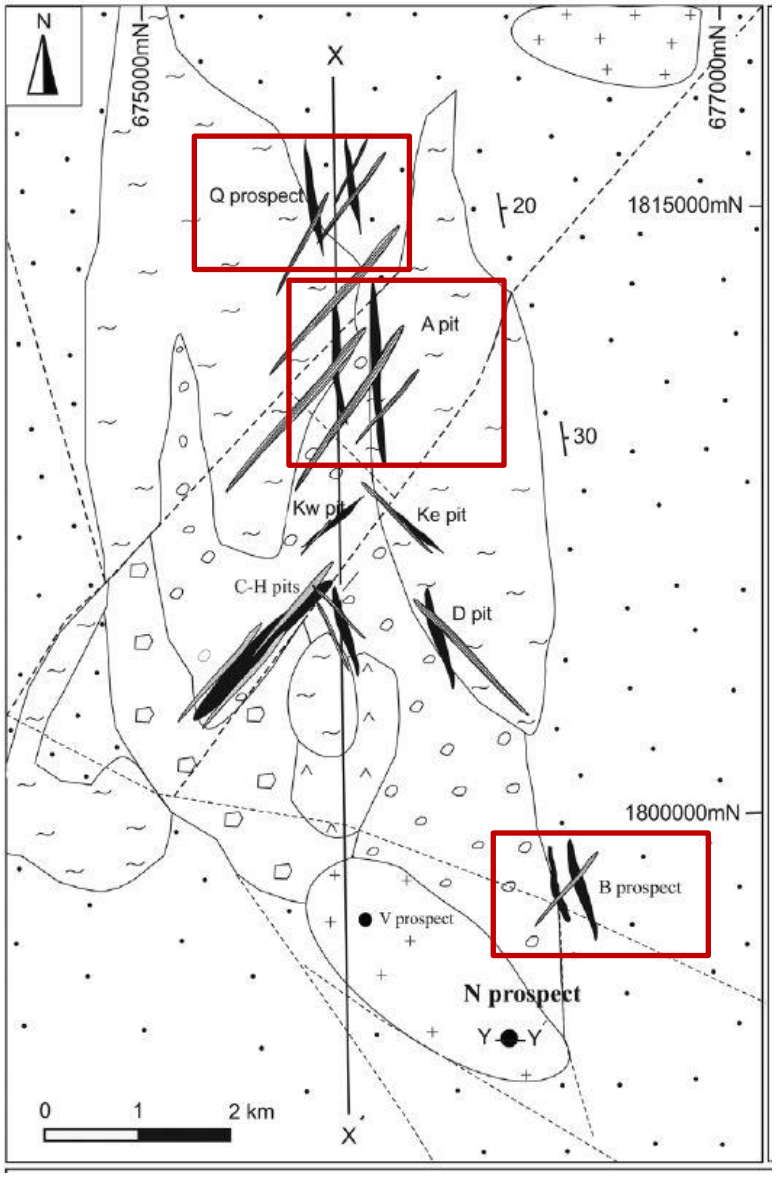

Fig. 5.6 Map of Chatree deposit showing A pit, Q prospect and B prospect (Tangwattananukul, 2014)

5.2.3 Alteration

Alteration zone of B-prospect can be divided into 3 zones which are compared to alteration zones of A pit of Salam (2013; Fig. 5.7) because the geology of A pit same as b-prospect. Quartz-adularia zone in this study can be equivalent to the qtz-ill-adl-py (Silicic alteration) of A pit. Qdularia-sericite-illite-quartz±calcite zone and sericite-illite±chlorite±calcite±quartz zone (Phyllic alteration) can be equivalent to ill-qtz-adl-chl-cal-py (phyllic alteration) but A pit does not have sericite and quartz as B-prospect. However, B prospect in this study area does not have propylitic alteration because in this study is near ore zone and has many veinlets. In alteration zones of section 1800085N has the presence of quartz-adularia (silicic alteration) without the ore zone nearly that can be implied to have ore zone in the other sections. Finally, there is adularia found in B-prospect which is the indicator of epithermal low sulfidation system (Dong and Morrison, 1995).

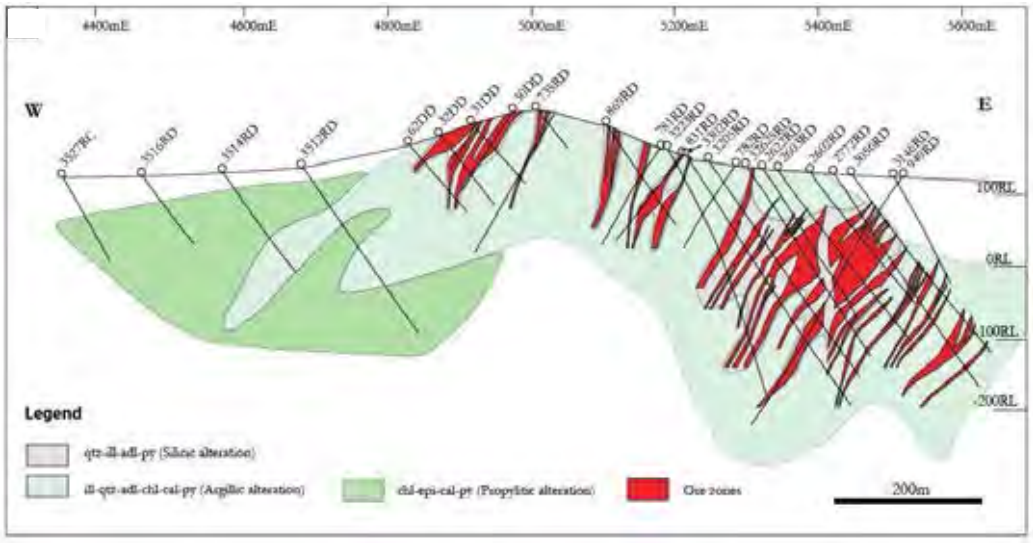

Fig. 5.7 Alteration zone of A pit in Chatree deposit (Salam, 2013)

5.3 Conclusion

The geology of B-prospect in section 1800085N can be divided into 4 rock units that are polymictic breccia unit (Unit 1), volcanogenic sedimentary unit (Unit 2), fiamme breccia unit (Unit 3), and andesitic breccia unit (Unit 4). In the part of stratigraphy, Andesitic breccia unit is the base of the sequence. Then, Fiamme breccia unit and volcanogenic sedimentary unit are overlain on the andesitic breccia unit respectively. Finally, polymictic breccia unit is covered on the top of the sequence. In the part of mineralization, ore zone can be found in the term of veins and veinlets as the lens in top of the section. The paragenesis sequence of this study can be divided into 3 stages are pre Au-Ag mineralization stage, main Au-Ag mineralization stage and post Au-Ag mineralization stage. The pre Au-Ag mineralization stage has quartz-pyrite veins. The main Au-Ag mineralization stage has quartz ± carbonate – sulfides - electrum veins. The post Au-Ag mineralization stage has quartz ± carbonate veins. The purity of gold (Fineness) is 619.94 that can be defined to electrum which higher value when grain size is increase. The alteration zone of b-prospect in this section can be divided into 3 zones that are quartz-adularia zone, adularia-sericite-illite-quartz-calcite zone and sericite-illite-chlorite-calcite-quartz zone. The zones are proximal to the ore zone and distal from the ore zone respectively. In the alteration minerals can be found for adularia which is the indicator of alteration mineral of epithermal low sulfidation system. The mineralization at B-prospect can be distinguished from Chatree deposit by its simple mineral assemblages. And it can be classified as a low-sulfidation epithermal deposit.

Recommendations for future works

The future work can be studied in the detail about more data of drill core and geochemistry:

1) In part of field details, the future study can be expanded to more section that can be correlated to be 3 dimensions.

2) In part of geochemistry, the future study can be study in more detail of geochemistry about stable isotope e.g. oxygen isotope, sulfur isotope that can be implied to create the model of the deposit. In addition, the chemistry of pyrites can be studied by LA-ICP MS.

References

Bunopas, S. and Vella, P.,1983. Tectonic and geologic evolution of Thailand. *In* Nutalaya, P. (ed.) Proc. of the workshop on stratigraphiccorrelation of Thailand and Malaysia. Geological Society of Thailand and Geological Society of Malaysia, 8th–10th Sept., 1983, Haad Yai, Thailand, 212–232.

Charusiri, P., Daorerk, V., Archibald, D., Hisada, K. & Ampaiwan, T., 2002. Geotectonic evolution of Thailand: a new synthesis. Journal of the Geological Society of Thailand 1, 1–20.

De Little, J.V., 2005. Geological setting, nature of mineralization, and fluid characteristics of the Wang Yai prospect, central Thailand, University of Tasmania.

Dong, G., Morrison, G.W., 1995. Adularia in epithermal veins, Queenland: morphology, structural state and origin, Mineral Deposita 30,11-19 (1995).

Khin Zaw and Meffre, S., 2007, Supplementary Report, Geochronology, metallogenesis and deposit styles of Loei Foldbelt in Thailand and Laos PDR, ARC Linkage Project.

Kromkhun, K., 2005, Geological setting, mineralogy, alteration, and nature of ore fluid of the H zone, the Chatree deposit, Thailand, University of Tasmania.

Paipana, S., 2014. Geology and mineralisation characteristics of bo thong antimony ± gold deposit, chonburi province, eastern Thailand, University of Tasmania.

Salam, A., Khin Zaw,Meffre, S.,McPhie, J., Lai, C.K., 2014. Geochemistry and geochronology of epithermal Au-hosted Chatree volcanic sequence: implication for tectonic setting of the Loei Fold Belt in central Thailand, Gondwana Research.

Salam, A., 2013. A geological, geochemical and metallogenic study of the Chatree epithermal deposit, Petchabun Province, Central Thailand. Unpublished PhD thesis, ARC Centre of Excellence in Ore Deposits (CODES) University of Tasmania, Hobart, Australia, p. 250.

Salam, A., Zaw, K., Meffre, S., Golding, S., McPine, J., Suphananthi, S. & Jamws, R. 2008. Mineralisation and Oxygen Isotope Zonation of Chatree Epithermal Gold-Silver Deposit, Phetchabun Province, Central Thailand. PACRIM Congress.

Sangsiri, P., Pisutha-Arnond, V., 2008. Host Rock Alteration at the A Prospect of the Chatree Gold Deposits, Phichit Province, Central Thailand: A Preliminary Re-

Evaluation, Proceedings of the International Symposia on Geoscience Resources and Environments of Asian Terranes (GREAT 2008), 4th IGCP 516, and 5th APSEG.

Shikazono, N. and Shimizu, M., 1987. The Ag/Au ratio of native gold and electrum and the geochemical environment of gold vein deposits in Japan, Mineral Deposita 22, 309-314.

Tangwatthananukul, L. and Ishiyama, D. 2017.Characteristics of Cu-Mo mineralization in the Chatree Mining Area, Central Thailand. Resource Geology Vol. 68, 83-92.

Tangwattananukul, L., Ishiyama, D., Matsubuya, O., Mizuta, T., Charusiri, P., Sato, H., & Sera, K., 2014. Characteristics of Triassic epithermal Au mineralization at the Q prospect, Chatree mining area, Central Thailand, Resource Geology, 1-8.

APPENDIX

A. XRD results

The XRD results of altered rock samples are used to support the petrographic results.

Table A.1 XRD result of sample 4562-114.0

Left Angle	Right Angle	Net Height	Raw Area	Net Area	%	SS-VVV-PPPP	Compound Name	Formula	System
2-Theta °	2-Theta °	Cps	Cps x 2-Theta °	Cps x 2-Theta °					
26.44	26.88	292	65.41	57.83	99.85	01-085-0930 (C)	Quartz	SiO2	Hexagonal
26.92	27	1.61	1.244	0.084	0.15	01-071-0956 (C)	Adularia	K4Al4Si12O32	Monoclinic
33.04	33.08	0.16	0.232	0.004	0.01	00-024-0076 (D)	Pyrite	FeS2	Cubic
				57.918	100				

Table A.2 XRD result of sample 4562-238.9

Left Angle	Right Angle	Net Height	Raw Area	Net Area	%	SS-VVV-PPPP	Compound Name	Formula	System
2-Theta °	2-Theta °	Cps	Cps x 2-Theta °	Cps x 2-Theta °					
26.52	26.9	186	45.54	35.47	90.88	01-085-1054 (C)	Quartz alpha	SiO2	Hexagonal
37.6	37.66	0.53	0.422	0.021	0.05	01-072-1385 (C)	Chlorite, chromian	Mg5.1Al1.2Si3Cr.7O10(OH)8	Triclinic
26.94	27.04	1.24	1.696	0.102	0.26	01-071-1543 (C)	Adularia	K(AlSi3O8)	Monoclinic
33	33.12	0.98	1.214	0.082	0.21	00-024-0076 (D)	Pyrite	FeS2	Cubic
35.22	35.3	0.58	0.977	0.036	0.09	00-003-0197 (D)	Sericite [NR]	K2O·3Al2O3·6SiO2·2H2O	Monoclinic
34.8	34.9	0.7	1.545	0.05	0.13	00-009-0334 (D)	Illite 2M1	K-Na-Mg-Fe-Al-Si-O-H2O	Monoclinic
27.36	27.82	13.4	7.878	3.269	8.38	01-071-1156 (C)	Albite high	Na(AlSi3O8)	Triclinic
				39.03	100.00				

Table A.3 XRD result of sample 4564-193.5

Left Angle 2-Theta °	Right Angle 2-Theta °	Net Height Cps	Raw Area Cps x 2-Theta °	Net Area Cps x 2-Theta °	%	SS-VVV-PPPP	Compound Name	Formula	System
26.48	26.86	228	55.02	43.44	87.45	01-085-1054 (C)	Quartz alpha	SiO2	Hexagonal
37.56	37.68	0.29	0.761	0.015	0.03	01-072-1385 (C)	Chlorite, chromian	Mg5.1Al1.2Si3Cr.7O10(OH)8	Triclinic
27.36	27.78	17.9	7.879	3.714	7.48	01-071-1543 (C)	Adularia	K(AlSi3O8)	Monoclinic
19.66	19.8	1	1.074	0.076	0.15	00-012-0216 (D)	Sericite [NR]	KAl2(Si3Al)O10(OH,F)2	
19.8	19.94	1.02	1.046	0.095	0.19	00-009-0334 (D)	Illite 2M1	K-Na-Mg-Fe-Al-Si-O-H2O	Monoclinic
32.92	33.26	12.6	4.462	2.334	4.70	00-024-0076 (D)	Pyrite	FeS2	Cubic
				49.674	100.00				

Table A.4 XRD result of sample 4576-21.2

Left Angle 2-Theta °	*Right Angle 2-Theta °*	*Net Height Cps*	*Raw Area Cps x 2-Theta °*	*Net Area Cps x 2-Theta °*	*%*	*SS-VVV-PPPP*	*Compound Name*	*Formula*	*System*
26.42	*26.94*	*70.9*	*25.82*	*19.31*	*73.05*	*01-085-1054 (C)*	*Quartz alpha*	*SiO2*	*Hexagonal*
12.12	*12.68*	*7.11*	*3.345*	*2.071*	*7.83*	*01-072-1385 (C)*	*Chlorite, chromian*	*Mg5.1Al1.2Si3Cr.7O10(OH)8*	*Triclinic*
26.94	*27*	*0.79*	*1.059*	*0.031*	*0.12*	*01-071-1543 (C)*	*Adularia*	*K(AlSi3O8)*	*Monoclinic*
33	*33.08*	*0.26*	*0.193*	*0.012*	*0.05*	*00-024-0076 (D)*	*Pyrite*	*FeS2*	*Cubic*
8.78	*8.9*	*0.22*	*0.038*	*0.016*	*0.06*	*00-009-0343 (D)*	*Illite, trioctahedral*	*K0.5(Al,Fe,Mg)3(Si,Al)4O10(OH)2*	*Orthorhombic*
19.9	*20*	*0.74*	*0.645*	*0.039*	*0.15*	*00-003-0197 (D)*	*Sericite [NR]*	*K2O·3Al2O3·6SiO2·2H2O*	*Monoclinic*
27.32	*27.84*	*17.2*	*9.408*	*4.955*	*18.74*	*01-083-1609 (C)*	*Albite high*	*Na(AlSi3O8)*	*Triclinic*
				26.434	*100.00*				

Table A.5 XRD result of sample 4576-44.1

Left Angle 2-Theta °	Right Angle 2-Theta °	Net Height Cps	Raw Area Cps x 2-Theta °	Net Area Cps x 2-Theta °	%	SS-VVV-PPPP	Compound Name	Formula	System
26.5	26.96	152	39.57	30.78	98.60	01-085-0930 (C)	Quartz	SiO2	Hexagonal
26.96	27.06	1.29	2.164	0.1	0.32	01-071-0956 (C)	Adularia	K4Al4Si12O32	Monoclinic
19.7	19.76	0.39	0.378	0.014	0.04	00-012-0216 (D)	Sericite [NR]	KAl2(Si3Al)O10(OH,F)2	
18.1	18.14	0.26	0.225	0.005	0.02	00-009-0334 (D)	Illite 2M1	K-Na-Mg-Fe-Al-Si-O-H2O	Monoclinic
33.04	33.2	2.96	1.311	0.319	1.02	00-024-0076 (D)	Pyrite	FeS2	Cubic
				31.218	100.00				

Table A.6 XRD result of sample 4576-97.8

Left Angle 2-Theta °	Right Angle 2-Theta °	Net Height Cps	Raw Area Cps x 2-Theta °	Net Area Cps x 2-Theta °	%	SS-VVV-PPPP	Compound Name	Formula	System
26.48	26.88	247	56.03	47.45	99.79	01-085-1054 (C)	Quartz alpha	SiO2	Hexagonal
26.94	27	2	1.013	0.066	0.14	01-071-1543 (C)	Adularia	K(AlSi3O8)	Monoclinic
33.04	33.12	0.61	0.656	0.036	0.08	00-024-0076 (D)	Pyrite	FeS2	Cubic
				47.552	100.00				

Table A.7 XRD result of sample 4576-129.3

Left Angle 2-Theta °	Right Angle 2-Theta °	Net Height Cps	Raw Area Cps x 2-Theta °	Net Area Cps x 2-Theta °	%	SS-VVV-PPPP	Compound Name	Formula	System
26.44	26.88	259	59.55	52.11	98.88	01-085-1054 (C)	Quartz alpha	SiO2	Hexagonal
26.94	27.06	1.6	1.591	0.112	0.21	01-071-1543 (C)	Adularia	K(AlSi3O8)	Monoclinic
32.82	33.14	2.47	1.492	0.476	0.90	00-024-0076 (D)	Pyrite	FeS2	Cubic
				52.698	100.00				

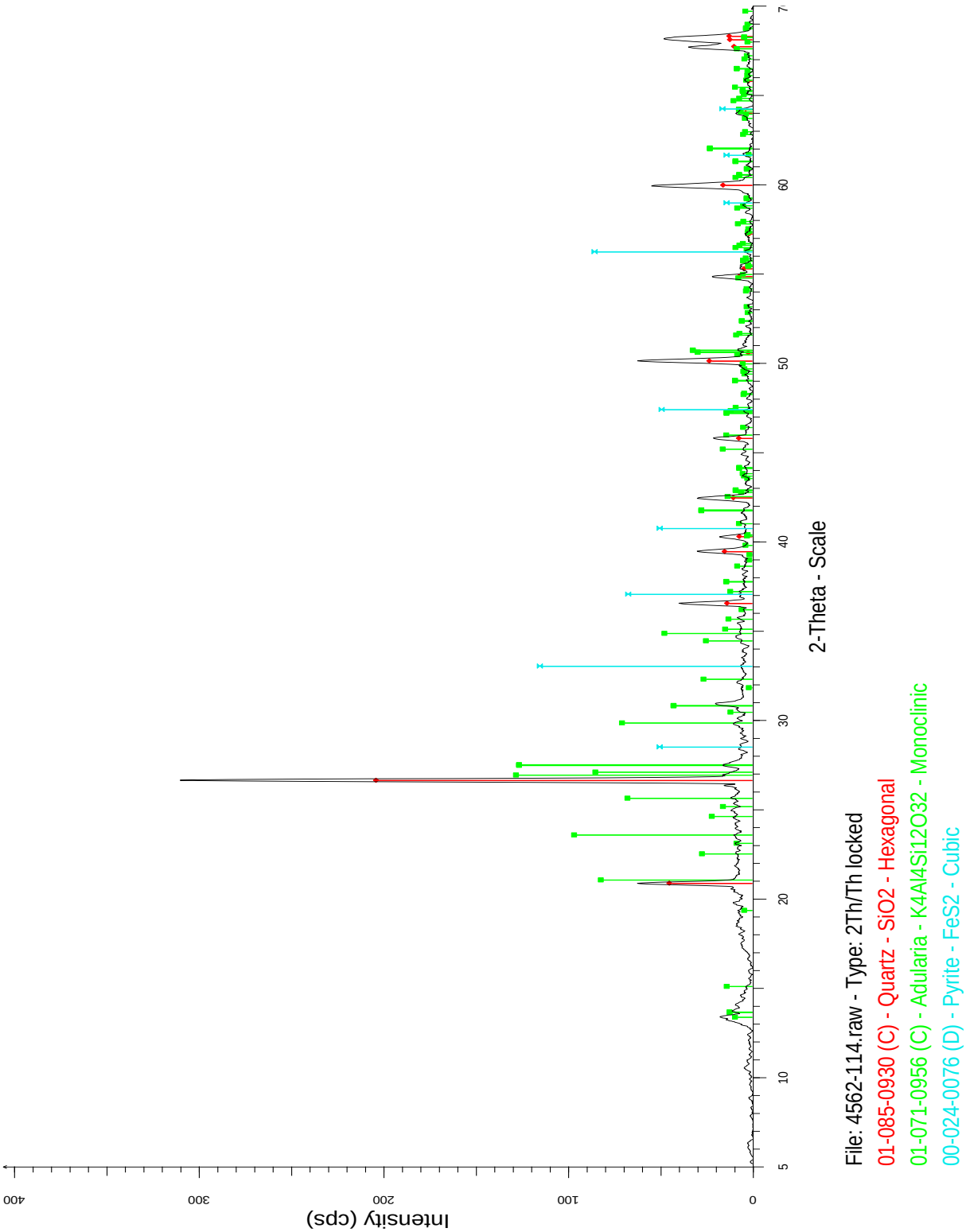

Fig. A.1 XRD result of sample 4562-114.0

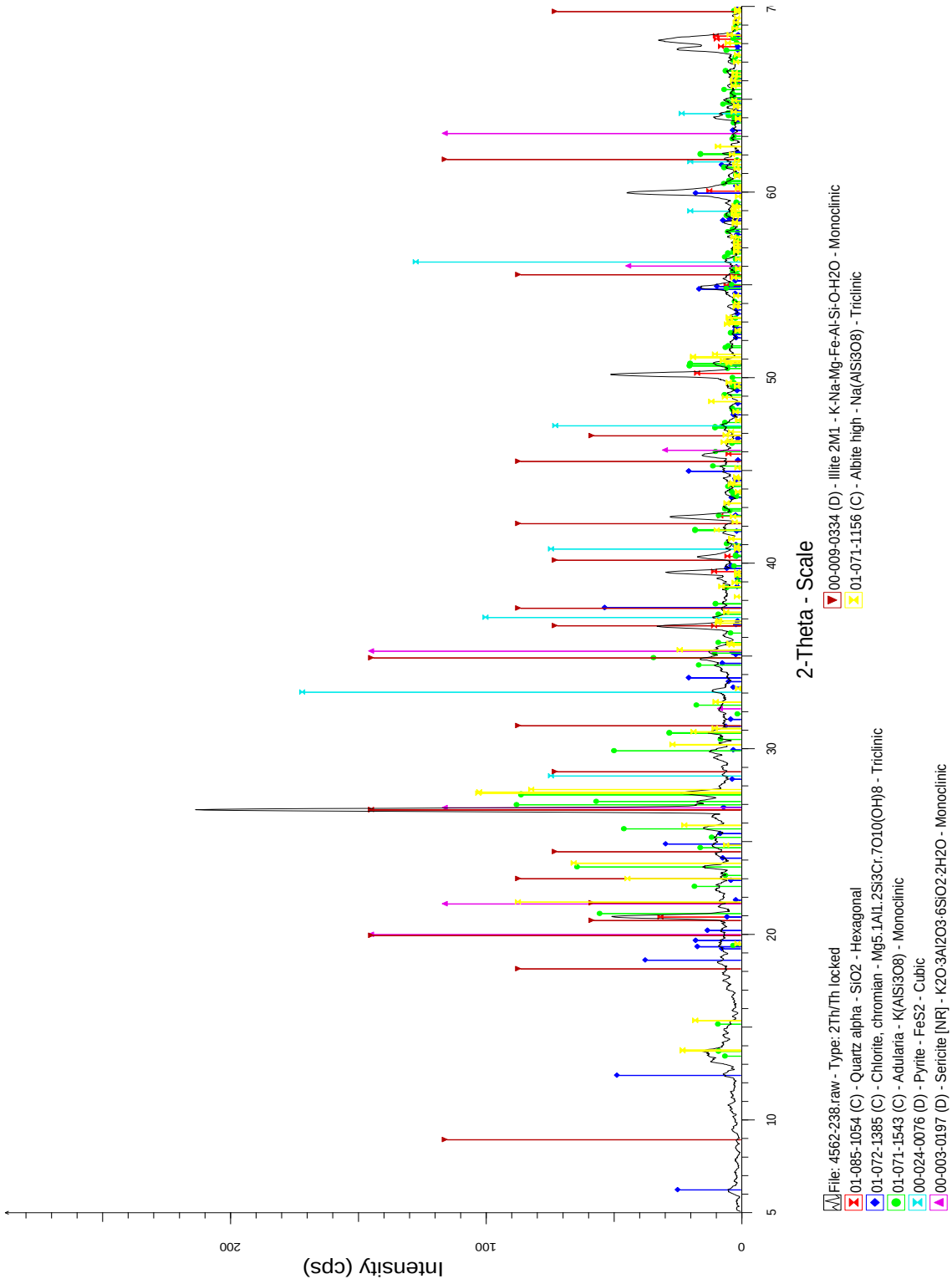

Fig. A.2 XRD result of sample 4562-238.9

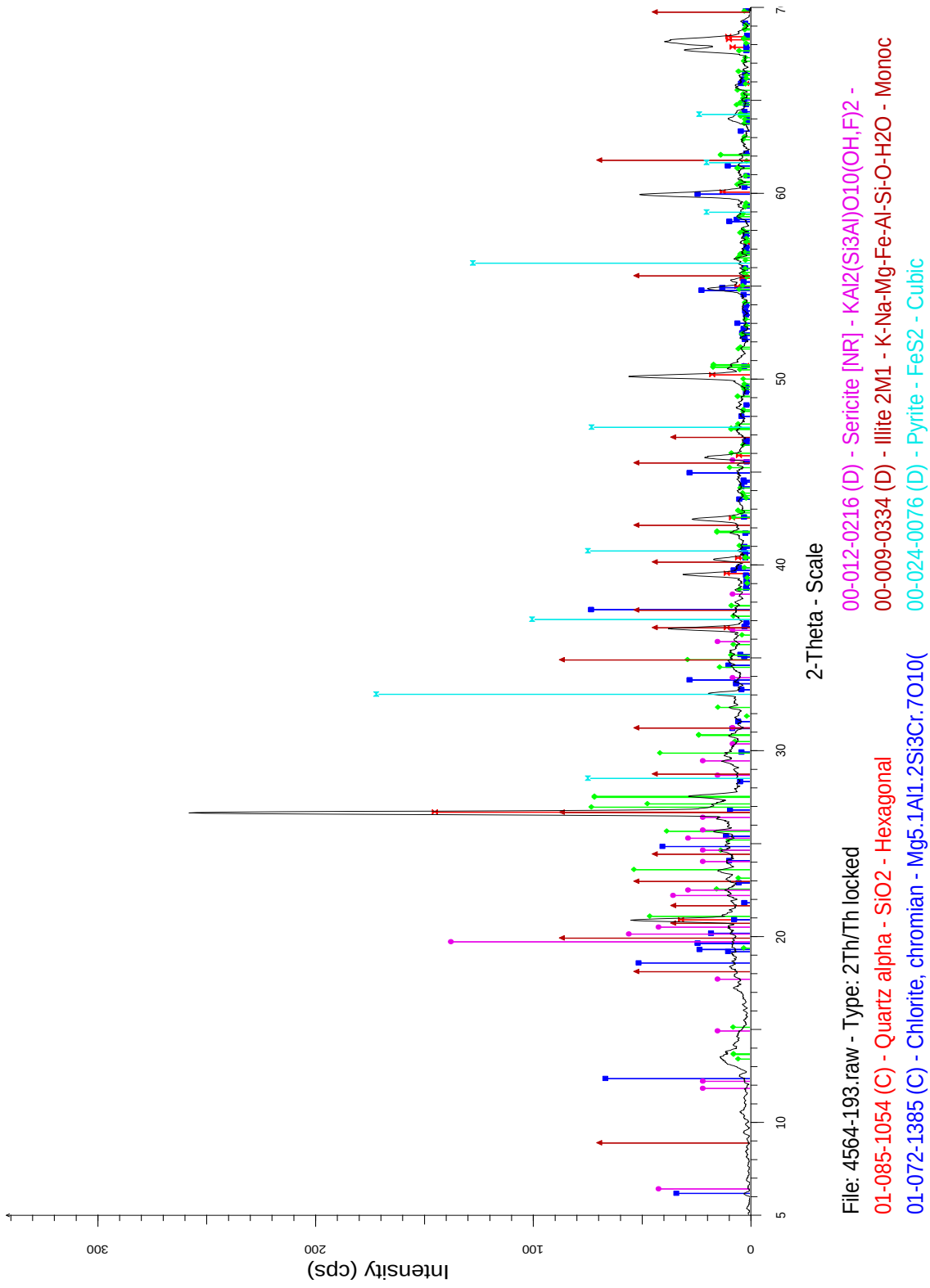

Fig. A.3 XRD result of sample 4564-193.5

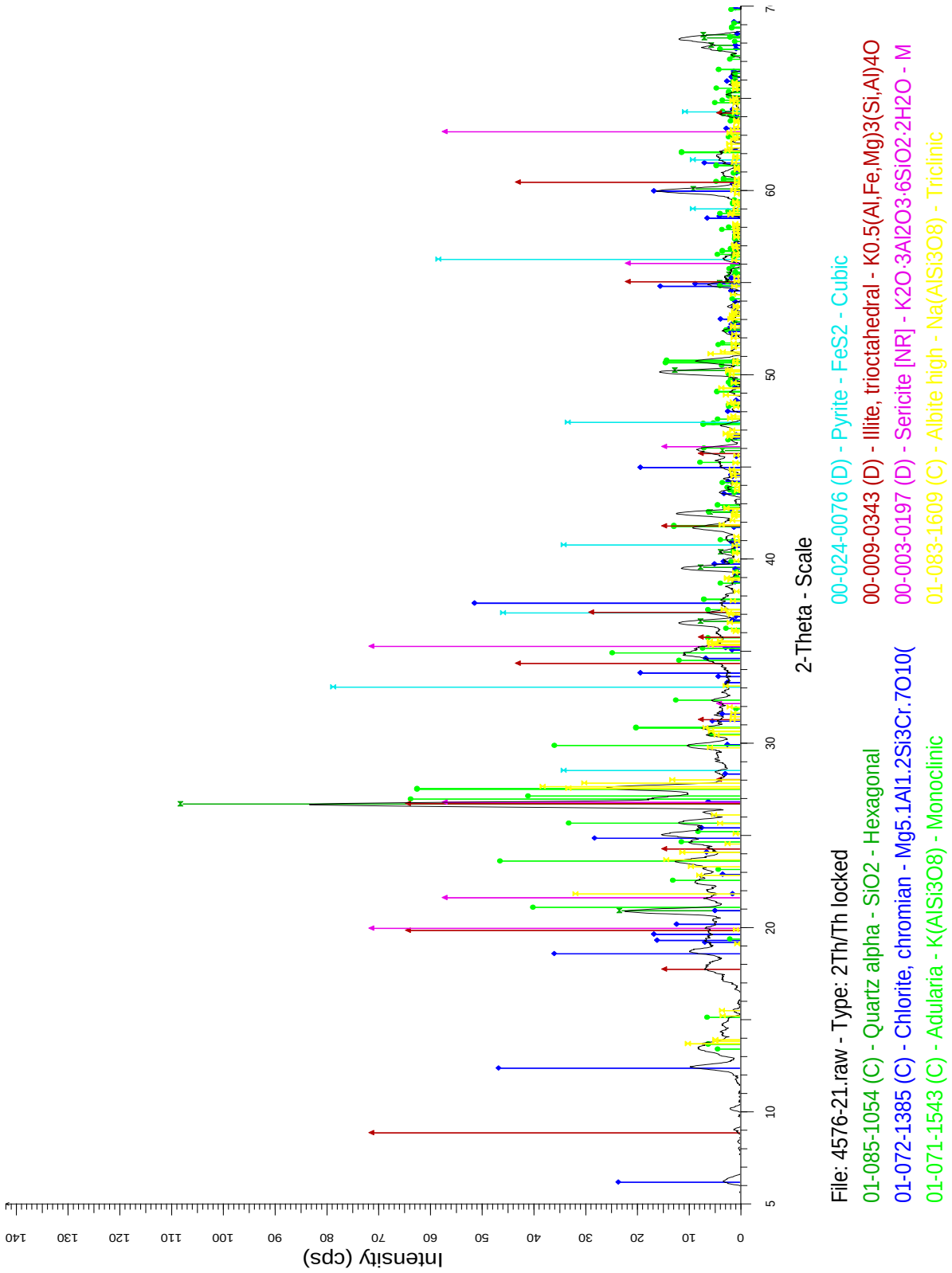

Fig. A.4 XRD result of sample 4576-21.2

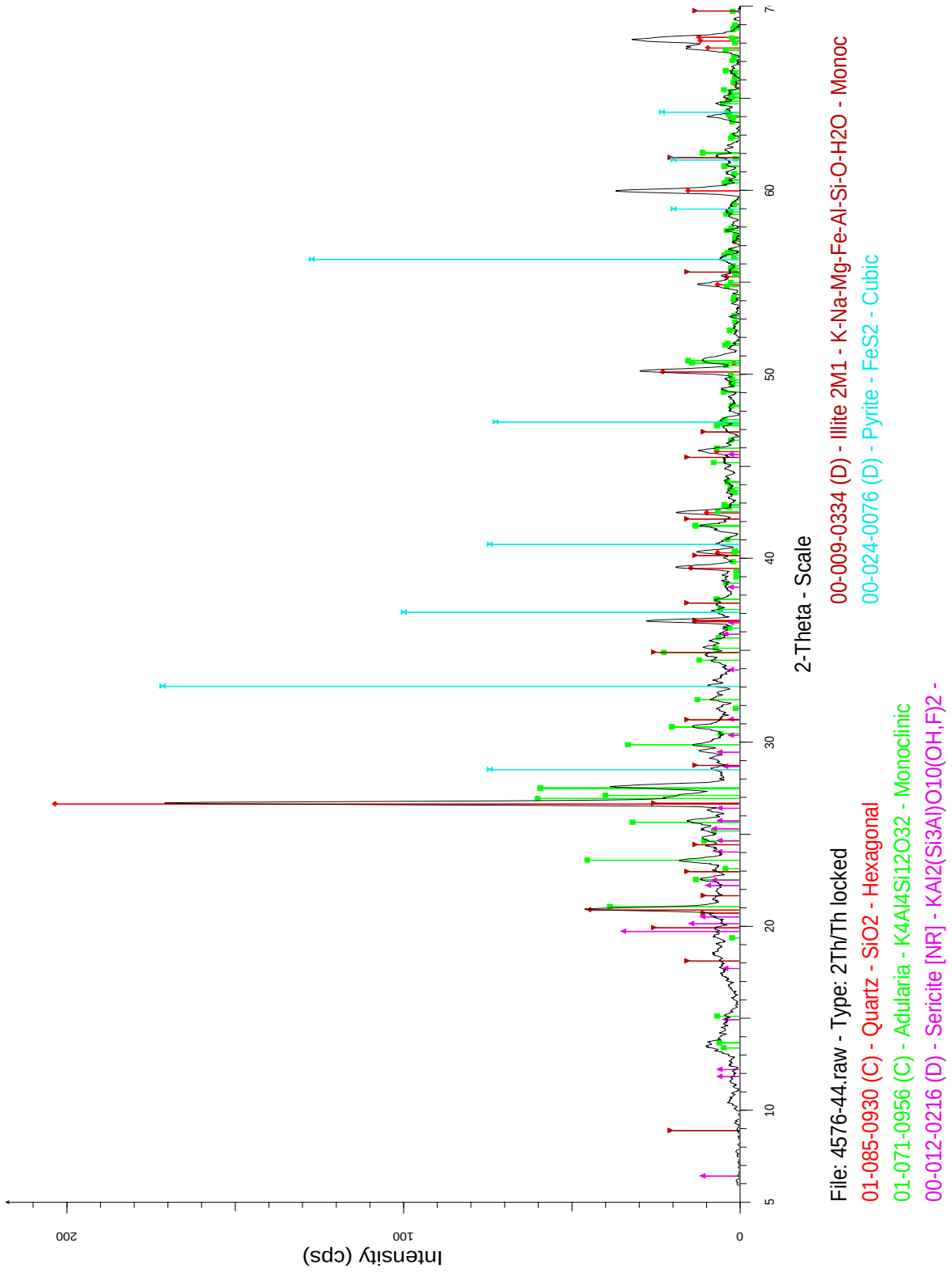

Fig. A.5 XRD result of sample 4576-44.1

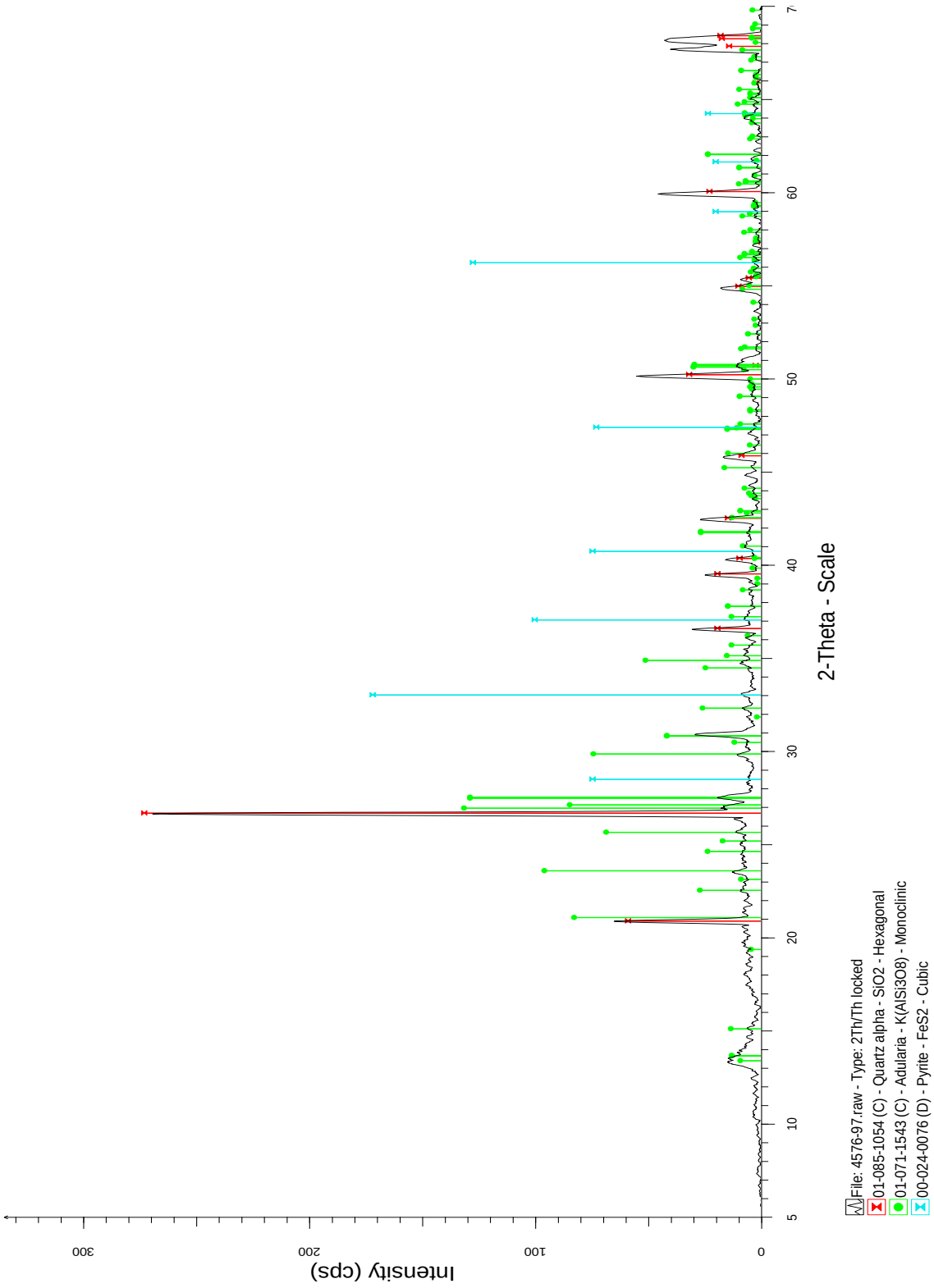

Fig. A.6 XRD result of sample 4576-97.8

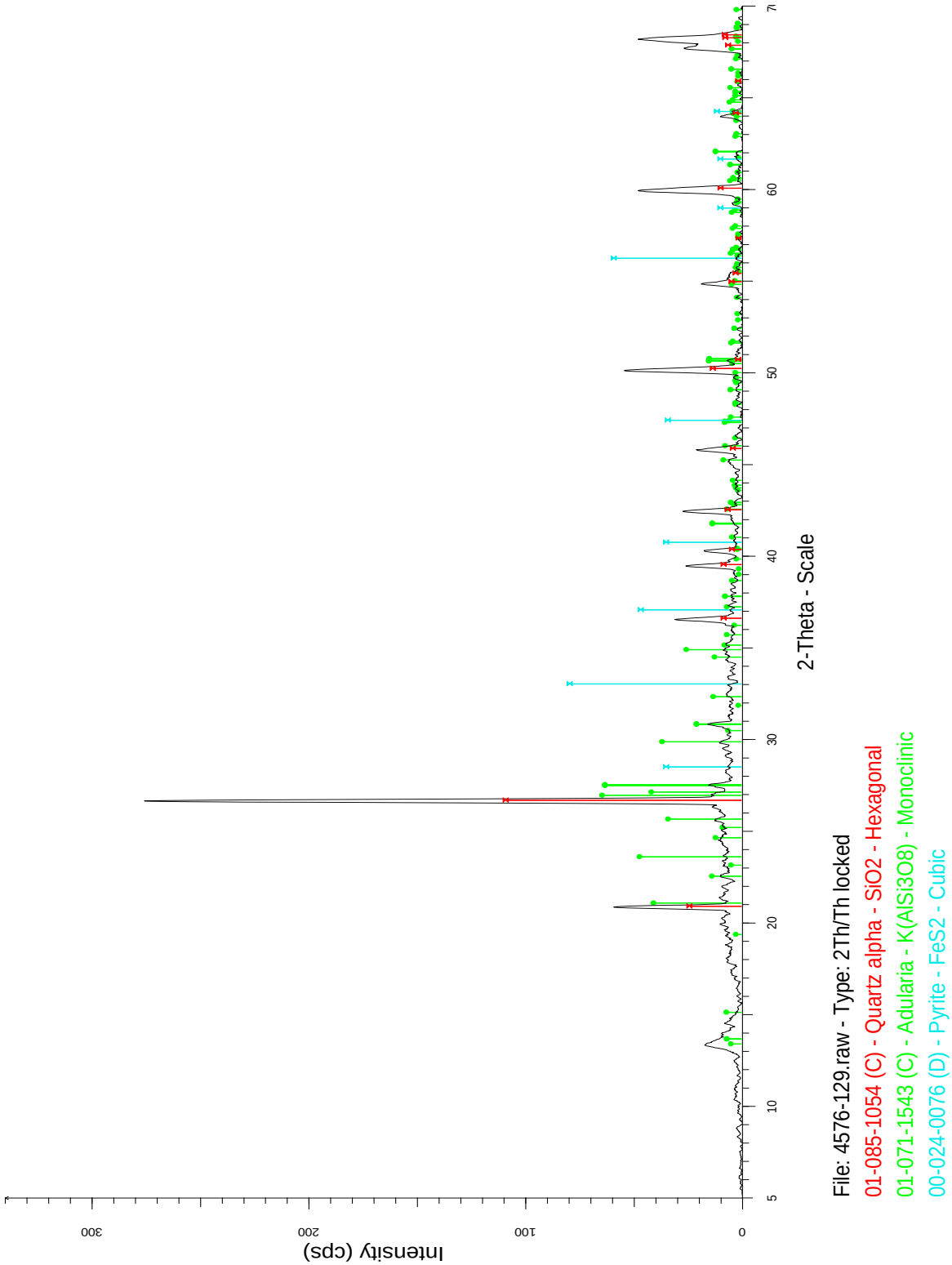

Fig. A.6 XRD result of sample 4576-129.3

B. EPMA result

Table B.1 EPMA result of sample 4562-97.8-2

No.	S	Pb	Cu	Fe	Zn	As	Au	Ag	Total	Comment
1	0	0	0.023	0.052	0	0	59.373	37.263	96.711	B2-F-1
2	0.005	0	0	0.002	0	0	59.208	37.391	96.606	B2-F-2
3	0.005	0	0.032	0.02	0	0	56.88	35.855	92.792	B2-F-3
4	0.01	0	0	0	0	0	56.26	36.372	92.642	B2-F2-1
5	0.068	0	0	0	0	0.022	38.694	26.08	64.864	B2-F2-2
6	0.04	0	0.016	0.042	0	0	52.913	35.006	88.017	B2-F2-3
7	0.006	0.054	0	0.061	0	0	57.94	36.671	94.732	B2-F3-1
8	0.02	0	0	0.036	0	0	58.827	36.452	95.335	B2-F3-2
9	0.005	0	0.013	0.004	0	0.01	0.218	0.037	0.287	B2-F3-3
10	11.98	0	0.297	6.66	0.557	0.014	34.374	32.052	85.934	B2-F4-1
11	8.944	0	0	20.788	0	0	61.055	23.124	113.911	B2-F4-2
12	0.053	0	0	0.152	0	0	59.257	37.316	96.778	B2-F4-3
13	3.222	0	0.115	3.359	0	0	56.259	34.346	97.301	B2-F5-1
14	47.292	0	0.07	41.318	0.026	0.065	0.274	0.009	89.054	B2-F5-2
15	46.921	0	0.049	40.616	0	0.032	0.445	0.078	88.141	B2-F5-3
16	0.005	0.018	0	0.011	0	0.015	63	37.256	100.305	B2-F6-1
17	0	0.031	0.069	0.017	0	0	60.25	37.313	97.68	B2-F6-2
18	0	0	0.052	0	0	0	60.067	36.5	96.619	B2-F6-3
19	0.092	0	0.006	0.056	0	0.065	59.6	36.387	96.206	B2-F7-1
20	0.015	0	0	0	0	0	62.03	36.453	98.498	B2-F7-2
21	0.034	0	0	0.003	0	0	17.986	15.573	33.596	B2-F7-3
22	0.02	0.064	0	0.395	0	0	60.68	36.666	97.825	B2-F8-1
23	0.026	0.053	0	0.062	0	0	62.222	36.947	99.31	B2-F8-2
24	0.014	0.035	0.01	0.1	0	0.016	63.39	36.837	100.402	B2-F8-3
25	0.066	0.046	0.02	0.443	0	0	60.727	37.197	98.499	B2-F9-1

26	1.012	0	0.029	2.956	0.009	0.006	57.509	36.402	97.923	B2-F9-2
27	44.062	0	0.03	35.751	0.024	0.045	0	0.007	79.919	B2-F9-3
28	0	0	0.011	0.359	0	0.026	60.746	37.542	98.684	B2-F10-1
29	0	0	0	0.179	0	0	61.821	36.961	98.961	B2-F10-2
30	0.063	0	0.084	0.348	0	0	62.041	36.493	99.029	B2-F10--3
31	0.492	0	0.002	2.24	0	0.009	59.329	36.099	98.171	B2-F11-1
32	0.941	0	0.045	1.808	0	0	58.808	36.009	97.611	B2-F11-2
33	22.502	0	0	21.193	0	0.073	28.008	17.728	89.504	B2-F11-3
34	0.001	0	0	0.283	0	0	62.101	36.82	99.205	B2-F12-1
35	0.037	0	0	0.61	0	0	62.11	36.54	99.297	B2-F12-2
36	0.022	0	0	0.287	0	0	60.829	36.89	98.028	B2-F12-3
37	0.019	0.035	0	0.023	0	0.02	56.748	36.512	93.357	B2-F13-1
38	0.099	0.022	0.054	0.05	0.104	0	57.704	36.818	94.851	B2-F13-2
39	0.017	0	0	0.323	0.04	0.016	3.277	2.248	5.921	B2-F13-3
40	0.027	0	0	0.446	0	0	63.333	36.491	100.297	B2-F14-1
41	0.011	0	0	0.074	0	0	62.389	37.266	99.74	B2-F14-2
42	0.006	0	0.026	0.042	0	0	61.209	36.619	97.902	B2-F14-3
43	0.034	0	0.028	0.659	0.012	0.004	60.37	36.787	97.894	B2-F15-1
44	46.453	0	0.027	40.016	0.032	0.541	1.303	0.498	88.87	B2-F15-2
45	39.571	0	0.017	36.467	0.01	0.488	8.442	4.21	89.205	B2-F15-3
46	0.153	0.135	0	0.436	0	0	61.047	36.968	98.739	B2-F16-1
47	3.291	0	0	3.201	0	0.001	55.746	33.691	95.93	B2-F16-2
48	0.02	0	0.031	0.128	0	0	59.505	36.665	96.349	B2-F16-3
49	0.012	0	0	0.072	0	0	63.071	36.299	99.454	B2-F18-1
50	0.022	0	0.047	0.128	0	0	62.684	36.256	99.137	B2-F18-2
51	0.041	0	0	1.191	0	0	60.697	36.154	98.083	B2-F18-3
52	45.084	0	0.022	39.57	0.025	0	1.865	1.157	87.723	B2-F19-1
53	50.031	0	0.043	41.452	0	0.019	0	0.013	91.558	B2-F19-2
54	0.024	0	0	0.507	0	0	61.211	37.194	98.936	B2-F19-3

55	0.003	0.015	0.002	0.054	0	0	60.916	36.948	97.938	B2-F20-1
56	0	0	0	0.051	0	0	61.839	36.995	98.885	B2-F20-2
57	0.01	0.048	0.034	0.096	0	0	63.514	37.489	101.191	B2-F20-3
58	0.018	0.083	0.007	0.088	0	0.004	63.085	37.153	100.438	B2-F21-1
59	0	0.004	0	0.065	0	0	62.89	37.566	100.525	B2-F21-2
60	0.03	0	0.015	0.204	0	0	60.016	37.725	97.99	B2-F21-3
61	0.042	0	0	0.004	0	0	63.098	37.054	100.198	B2-F22-1
62	0.053	0	0.045	0.327	0	0.002	44.572	31.097	76.096	B2-F22-2
63	0	0	0	0.164	0	0	61.964	36.937	99.065	B2-F22-3
64	0.027	0	0.078	0.004	0	0	62.054	36.563	98.726	B2-F23-1
65	0.004	0	0.01	0.094	0	0	61.402	36.965	98.475	B2-F23-2
66	0.032	0.002	0	0.349	0	0.013	43.002	29.505	72.903	B2-F23-3
67	3.398	0	0.018	4.377	0.002	0.009	53.116	35.151	96.071	B2-F24-1
68	45.793	0	0.036	37.421	0.048	0.026	0.682	0.116	84.122	B2-F24-2
69	0.058	0	0	1.135	0	0	59.742	36.792	97.727	B2-F24-3
70	0.127	0	0.049	1.615	0.041	0.043	2.918	2.871	7.664	B2-F25-1
71	0.047	0.056	0.043	0.247	0	0	61.767	37.19	99.35	B2-F25-2
72	0	0	0.034	0.055	0	0	59.708	37.254	97.051	B2-F25-3
73	0.019	0	0	0.149	0	0.006	62.382	37.593	100.149	B2-F26-1
74	0.004	0.013	0.053	0.038	0	0.012	62.582	37.1	99.802	B2-F26-2
75	21.219	0	0	17.813	0.01	0.024	29.859	21.259	90.184	B2-F26-3
76	0.006	0	0.045	0.076	0	0.014	62.457	37.089	99.687	B2-F27-1
77	0.009	0.015	0.044	0.045	0	0.006	61.36	36.746	98.225	B2-F27-2
78	0	0	0.006	0.011	0	0.043	61.127	36.858	98.045	B2-F27-3
79	0.022	0	0.107	0.158	0	0	63.252	37.11	100.649	B2-F28-1
80	0.01	0	0.002	0.018	0	0	61.104	37.28	98.414	B2-F28-2
81	0.008	0	0	0.016	0	0.008	57.337	40.773	98.142	B2-F28-3
82	0	0	0	0.028	0	0	60.678	36.89	97.596	B2-F29-1
83	0	0	0.05	0.062	0	0.007	61.182	37.126	98.427	B2-F29-2

84	0.024	0	0.006	0.001	0	0	61.215	36.852	98.098	B2-F29-3
85	0.019	0	0.047	0	0	0	61.057	37.16	98.283	B2-F30-1
86	0	0.002	0.011	0.02	0	0.001	59.113	36.235	95.382	B2-F30-2
87	0.005	0	0.073	0.381	0.013	0	61.602	37.204	99.278	B2-F30-3
88	0.008	0	0.03	0.104	0	0	61.925	37.634	99.701	B2-F31-1
89	0.091	0	0	0.09	0	0.02	61.68	36.622	98.503	B2-F31-2
90	0.005	0	0	0.026	0	0	61.412	37.594	99.037	B2-F31-3
91	0	0	0.022	0.04	0	0.003	61.926	36.915	98.906	B2-F32-1
92	0	0	0	0.017	0	0	61.523	36.978	98.518	B2-F32-2
93	0.022	0.017	0.024	0.069	0	0	60.575	36.657	97.364	B2-F32-3
94	0.022	0	0	0.267	0	0	61.333	37.428	99.05	B2-F33-1
95	0	0.011	0.027	0.148	0	0	60.017	37.196	97.399	B2-F33-2
96	0.03	0.017	0.006	0.272	0	0	60.417	37.28	98.022	B2-F33-3
97	0	0.009	0.011	0.583	0	0	51.778	40.957	93.338	B2-F34-1
98	0.022	0.11	0	0.129	0	0	58.711	37.819	96.791	B2-F34-2
99	0.007	0	0.028	0.086	0	0	61.189	37.692	99.002	B2-F34-3
100	0.014	0.069	0.013	0.047	0	0.021	60.085	37.14	97.389	B2-F35-1
101	0.006	0.084	0.001	0.045	0	0	59.381	37.557	97.074	B2-F35-2
102	0.006	0.039	0	0.081	0	0.003	60.409	37.924	98.462	B2-F35-3
103	0.003	0	0.018	0.106	0	0	62.019	36.905	99.051	B2-F36-1
104	0	0	0.041	0.066	0	0.009	61.474	37.613	99.203	B2-F36-2
105	0.02	0	0	0.149	0	0.019	60.48	36.569	97.237	B2-F36-3
106	0	0	0.111	0.009	0	0	63.079	36.981	100.18	B2-F37-1
107	0.008	0	0.008	0.026	0	0	63.371	36.972	100.385	B2-F37-2
108	0.007	0	0	0.027	0	0	61.089	37.966	99.089	B2-F37-3